Evaluating Mineralogical, Geochemical and Microbial Relationships Within Sulfur-Bearing Mine Wastes; A Multianalytical and Multivariate Statistical Approach

by

Emilia Principe

A thesis submitted in partial fulfillment
of the requirements for the degree of
Master of Science (MSc) in Geology

The Faculty of Graduate Studies
Laurentian University
Sudbury, Ontario, Canada

THESIS DEFENCE COMMITTEE/COMITÉ DE SOUTENANCE DE THÈSE
Laurentian Université/Université Laurentienne
Faculty of Graduate Studies/Faculté des études supérieures

Title of Thesis
Titre de la thèse: EVALUATING MINERALOGICAL, GEOCHEMICAL AND MICROBIAL RELATIONSHIPS WITHIN SULFUR-BEARING MINE WASTES; A MULTIANALYTICAL AND MULTIVARIATE STATISTICAL APPROACH

Name of Candidate
Nom du candidat: Principe, Emilia

Degree
Diplôme: Master of Science

Department/Program
Département/Programme: Geology

Date of Defence
Date de la soutenance March 27, 2018

APPROVED/APPROUVÉ

Thesis Examiners/Examinateurs de thèse:

Dr. Nadia Mykytczuk
(Co-Supervisor/Co-directrice de thèse)

Dr. Michael Schindler
(Co-Supervisor/Co-directeur de thèse)

Dr. Lindsay Robertson
(Committee member/Membre du comité)

Dr. Graeme Spiers
(Committee member/Membre du comité)

Dr. Matthew Lindsay
(External Examiner/Examinateur externe)

Approved for the Faculty of Graduate Studies
Approuvé pour la Faculté des études supérieures
Dr. David Lesbarrères
Monsieur David Lesbarrères
Dean, Faculty of Graduate Studies
Doyen, Faculté des études supérieures

ACCESSIBILITY CLAUSE AND PERMISSION TO USE

Abstract

Mine tailings harbour a dense population of extremophiles that play key roles in metal and mineral transformations. While microbially mediated mineral oxidation and reduction within sulfur-bearing mine waste has been widely reported, linkages and statistical significance between environmental parameters and geochemical and mineralogical compositions with microbial community diversity has not yet been documented. A combined geochemistry, mineralogy, and genomics approach has been used in this study to better understand the biogeochemical processes occurring within a gradient of tailings dam materials both at surface and down a depth profile. Complex microbial diversity patterns across sample types, environmental conditions, spatial locations, and geochemical and mineralogical compositions, are addressed using multivariate statistical analysis. Additionally, scanning electron microscopy (SEM) and transmission electron micrscopy (TEM) are used to analyze the compositional and morphological features of microbe-mineral assemblages. A total of 40 sulfur-bearing tailings samples have been collected aseptically from five constructed tailing dam structures, in Sudbury, Ontario. Samples have been grouped into three zones including oxidized, transition, and unoxidized, which are distinguished by pH, munsell colour and mineralogical composition. Oxidized material is composed of silicates and iron-hydroxides (goethite) and iron-hydroxy sulfate minerals (jarosite, schwertmannite), with contact pH ranging from 2.6 - 4.5. Material from the unoxidized zone consists mainly of silicates and sulfides (pyrite, pyrrhotite, chalcopyrite and greigite), with a higher contact pH ranging from 4.14 - 5.71. Transitional material is dominantly composed of silicates, but contains both sulfides and secondary iron and sulfate minerals, with pH ranging from 3.6 - 5.31. Microbial community composition and structures are often attributed to their surrounding geochemical environments. However, no significant correlations are observed between total metal content and microbial community compositions across the analyzed samples. However, community compositions and structures exhibit significant changes based on the contact pH ranges and mineralogical

compositions of the analyzed tailings material. Oxidized, transition, and unoxidized material exhibit similar taxa, however, relative abundance of taxa exhibits extensive variability across the identified zones. Key indicator species are statistically tested across the three alteration zones, with microorganisms whose metabolic functions underpin iron and/or S oxidation and/or reduction identified as microorganisms characterizing alteration zones. Microbial-mineral assemblages analyzed at the nano-scale exhibit minerals that were not identified by routine whole sample analysis (XRD), thereby indicating the importance of performing both SEM and TEM to fully understand microbial-mineral interactions. The microbial-mineral relationships observed in this study both at the micro- and nano-meter scale have resulted in furthering understanding of biogeochemical processes occurring within the analyzed sulfur-bearing tailings material.

Acknowledgements

To Dr. Nadia Mykytczuk, thank you, for not only being a supportive and patient supervisor but for also being my mentor. For helping guide me in the sometimes arduous politics of academia. For reaffirming what I always thought was true; that being a woman in science can be glamorous, so long as you are willing to redefine what you believe to be glamourous.
If not for Nadia's willingness to train me as an undergraduate student, this project would likely not have happened.

To Dr. Michael Schindler, thank you for constantly challenging me. For the encouragement and levity; whether in a coffee shop, the lab, or Virginia. For the impromptu German lessons, the 24-hour email service, and allowing myself a glimpse into your encyclopedic mind.
Prost.

To Dr. Graeme Spiers, a heartfelt thank you for all of your advice over the years and for always having your door open. Thank you Lindsay Robertson, for collaborating and for being an understanding employer, and more importantly, the ongoing support.

An additional thank you to the Basiliko & Mykytzcuk lab and friends at the Vale Living with Lakes Center. To William Zhe, at the Laurentian University GeoLabs, thank you for always insisting that I wasn't a bother when my sample preparation inevitably failed time and time again. To Ido Hatam, I simply can't thank you enough for your help and friendship along the way. Finally, to fellow graduate students in the Earth Science department, thank you for the camaraderie. It was this support that made this process greatly enjoyable.

Emilia

Table of Contents

Table of Figures

1 General Introduction

1.1 Sulfidic tailings material; production, composition, environmental impact and storage

Mine wastes, defined as mining by-products that are of sub economic value, constitute the largest global proportion of waste industrially produced (Lottermoser, 2007). Mine wastes may be subdivided into numerous types, determined by the physical and chemical characteristics, namely the mineralogical and geochemical composition. One such type of mine wastes are sulfidic tailings, which are fine grained crushed, ground, and milled sulfidic waste rock that are generated as a by-product from mineral extraction (Lottermoser, 2007). Sulfidic tailings are often deposited as a slurry, and may include metals (often sub economic to uneconomic grades), processing chemicals, organic amendments, processing waters, and ground gangue minerals from the processed ore-bearing geological materials. The minerals often include silicates, oxides, hydroxides, carbonates, sulfates and sulfides (Lottermoser, 2007). Despite advanced extraction technologies, recoveries of the relevant minerals are never 100 %, and thus tailings materials will include sulfide minerals. Within metal ores, such as base metal (Ni Cu) massive sulfide deposits, relevant minerals often include sulfides, which incorporate metals within their crystal structure.

The Earth's mantle and crust is composed of a small amount of sulfur, totaling at only 0.025% (Vaughan and Corkhill, 2017). Intrinsically, sulfide minerals, which are compounds where sulfur is bound to a cation(s) and/or to anions such as As, Sb, and S, are a minor, yet common component of Earth's crust (Lottermoser, 2007; Vaughan and Corkhill., 2017). Sulfide minerals have been expressed as the most important socioeconomic group of ore minerals by Vaughan and Corkhill (2017), as they are not only important for incorporating metals within their crystal structures, but are responsible for environmental degradation. A considerable number of sulfide minerals have been identified, with five expressed as 'abundant accessory rock forming' minerals (Bowles et al., 2011). These include the following; pyrite (FeS_2), pyrrhotite ($Fe_{1-x}S$), chalcopyrite ($FeCuS_2$),

sphalerite (ZnS) and galena (PbS). Another important group are poorly crystalline metastable sulfides, otherwise defined as 'amorphous iron sulfides' (Vaughan et al., 2017), include the minerals greigite (Fe_2S_4) and mackinawite (FeS). These two minerals precipitate within low temperature environments (<100°C) under reducing conditions (Schieber et al., 2011).

Low temperature sulfide geochemistry within sulfidic tailings is of critical importance, due to its relevance in metal and metalloid release and/or attenuation through oxidative and/or reductive dissolution reactions. Specifically, the degree of weathering and/or alteration of sulfide minerals have been analyzed and reviewed in order to further understand biogeochemical processes occurring within sulfidic mine wastes. Jambor and Blowes (1990) established a sulfide alteration index (SAI), whereby sulfide minerals are ranked as least to most altered from 0 – 1, respectively. Alteration is based on microscopic examinations, whereby dissolution, alteration, and/or replacement (i.e: pseudomorphism) are indications of the alteration degree.

Extensive environmental impacts from mining are associated with metal release and, as a result, mine wastes must be disposed in an isolated facility where ongoing monitoring and treatment is to be maintained (Lottermoser, 2007). The majority of tailings materials produced are disposed of into tailings storage facilities, which are impoundments that act as storage structures. These structures can range from natural depressions (i.e: lakes), dry-stack piles, man-made ponds, fields, etc. Additionally, the perimeter of these impoundments may be encompassed by tailings dam structures. Tailings dams are large surface embankments which are often composed of the tailings material themselves that are designed to isolate mine wastes and they range from a few to thousands of hectares in size. Due to this immense size, tailings dam structures are considered to leave the largest footprint of all mining activities (Lottermoser, 2007). The mineralogical and geochemical compositions of material used to construct these tailings dams must be analyzed and

identified prior to construction and throughout monitoring procedures, to ensure effective construction and resistance to environmental degradation, erosion and failure (Lottermoser, 2007).

1.2 Biogeochemical cycling of iron and sulfur within sulfidic tailings material

1.2.1 Weathering of sulfidic tailings

Sulfidic tailings are invariably heterogeneous and polymineralic and the mineralogical composition of sulfidic tailings is dependent on the ore deposit from which it originates. Sulfidic tailings are composed of various minerals, including, but not limited to, silicates, oxides, hydroxides, carbonates, and sulfides, with silicates as the most common gangue phases (Lottermoser, 2007). Upon exposure to air, water and/or microorganisms, minerals within sulfidic tailings become chemically unstable (Jamieson, 2011). The rate and weathering pathway of a mineral in mine tailings depends on the solubility of the mineral, dissolution kinetics, environmental conditions (pH, Eh, T) and ionic strength and microbial activities. Understanding the interplay of these factors and their effects on the weathering of contaminant bearing minerals is thereby of notable importance to wide in the prediction of mine drainage quality and chemistry.

1.2.2 Sulfide oxidation; an overview

A key reaction in the development of acid rock drainage and metal leaching (ARD/ML) is the oxidation of sulfide minerals such as pyrite and pyrrhotite. The oxidation of pyrite may proceed through many reactions and is demonstrated in reactions 1-4.

Reaction 1 $FeS_2 + 7/2O_2 + H_2O \rightarrow Fe^{2+} + 2SO_4^{2-} + 2H^+$

Reaction 2 $Fe^{2+}_{(aq)} + 1/4O_{2(g)} + H^+ \rightarrow Fe^{3+}_{(aq)}\ 1/2H2O_{(l)}$

Reaction 3 $FeS_{2(s)} + 14Fe^{2+}_{(aq)} + 8H_2O_{(l)} \rightarrow 15Fe^{2+}_{(aq)} + 2SO_4^{2-}{}_{(aq)} + 16H^+_{(aq)}$

Reaction 4 $Fe^{3+}_{(aq)} + 3H_20_{(l)} \rightarrow Fe(OH)_{3(s)} + 3H^+_{(aq)}$

Reaction 1, referred to as the "initiator reaction" illustrates the chemical oxidation of pyrite and occurs in the presence of both oxygen and water. This reaction results in the release of ferrous iron from the pyrite crystal lattice into the surrounding environment, and the corresponding release of H^+ protons ultimately configures a pH regime optimal for acidophilic bacterial growth (Konhauser, 2007). If the acidity is not buffered and the pH is lowered, conditions may become optimal for acidophilic bacterial growth.

The liberated ferrous iron is subjected to enzymatic oxidation in the presence of dissolved oxygen, producing ferric iron (Reaction 2). Oxidation of ferrous to ferric iron can be a consequence of either biotic or abiotic processes, or a combination of the two. The oxidation of ferrous iron to ferric iron is accelerated by ferrous iron oxidizing bacteria, as they accelerate the production of ferric iron by five to six orders of magnitude greater than the exclusive abiotic chemical oxidation (Robertson, 1992). For example, *Acidithiobacillus ferrooxidans* and *Leptospirillum ferrooxidans*, actively oxidize ferrous iron and sulfur and/or sulfur compounds during metabolic reactions, resulting in accelerated sulfide oxidation and increase in acidity.

As illustrated in reaction 3 and 4, produced ferric ions can either directly oxidize pyrite or hydrolyze and precipitate as amorphous ferric (hydr)oxides, respectively. Within reaction 3, soluble ferric ions produced from reaction 2 directly oxidize pyrite, releasing additional sulfate and ferrous ion (Moncur et al., 2009). The released ferrous ion can then be further utilized as an energy generating process for microbial growth, establishing a propagation cycle (Lottermoser, 2007). Within reaction 4, the precipitation of ferric iron produces not only iron-(hydr)oxides but also extensively produces H^+ protons. The increase in surrounding acidity can then activate and

exhilarate further mineral dissolution, particularly gangue minerals, such as silicates (Konhauser, 2007). Concurrently throughout this reaction, the presence of sulfate released from reaction 1 and 4 in conjunction with the presence of ferric iron could result in the formation of secondary minerals (i.e: jarosite) (Konhauser, 2007). The reactions are continuous and they occur simultaneously, establishing the cyclic iron cycle within sulfur-bearing mine waste environments.

1.2.3 Sulfur oxidation

As previously mentioned in Section 1.3.2, sulfide oxidation may be amplified with the presence of sulfur and iron oxidizing bacteria. Sulfur oxidizing bacteria may be subdivided into two groups, including a class of bacterium which thrive at neutral pH, and a class that thrives within acidic environments (Konhauser, 2007). Within the latter, the predominant microorganisms include *Acidithiobacillus*, *Sulfolobus* and *Acidianus* spp. (Konhauser, 2007). Other sulfur oxidizing bacteria, including *Acidithiobacillus thiooxidans* and *Acidithiobacillus caldus*, have exhibited substantial involvement with pyrite oxidation as these microorganisms oxidize intermediate sulfur compounds, resulting in the formation of sulfuric acid (Chen et al., 2014).

Sulfur-oxidizing microorganisms accommodate a large suite of metabolic processes to oxidize sulfur compounds. The oxidation of a reduced sulfur compound (-1 valence state), to sulfate (+6 valence state), is an 8e- step. Numerous intermediate S species are formed over the six intermediate oxidation states of sulfur between sulfide and sulfate throughout the oxidation process (Johnston, 2010; Hansel, 2015). Indeed, an oxidant is required to achieve sulfur oxidation throughout these reactions and oxygen is often used as a terminal electron acceptor for sulfur-oxidizing bacteria. Within systems where oxygen is limited, some sulfur oxidizing bacteria are capable of utilizing NO^{3-}, NO^{2-} or ferric iron in place of oxygen (Fossing et al., 1995; Johnston, 2010).

Biotic sulfide oxidation produces two distinct outcomes; direct leaching and indirect leaching (Johnson et al., 1993). Direct leaching occurs as a result of microbial adsorption to the sulfide surface, where oxidation and solubilization is controlled through enzymatic reactions (Johnson et al., 1993). Indirect leaching includes the enzymatic oxidation of ions in solution in the presence of dissolved oxygen (i.e. ferrous iron to ferric iron), where the resulting ferric iron can either directly oxidize sulfides or hydrolize and be precipitated as amorphous ferric iron-oxy(hydr)oxides (Johnson et al., 1993). Larson et al (1993) has suggested that every individual cell of *A. ferrooxidans* and *A. thiooxidans*, is required to be directly adhered to the sulfide surface in exchange for energy uptake. Placement of attachment is both meticulous and sufficient as bacteria tend to adhere to surface areas with high surface energy within minutes (Kohnhauser, 2007). A study conducted by Pace et al (2005) exhibited that *A. ferrooxidans* adhering and colonizing on a pyrite surface was dependent upon the presence and occurrence of phosphate enriched sites. Upon attachment, *A. ferrooxidans* tightly adhere to the pyrite surface with the use of lipopolysaccharides, which may or may not be acidic (Southam and Beveridge, 1993; Pace et al., 2005). The resulting release of ferric iron from the microbial oxidation of ferrous iron may then chemically react with pyrite, to further pyrite oxidation (Konhauser, 2007). Notably, Edwards et al (2000) states that the microbially produced ferric iron may react with non-specific surfaces, and thus may oxidize other minerals as well. The released ferric iron serves as evidence for an acidic microenvironment within the lipopolysaccharides, as ferric iron remains soluble within this environment (Pace et al. 2005). Additional studies support this representation of microbial colonization, as Dockrey et al (2014) exhibits bacteria colonizing pyrite surfaces by direct attachment, followed by cementation and the formation of an acidic microenvironment.

As mentioned above, various intermediate sulfur species are formed during the transformation of S^{2-}as to $(SO_4)^{2-}$. Pyrite is the one of the most common sulfide minerals in mine tailings and as such the mechanisms of pyritic weathering have been studied in great detail.

Upon initial oxidation of ferrous iron (structurally bound within the crystal lattice of pyrite), partially protonated sulfur ligands are exposed at the surface of pyrite, and will attach to available O_2 (Goldhaber, 1983). With the additional presence of water, the double bond between the O_2 molecules will break, H_2O will bind with iron and the displacement of $2S_2OH^-$ groups will ensue (Goldhaber, 1983).

At circumneutral pH (between pH 6.5 - 7.5), $2S_2OH^-$ groups will oxidize to sulfate (reaction 5) through the aforementioned sulfur intermediates, which include: thiosulfate ($S_2O_3^{2-}$), polythionates ($S_nO_6^{2-}$) and sulfite (SO_3^{2-}) (Konhauser, 2007). The oxidation of the listed intermediate sulfur compounds is yet not entirely understood, as many of these intermediates are short-lived and present in exceptionally low concentrations within the micro molar range. Despite their brief presence, their interactions with the surrounding environments are significant, and should be identified (Konhauser, 2007; Hansel, 2015). Thiosulfate ($S_2O_3^{2-}$) is the first intermediate S species to form, and is most stable at neutral pH, as shown in reaction 6 (Xu and Schoonen, 1995). Thamdrup et al (1993) discovered bacterial sulfur disproportionation, which is a process whereby thiosulfate disproportionates to elemental sulfur and sulfite (reaction 7). Thiosulfate can also be oxidized by O_2 (reaction 8), resulting in the formation of tetrathionate (a polythionate), which is most stable at low pH (Konhauser, 2007). Due to the instability of sulfite under alkaline conditions, the resulting sulfite within reaction 2 can further react with oxygen, resulting in the production of sulfate (reaction 9). Reaction 10 illustrates elemental sulfur oxidization to sulfate which would also occur within alkaline conditions, as elemental sulfur is not stable within alkaline conditions. Under acidic conditions, sulfate and tetrathionate would be the sulfur intermediate species in greatest abundance (Hansel, 2015).

Reaction 5 $S_2OH^- + 3O_2 + H_2O \rightarrow 2SO_4^{2-} + 3H^+$

Reaction 6 $S_2OH^- + O_2 \rightarrow S_2O_3^{2-} + H^+$

Reaction 7 $S_2O_3^{2-} \rightarrow S^0 + SO_3^{2-}$

Reaction 8 $2\ S_2O_3^{2-} + 0.5O_2 + 2H^+ \rightarrow S_4O_6^{2-} + H_2O$

Reaction 9 $SO_3^{2-} + 0.5O_2 \rightarrow SO_4^{2-}$

Reaction 10 $S^0 + 1.5O_2 + H_2O \rightarrow SO_4^{2-} + 2H^+$

1.2.4 Dissimilatory sulfate reduction

Dissimilatory sulfate reduction, the process where microorganisms reduce sulfate to H_2S, is of critical importance within sulfidic mine waste environments. Sulfur-reducing bacteria are well known to work strictly under anaerobic conditions. However, in recent research, it has been shown that many species of sulfur reducing bacteria may endure hours of oxygen exposure, with some persisting under oxidizing conditions (Konhauser, 2007; Johnston, 2010; Wu, 2012). Prevalent sulfate reducing bacteria include the following mesophilic genera: *Desulfotomaculum*, *Desulfosporosinus*, and *Thermoacetogenium*, and the following thermophilic genera include *Thermodesulfobacterium*, *Thermodesulfovibrio* and *Thermodesulfobium* (Konhauser, 2007). Sulfate reducing bacteria may be subdivided into two metabolic groups, where one group can oxidize acetate, and the other cannot (Konhauser, 2007). Within these two groups, some microorganisms have the ability to function chemolithoautotrophically (obtains energy via oxidation of inorganic compounds, such as CO_2, N, Fe, etc.), with some using H_2 as an electron donor. Similar to sulfur oxidizing bacteria, sulfate reducing bacteria operate a suite of metabolic processes, and the overall reduction of sulfate to sulfide occurs through reactions with intermediate S species which undergoes an 8e- reduction, as seen in reactions 1 and 2 (Konhauser, 2007; Johnston, 2010). In reaction 11, energy is gained by coupling the oxidation of H_2 to sulfate

reduction. In reaction 12, energy is gained by coupling the oxidation of acetate (CH_3COO^-) to the reduction of sulfate.

Reaction 11 $4H_2 + SO_4^{2-} \rightarrow H_2S + 2OH^- + 2H_2O$

Reaction 12 $CH_3COO^- + SO_4^{2-} + H_2O \rightarrow H_2S + 2HCO_3 + OH^-$

Intermediate sulfur species are not mentioned in the above simplified reactions. Electrons, derived from H_2 donating electrons (H_2 is sourced from environmental gas or organic substrates), are transported through the cell, eventually crossing the plasma membrane to a cytoplasmic Fe-S bearing protein (Konhauser, 2007). Additional low molecular weight compounds may be used as electron donors, including lactate, formate, acetate or ethanol (Sahinkaya et al., 2007). Sulfate is then activated by adenosine-5'-triphosphate (ATP) by means of the enzyme ATP-sulfurylase (Konhauser, 2007). Sulfate will then be transported to the cytoplasm, where it reacts with a phosphate group to produce adenosine phosphosulfate (APS). APS is then reduced to sulfite enzymatically, and is ultimately reduced to H_2S via various intermediate reactions, including $S_3O_6^{2-}$ and $S_2O_3^{2-}$ (Konhauser, 2007; Johnston, 2010). H_2S is released from the cell and the intermediate sulfur species may also be excreted (Konhauser, 2007).

Sulfate is often in abundance within sulfidic mine waste environments, and thus the growth and rate limiting factor for sulfate reducing bacteria includes the availability of organic carbon (Ulrich et al., 2003). Within sulfidic tailings environments, organic matter may be derived from an amendment, natural soils, and/or dead organic biomass (i.e: dead microbial cells). Fortin and Beveridge (1997) state that very little organic carbon is required in order to sustain sulfate reducing bacteria, as they have adapted to their environments and successfully form H_2S rich microenvironments within the anoxic zones in sulfidic tailings.

1.2.5 Iron oxidation

Within oxygenated environments at neutral pH, ferrous iron oxidizes to ferric iron rapidly, which results in the hydrolyzation of ferric iron and the precipitation of nanocrystalline ferric hydroxides, as seen in reaction 13 (Kohnhauser, 2007). In environments of low pH and/or low oxygen concentrations, ferrous iron remains stable. Therefore, microorganisms which utilize the oxidation of ferrous iron to ferric iron for energy fixation are either acidophilic and/or microaerophilic. The most recognized acidophillic iron-oxidizing bacteria include *Acidithiobacillus ferrooxidans* and *Leptospirillum ferrooxidans*. Microorganisms such as *Acidithiobacillus ferrooxidans*, *Leptospirillum ferrooxidans* and *Ferroplasma acidiphilum*, have the ability to oxidize ferrous iron and thereby quickly generate ferric iron to further oxidation, resulting in the acceleration of pyrite oxidation (Chen et al., 2014). These organisms thrive in sulfidic mine waste environments, where growth of the former and latter are favourable within a pH range of 1.8 - 2.5 and below pH = 1.8, respectively (Konhauser, 2007).

Reaction 13 $4Fe^{3+} + 10H_2O + O_2 \rightarrow 4Fe(OH)_3 + 8H^+$

The metabolic processes of microbial ferrous iron oxidation begins with the transport of an electron, derived from ferrous iron, through the cell to an acid-stable Cu-bearing protein called rusticyanin (Kohnhauser, 2007). Ferrous iron is not transported through the cell and, instead, is regarded to have oxidized within the periplasm due to toxicity and insolubility of ferric iron (Ingledew et al., 1977). The neoformed ferric ion is then excreted from the cell through a diffusional gradient (Konhauser, 2007). Due to a high abundance of protons (i.e: H^+), ferric iron will either attach weakly, or not attach at all, to cells with highly protonated outer surfaces. This simplified metabolic description of microbial ferrous iron oxidation is not yet fully understood, as researchers currently lack a thorough understanding on mechanisms and pathways involved in the electron transfer (Melton et al., 2014).

1.2.6 Dissimilatory iron reduction

A wide variety of bacterial genera have the capability to reduce ferric iron, whether its occurring as a free ion, structurally incorporated within a mineral structure, or adsorbed to a surface (Konhauser, 2007). Within sulfidic mine waste environments, ferric iron occurs in a variety of forms. Notably, ferric iron often occurs in greatest abundance within nano-crystalline Fe-(hydr)oxide and iron-hydroxy sulfates, such as ferrihydrite, goethite and schwertmannite. Minerals such as jarosite, hematite and magnetite are also sources for microbial ferric iron reduction, and are often present within these environments. However, the amount of energy derived from ferric iron reduction from different mineral sources remains unresolved (Roden et al., 1996; Loveley et al., 2004). Nonetheless, ferric iron reducing bacteria use the coupling of ferric iron reduction to the oxidation of various compounds (H_2, fermentation products, monogrammatic compounds), from both amorphous and crystalline minerals sources containing ferric iron, as seen in reactions 14 and 15 (Konhauser, 2007; Melton et al., 2014). Alternative compounds which microbes utilize as an electron donor for ferric iron reduction include elemental sulfur, glucose and pyruvate (Lovley, 1993; Cummings et al., 2000). Upon the enzymatic reduction of ferric iron, microorganisms release carbon dioxide. This released carbon dioxide may form complexes with soluble metals and/or metalloids that are present within the surrounding environment, resulting in the formation of metal carbonate. This occurrence may mitigate environmental impacts on surrounding waters, as metals and/or metalloids may be incorporated within the resulting carbonate phase (Chen et al., 2005).

Reaction 14 $0.5H_2 + Fe(OH)_3 \rightarrow Fe^{2+} + 2OH^- + H_2O$

Reaction 15 $CH_3COO^- + 8Fe(OH)_3 \rightarrow 8Fe^{2+} + 2HCO_3^- + 15OH^- + 5H_2O$

There are numerous metabolic mechanisms of electron transfer that ferric iron reducing bacteria use when reducing ferric iron from ferric iron-bearing minerals. Direct contact between the

bacteria cell and mineral surface facilitates electron transfer. These electrons originate from a reduced source within the cells cytoplasm (Konhauser, 2007). Electrons are transferred through the cell and, ultimately, to the cells outer membrane, where iron reductase enzymes transfer the electrons to the ferric iron-bearing mineral surface of which the bacterium is attached (Konhauser, 2007). Subsequently, iron-oxygen bonds within the ferric iron-bearing mineral weaken (due to greater electron density) and allow the release of ferrous iron and reductive dissolution ensues (Lower et al., 2001; Konhauser, 2007). Other metabolic mechanisms do not require the direct attachment between the bacterial cell and the mineral surface for ferric iron reduction. Some bacteria, such as S. oneidensis, use oxidized metal chelators to solubilize ferric iron within environments that are deficient in ferric iron (Melton et al., 2014). Lovley (1991) demonstrates that soluble, chelated ferric iron is reduced at a faster rate than insoluble ferric iron oxides. Redox-active electron shuttles offer another mechanism to reduce ferric iron in which bacteria do not require direct attachment to the ferric iron-bearing mineral surface. Electron shuttles may be sourced microbially or from the surrounding environment, including flavins and humic substances, respectively (Melton et al., 2014). These shuttles transfer electrons from ferric iron-reducing bacteria to the ferric iron-bearing mineral surface, establishing ferric iron as the electron acceptor, and may be of importance when minerals are occluded in pore spaces (Melton et al., 2014; Konhauser, 2007). The three mechanisms, including direct cell-mineral contact, chelating agents, and electron shuttles are facilitated at the nm scale in close proximity to the mineral surface. When distal (within μm distance from the mineral surface) bacteria may use redox-active conductive pili (nanowires) or multistep electron hopping to transfer electrons (Melton et al., 2014). Microbial nanowires occur within microbial biofilms and transport electrons towards ferric iron-bearing minerals (Richter et al., 2011; Melton et al., 2014). Multistep electron hopping occurs over redox-active cofactors that are present within microbial biofilms. Here, electrons are transferred from the cells extracellular space, along co-factors and eventually, to the ferric iron-bearing mineral surface.

1.3 Biogenic mineral formation

Biogenic mineral formation, also termed biomineralization, may occur by two different mechanisms; biologically induced biomineralization and biologically controlled biomineralization (Konhauser, 2007). The former is not regulated by microorganisms and simply occurs as a byproduct of microbial metabolic activity and/or through interactions between microorganisms and their surrounding environment (Konhauser, 2007). The latter, however, is facilitated by microorganisms, as they will precipitate minerals within the cytoplasm (intracellular) or on the cell wall and bacterial polymers (extracellular) in order to provide a form of physiological purpose (Fortin and Langley, 2005). The next section will focus on the biomineralization of iron-(hydr)oxides, sulfates and sulfides, as these minerals are widespread within sulfidic mine waste environments.

1.3.1 Mineralization; nucleation and growth

The fundamental thermodynamics of biomineralization is equivalent to abiotic mineralization, only occurring when the amount of energy released from bond formation exceeds the activation energy barrier. Nucleation, the first step in mineral formation, occurs when supersaturation is reached. In other words, the activity of ions (IAP) in solution must meet or surpass the solubility product (Ksp) of the mineral of interest (Stumm and Morgan, 1996). Mineral growth would then ensue, as ions similar to those of the substratum, adsorb to the available critical nuclei (Konhauser, 2007). The first mineral phase to form is often poorly crystalline, with poorly crystalline phases such as ferrihydrite, are kinetically favoured over crystalline phases. This is due to lower interfacial free energy and fast nucleation rates of the nanocrystalline phases, which are often too fast to allow for crystalline analogs to form initially (Nielson et al., 1971; Steefel et al., 1990). Therefore, the transformation sequence of mineralization within low temperature environments commences with

the precipitation of nanocrystalline metastable phases, followed by the mineralization of crystalline mineral phases (Konhauser, 2007).

Crystallization by particle-attachment (CPA) is a crystallization process which includes the attachment of a range of particles, such as nanoparticles, multi-ion complexes, and oligomers (Yorero et al., 2015). As stated, when supersaturation is reached, mineral nucleation and growth ensues (Yorero et al., 2015). However, processes involved with the transition of an amorphous phase to crystalline phase, in addition to essential aspects of CPA (i.e: interconnections between particle motion, interfacial forces and solution structure), remains relatively unknown (Yorero et al., 2015).

1.3.2 Microbial nucleation sites

The role of microorganisms within iron and sulfur cycling does not end after metabolic oxidative and reductive reactions, as they may also serve as surfaces available for mineral nucleation (Konhauser, 2007). Microbial cell walls are abundant in ionized ligands (often negatively charged), and a result, is a favoured location for sorption reactions with positively charged minerals, due to electrostatic attaction (Glasauer et al. 2001). Microbial cell walls encrusted in amorphous iron oxides, such as two-line ferrihydrite, have been observed within various environments (Tipping et al (1989); Emerson (2000)). The specificity of each cation binding with microbial cell ligands is complex, as the structure and composition of microbial cell walls vary across species and physiochemical properties differ for unique cations (Konhauser, 2007).

1.3.3 Biogenic Iron Oxides

Biogenic iron oxides constitute iron oxides that are found in close association with microbial activity (Fortin and Langley, 2005). Fortin and Langley (2005) state that the physiochemical

characteristics of biogenic iron oxides are similar to abiotic iron oxides, resulting in challenging interpretations of biogenic origins. Common iron oxides may be subdivided into three distinct groups including; amorphous to poorly ordered phases (i.e: two- and six-line ferrihydrite), oxyhydroxides (i.e: goethite, lepidocrocite) and oxides (i.e: hematite, magnetite) (Cornell and Schwermann, 2003). These oxides are commonly small in diameter, ranging from 2-500 nm (Fortin and Langley, 2005). The biological role involved with the precipitation of iron oxides includes the oxidation of ferrous iron to ferric iron, under various conditions, including low to neutral pH and oxic to anoxic environments (Fortin and Langley, 2005).

Both the abiotic and biotic oxidation of ferrous iron to ferric iron is heavily dependent on the pH and oxygen concentrations of the surrounding environment (Fortin et al., 2005). The abiotic oxidation of ferrous iron to ferric iron occurs rapidly, resulting with limited dissolved ferrous iron (Konhauser, 2007). Despite rapid chemical oxidation, microorganisms are commonly observed in association with iron oxides in both neutral and acidic pH environments (Fortin et al., 2005; Guo and Barnard, 2013). Within low pH environments, such as within sulfidic mine waste environments, the oxidation of ferrous iron to ferric iron is catalyzed and mediated by microorganisms and thus the formation of ferrihydrite is produced by iron-oxidizing microorganisms (Guo and Barnard, 2013). Ferryhydrite, the most common biomineralized iron oxide mineral, and due to its low interfacial free energy, it is often the first phase to form. Consequently, it often serves as a precursor phase for more stable iron oxide phases, such as goethite and hematite, where they form via dissolution – precipitation processes (Guo and Barnard, 2013).

The formation of ferrihydrite is considered to be both biologically controlled and biologically induced, where its directly and indirectly formed by microbial activity, respectively (Guo and Barnard, 2013). The formation of ferrihydrite may proceed through the oxidation and hydrolysis of ferrous iron that is bound to the microbial cell wall, the attachment of iron colloids or ferric ion

species to microbial ligands, or by changing environmental parameters (Eh and pH) from microbial metabolic activity (Konhauser, 2007).

1.3.4 Iron sulfates

Jarosite ($KFe_3(SO_4)_2(OH)_6$) and schwertmannite (ideally $Fe_8O_8(OH)_6SO_4$) are common iron-hydroxysulfate minerals in sulfidic mine tailings, due to the environments low pH and abundance of sulfate. Jarosite and schwertmannite precipitate upon the oxidation and hydrolysis of ferrous iron (reactions 16 and 17). Konhauser (2007) states the role microorganisms play in the mineralization of these two phases is not yet well understood. However, Oggerin et al (2013) has suggested that the identified fungal strain, *Purpureocillium lilacinum,* induced the formation of hydronium-jarosite, with it nucleating along the fungal cell wall. Mori et al (2016) observed a new ferrous iron oxidizing strain, C25, forming iron-rich filaments throughout growth. These cellular filaments formed spheres, which developed into schwertmannite mineral assemblages. This method of biomineralization did not encapsulate the entirety of the cell volume, thus permitting the microorganism to further oxidation of dissolved ferrous iron ions. A biogenic schwertmannite-like mineral (SAED diffraction pattern similar to that of schwertmannite) phase was present amongst precipitates on or around algal cells (Akai et al., 1999).

Reaction 16 $K^+ + 3Fe^{3+} + 2SO_4^{2-} + 6H_2O \rightarrow KFe_3(SO_4)_2(OH)_6 + 6H^+$

Reaction 17 $8Fe^{3+} + SO_4^{2-} + 14H_2O \rightarrow Fe_8O_8(OH)_6SO_4 + 22H^+$

1.3.5 Secondary sulfides; abiotic and biotic mineralization

The formation of low temperature (<100°C) sulfides is indirectly linked with dissimilatory sulfate reduction, as discussed in Section 1.3.4. As seen in reaction 12 (Section 1.3.4), the microbially reduced sulfate, in addition to microbial enzymatic reactions, generates dissolved hydrogen sulfide. The dissolved hydrogen sulfide, then in turn, may react abiotically with surrounding free ions and/or mineral phases resulting in the formation of a sulfide mineral.

Once again, pyrite is used here as an example as it is one of the most common sulfides within sulfidic mine waste environments. The direct mechanisms involved in the formation of pyrite within low temperature environments still remains a topic of debate. However, it is widely accepted that the steps involved include a number of iron-sulfide precursors (Sweeney et al., 1973). The first step involves the precipitation of a nanocrystalline iron monosulfide phase, such as FeS, due to its low interfacial free energy. This precipitation process may occur by two mechanisms, as seen in reactions 1 and 2. In reaction 18, bisulfide (HS^-) reacts with free ferrous iron, which may form from dissimilatory ferric iron reduction, producing a monosulfide (FeS). The other mechanism, as seen in reaction 19 includes the reaction between bisulfide and ferric oxyhydroxide which produces the monosulfide, FeS, and elementary S (Canfield, 1989).

Reaction 18 $Fe^{2+} + HS^- \rightarrow FeS + H^+$

Reaction 19 $6Fe(OH)_3 + 9HS^- \rightarrow 6FeS + 3S^0 + 9H_2O + 9OH^-$

The iron monosulfide will rapidly transition into the highly reactive and disordered mackinawite phase (FeS) (Wolthers et al., 2005; Konhauser, 2007). With a highly reactive surface, mackinawite may then transform into a more stable sulfide phase by reacting with various intermediate sulfur species (Konhauser, 2007). In reaction 20, mackinawite reacts with elemental sulfur, resulting in the formation of the metastable sulfide, greigite. Greigite may then transform into the stable sulfide phase, pyrite, through dissolution-precipitation reactions (Schoonen and Barnes, 1991). Luther

(1991) has proposed that mackinawite may react with other partially oxidized intermediate sulfur species, such as polythionates ($S_xO_6^{2-}$), thiosulfate ($S_2O_3^{2-}$) or polysulfides (S_x^{2-}), resulting in the direct precipitation of pyrite (FeS_2), as seen in reaction 21. The more stable sulfide (pyrite) does not precipitate initially within low temperature environments as the rate of nucleation of less stable precursors, such as mackinawite and greigite, is greater (Schoonen and Barnes, 1991).

Reaction 20 $3FeS + S^0 \rightarrow Fe_3S_4$

Reaction 21 $FeS + HS_x^- \rightarrow FeS_2 + S_{x-1}^{2-} + H^+$

2.0 Thesis objectives

The interdisciplinary field of biogeochemistry integrates concepts and perspectives from three key disciplines including geology, chemistry and biology (Shock et al., 2015). The emerging field differs from geomicrobiology, with emphasis on the geological and chemical roles that influence biochemical processes (Shock et al., 2015). The study of microorganisms and how they characterize their environmental surroundings dates back to the 19th century (Dick et al., 2015). However, only within the last few decades have scientists been gradually learning the links between microorganisms, their mineralogical substrate and surrounding environments (Dick et al., 2015).

This study used a combined mineralogy, genomics and geochemistry approach to gain an improved understanding of biogeochemical processes occurring within a gradient of tailings dam materials both at surface and down a depth profile. The thesis will be presented in two chapters, with Chapter 1 addressing complex microbial diversity patterns across sample types, environmental conditions, spatial locations, and geochemical and mineralogical compositions, using multivariate statistical analysis. In order to identify fundamental microbial roles in mineral

precipitation and/or dissolution within the analyzed tailings material, Chapter 2 will address microbial-mineral assemblages at the nano-scale.

This study is necessary to identify links that exist between microbial communities and tailings material type, as further understanding in mineral precipitation and/or dissolution within these tailings dams are pertinent. Improving our knowledge on the biogeochemical processes occurring at both surface, and at depths within the sampled tailing dam structures will aid in ameliorating environmental impacts from tailings, and provide information that may be used to improve tailings dam construction, operation and closure.

Chapter 1

3.0 Introduction

3.1 Mineralogy of mine wastes; characterization and categorization

Jambor (1994), Lottermoser (2010) and Jamieson et al (2011) have classified minerals analyzed within mine wastes into various groups. These groups represent the degree of mineral alteration, whereby primary minerals analyzed within mine waste material represent unaltered extracted minerals and secondary minerals represent products of weathering reactions. Specifically, Jambor (1994) considers secondary minerals as minerals that have formed by weathering of any minerals, whereas Lottermoser (2010), considers secondary minerals as minerals that have exclusively formed by the weathering of sulfide minerals. In this study, secondary minerals are discussed with respect to the definition by Jambor (1994) and primary minerals are defined as minerals that have formed prior to metal extraction.

The type of primary minerals present in a tailings impoundment is dependent upon the ore deposit of which was mined. Within studied sulfidic mine tailings, located in Sudbury, ON, McGregor et al (1998) identified oxides, silicates and sulfides as primary minerals. Oxides and silicate minerals identified as primary minerals within sulfidic mine waste in Sudbury, ON, include the following: quartz, chlorite, biotite, plagioclase, amphiboles, pyroxenes, talc, magnetite (Jambor and Owens, 1993; McGregor et al., 1998). Sulfides identified as primary sulfide minerals include the following: pyrrhotite, chacopyrite, pentlandite, pyrite and marcasite. Secondary minerals were identified as products of coupled oxidation and/or dissolution precipitation reactions at or within close proximity to the surface of the tailings. Secondary minerals include the following; gypsum, goethite, jarosite and hematite.

McGregor et al (1998) grouped tailings material from the Copper Cliff tailings area within Sudbury, ON, into three alteration zones including oxidized, transition and unoxidized zones. This study defines the three alteration zones based on the type of chemical processes assumed to be occurring in each zone. For example, the authors consider an oxidized zone as zone where sulfide oxidation and dissolution occurs and where trace metals are released into tailings pore water. In this zone, sulfide minerals also exhibited the strongest degree of alteration and occurred at the base of the oxidized zone (i.e: covellite). Similarly, the transition zone represented a zone in which secondary mineral phases formed and in the process attenuated metals through adsorption or structural incorporation. The latter processes occur as a result of precipitation reactions in migrating pore water, which carries metals released during sulfide oxidative dissolution in the oxidized zone. Following the classification by McGregor et al (1998), secondary mineral phases, such as goethite and jarosite, can thus occur in the oxidized and transition zone of sulfidic tailings. Lastly, the unoxidized zone had been considered as the zone with the highest concentration of total sulfur.

Gunsinger et al (2006) grouped tailings material in a similar manner. Pyrrhotite-rich tailings from Lynn Lake, Manitoba, were grouped into three categories based on the degree of alteration. The oxidized zone represented material of which was depleted in sulfides. The transition zone represented material that had been altered and weathered via oxidation reactions. Lastly, Gunsinger et al (2006) grouped tailings material exhibiting very little to no alteration into an 'unaltered' zone. Grouping tailings material based on degree of alteration is thereby common, however, the definition of each alteration zone changes across studies (McGregor et al., 1998; Gunsinger et al., 2006; Lottermoser, 2010; Jamieson, 2011).

3.2 Mineralogical and geochemical features of sulfidic mine wastes; mineral oxidation and dissolution

The processes involved in mineral oxidation and reduction proceed through many redox reactions, which ultimately result in the formation of secondary minerals and subsequently affect the transformation and attenuation of dissolved metals. Indeed, microorganisms may be directly or indirectly involved with these processes. Firstly, biotic oxidation or reduction produces two distinct outcomes: direct and indirect leaching. Direct leaching occurs as a result of microbial adsorption to the sulfide surface where oxidation, reduction and/or solubilization is controlled through enzymatic reactions. Indirect leaching includes the enzymatic oxidation or reduction of ions in solution in the presence of dissolved oxygen. For example, the enzymatic oxidation of ferrous iron results in ferric iron, which can either directly oxidize sulfides or hydrolize and be precipitated as amorphous ferric (oxy)hydroxides. Despite continuous geochemical fluxes, both microbial oxidation and reduction within sulfidic tailings indirectly form secondary minerals, typically dominated by jarosite ($KFe_3(SO_4)_2(OH)_6$), goethite, schwertmannite ($Fe_8O_8(OH)_6SO_4$), and ferrihydrite. The formation of these secondary minerals within sulfidic tailings influences the fate of metal mobility, as metals and metalloids can be adsorbed to these secondary mineral surfaces (ferrihydrite, goethite) and/or sequestered through their structural incorporation (jarosite).

Ultimately, the environmental fate of tailings-derived metals is fundamentally controlled by redox and microbial processes, in addition to mineral precipitation, transformation and/or dissolution.

3.3 Microbiology of mine wastes

Understanding the microbiology of sulfidic mine wastes is of critical importance, as it provides knowledge to advance biomining applications and remediation practices, in addition to guiding the amelioration of environmental impacts (Baker and Banfield, 2003; Lottermoser, 2007). Schippers et al (2010) states that more than 70 studies on the microbiology of sulfidic mine wastes and bioleaching heaps have been published, with the majority using culturing techniques (growing bacteria). With recent advancements, molecular techniques are widely being implemented to examine entire microbial community structures and diversity (Schippers et al., 2010). As such, microbial diversity within sulfidic tailings have been studied using a 16S rRNA gene sequencing approach, providing high resolution community diversity and aiding in unravelling biodiversity within sulfidic tailings material.

Across the 70 studies investigated by Schippers et al (2010), 21 genera of bacteria that utilize iron and/or sulfur species and/or other metals for energy fixation have been identified. Microorganisms that oxidize ferrous iron and sulfur enhance sulfide oxidation, whereby microorganisms that reduce ferric iron and sulfate enhance the dissolution of ferric iron bearing mineralogical phases (i.e: iron (hyr)oxides) and the precipitation of sulfides, respectively (Bazylinksy and Frankel, 2000; Baker and Banfield, 2003; Konhauser, 2007; Hansel et al., 2015). Bacteria at the genus level that were identified to oxidize pyrite, other metal-bearing sulfides, ferrous iron and sulfur and reduce ferric iron within mine waste or heap environments include *Acidithiobacillus*, *Alicyclobacillus* and *Sulfobacillus*. Additional genera include the following: *Acidimicrobium* (oxidize pyrite and ferrous iron), *Acidiphilium* (oxidize sulfur and reduce ferric iron), *Thiobacillus* and *Thiomonas* (oxidize

sulfur and other metals), *Pseudomonas* (oxidize sulfur and reduce ferric iron), *Leptospirillum* (oxidize pyrite, other metals and ferrous iron) and *Gallionella* (oxidize ferrous iron). *Acidithiobacillus ferrooxidans* and *Leptospirillum* are common microbial members identified within acid mine drainage environments, including sulfidic mine wastes (Nordstrom et al., 2015). These two prevalent iron-oxidizing achaea exhibit different optimal conditions, whereby *Acidithiobacillus ferrooxidans* is psychrophilic to mesophilic, and *Leptospirillum* frequents acidic environments (pH values <1.5) at greater temperatures (Nordstrom et al., 2015). Korehi et al (2014) identified OTUs identified as families of Alicyclobacillaceae, Peptococcaceae (reduce sulfate), Hydrogenophilaceae (contains genus *Thiobacillus* which oxidizes sulfur) and Micrococcaceae as most abundant across tailing samples collected from three sulfidic mine waste sites. Genera that metabolically reduce ferric iron and sulfate include the following; *Desulfobacter*, *Desulfobacterium*, *Desulfobulbus*, *Desulfotomaculum* and *Desulfovibrio*. Genera which reduce sulfate for energy fixation include the following: *Desulfobotulus*, *Desulfococcus*, *Desulfonema*, *Desulfosarcina* and *Desulfotomaculum* (Schippers et al., 2010). Lastly, *Ferribacterium* has the ability to reduce ferric iron (Schippers et al., 2010).

Other inhabitants of mine waste environments include bacteria that degrade organic compounds for energy fixation. Schippers et al (2010) states that acidophilic heterotrophic bacteria which degrade organic compounds sometimes facilitate the growth of autotrophic ferrous iron and sulfur oxidizing bacteria. Additionally, *A. cryptum*, a heterotrophic species which has the ability to oxidize sulfur can only perform this metabolic reaction with an organic substate (Johnson and Roberto, 1997). Additionally, *A. cryptum* has been reported to use ferric iron for respiration (Bilgin et al., 2004). Baker and Banfield (2003) states that fixed carbon is present in low abundance within subsurface mine waste materials and, as such microorganisms within communities rely on specific metabolic products. For example, organoheterotrophs use fixed carbon produced by lithoautotrophs, which oxidize ferrous iron and sulfur for energy. The examination and analysis of

microbial communities is therefore necessary, in addition to merely analyzing microorganisms of interest.

4.0 Objectives

The objectives of Chapter 1 are to characterize and describe the geochemical and mineralogical compositions, in addition to the microbial community compositions of sulfur-bearing tailings material, to develop further understanding of the biogeochemical processes occurring both at surface, and down a depth profile. Mineralogical, geochemical and microbial community compositions will be linked using multivariate statistical analyses, with microbial indicators of mineral modification identified to improve metrics and resolution between mineralogy, geochemical and microbial relationships within sulfidic tailings material.

5.0 Methods

5.1 Study area

Silt-sand sized tailings material produced by the processing of Cu-Ni-Fe sulfides and platinum group minerals define the composition of the material deposited within the study area in Sudbury, ON. Sulfidic tailings material analyzed within this study were collected from five tailings dams, that differ in age of construction and occur in different locations across the study area.

5.2 Sampling and storage

A total of 41 tailings samples were collected aseptically from five vertical profiles through various depths (ranging from 1-50 ft) of tailings dam structures in Sudbury, ON. The collected tailings samples were selected based on differing colour, moisture content, depth, pH and ORP, in order

to obtain a wide variety of tailings material. Samples were collected with a steel scoopula, that was sterilized with 70% ethanol after each use to minimize cross-contamination. Samples were stored in a sterile 50mL falcon tube or sterile Whirl-pack® sampling bags and stored in a cooler with freezer packs, maintaining 4°C temperature, until arrival at the laboratory (<10 h upon sample collection). Tailings samples used for DNA extraction and isolation were stored in a freezer at -20°C, and samples used for mineralogical and geochemical characterization were stored at room temperature.

5.3 Field measurements

A waterproof and portable HANNAH meter was utilized to measure the pH, ORP (mV), conductivity (EC) and total dissolved solids (ppt), with a 1:2 soil to water ratio. The probe was calibrated with pH 4 and 7 buffer solution, and was rinsed and wiped with a Kimtech wipe in between samples.

5.4 Analytical techniques

5.4.1 DNA extractions and computational biology

Prior to DNA extractions, samples were washed with 3 volumes of phosphate buffer solution. Genomic DNA of the total microbial community within samples were extracted from cells pelleted from 0.25 g of tailings material, using the MO BIO PowerSoil DNA Isolation Kit (MoBio, Carlsbad Springs, USA), following manufacture protocols, with an additional 10 min initial heating period at 55°C. Duplicates of extracted genomic DNA were pooled and quantified using a Take3 spectrophotometry system on a Synergy HI microplate reader (BioTek, Winooski VT, USA).

Extracted genomic DNA was amplified by PCR in triplicate to reduce PCR bias. 25uL PCR reaction mixtures were prepared with the following: 5 μL of standard OneTaq buffer (5x),0.25 μL of 25mM dNTP, 0.5 μL of both the forward and reverse primers, 1 μL BSA (12 mg/ml), 0.125 μL of OneTaq DNA polymerase (New England Bio, MA, U.S.A.), and 1-10 ng DNA and water to equal a total reaction volume of 25 μL. PCR reactions were conducted with the following parameters: Initial denaturation at 95°C for a duration of 5 minutes, 35 cycles of denaturation at 68°C for 30 seconds, annealing period at 53°C for 16s for 45 seconds, extension period at 68°C for 1 min, and a final extension step at 72°C for 10 minutes. PCR products were verified by gel electrophoresis on a 2% agarose gel.

Confirmed DNA samples were sent for sequencing at Metagenom Bio Inc. (Toronto, Canada) for the bacterial 16s rRNA gene, using primers (5'-CCT ACG GGN BGC ASC AG-3') and Pro805R (5'-GAC TAC NVG GGT ATC TAA TCC-3) (Takahashi et al., 2014), on an Illumina MiSeq system (Illumina Biotechnology Co., San Diego, USA). DNA libraries were prepared using in-house protocols. Prior to cluster generation and sequencing, DNA samples were denatured and diluted with 0.2 N NaOH and hybridization buffer, respectively. Subsequently, samples were heat denatured. Sequencing template included denatured and diluted amplicon library and PhiX control, which were combined and heated at 96°C for 2 min, prior to loading onto MiSeq v3 reagent cartridge.

Raw Miseq reads were merged and preliminary quality processing was performed with PANDAseq for the 16S rRNA gene reads (Stamatakis et al., 2014). Supplementary quality filtering was performed using USEARCH v9.0.2132, and taxonomy was assigned using QIIME with the Green Genes (Version 1.5.3) database (DeSantis et al., 2006). Data was imported and analyzed in R using the phyloseq package (R Core Team, 2016; Holmes, 2013).

5.4.2 Inductively coupled plasma mass spectrometry (ICP-MS)

Elemental concentrations within the solid tailings material were analyzed by inductively coupled plasma mass spectrometry (ICP-MS) at a commercial lab (ALS Minerals, Vancouver, British Columbia, Canada). Quality assurance and control includes duplicate analysis, certified reference material data, procedural and calibration blanks, matrix matched standards and internal standards. Table 2 includes selected elemental concentrations of samples, expressed as mg/kg^{-1}.

5.4.3 Total ferrous iron and sulfide sulfur analysis

Total ferrous iron was determined by titration at a commercial lab (ALS minerals, Vancouver, British Columbia, Canada). Total sulfide sulfur was determined by infrared detection using a LECO analyzer, after leaching sulfate within samples with HCL (25%) at the commercial lab, ALS minerals (Vancouver, British Columbia, Canada). Sample replicates, blanks, and internal reference standards are used as part of quality control.

5.4.4 X-ray diffraction (XRD), scanning electron microscopy (SEM)

Powdered samples were prepared by crushing solid tailings material with an agate motor and pestle. The samples were measured with a Phillips PW 1729 X-ray diffractometer, using Co Kα (1.79Å) radiation, and operating at 40 kV and 30 mA. Diffraction patters were collected over a scan range of 10-60° with a step size of 0.02°2θ and dwell times of 4 seconds per step.

Samples for scanning electron microscopy (SEM) were prepared through gentle crushing of grain aggregates with an agate motor and pestle. The samples were embedded into epoxy and polished before their examination with an optical and a scanning electron microscope. Scanning Electron

Microscopy was conducted with a JEOL 6400 at 20 kV using detectors for backscattered (BSE) and secondary electrons (SE) detectors as well as an energy dispersive X-ray spectrometer (EDS).

5.5 Statistical analysis

Multivariate statistical analysis was conducted in R software (version 1.0.136) and included non-metric multidimensional scaling, redundancy analysis and an indicator species analysis. All Figures were prepared in R software (version 1.0.136), with the ggplot package.

5.5.1 Non-metric multidimensional scaling

Non-metric multidimensional scaling analysis (NMDS) was performed using the metaMDS and adonis function of the vegan package in R software (version 1.0.136). The absolute abundance of microbial data (OTUs) was log transformed and subjected to the Bray-Curtis dissimilarity calculation, with 300 iterations. Within the NMDS plots, points represent the microbial community composition of a sample within reduced 3D multidimensional space. The distance between two points (two samples) represents the difference between the two microbial community compositions of the two samples.

5.5.2 Redundancy analysis

A redundancy analysis (RDA) was performed using the dbrda function of the vegan package in R software (version 1.0.136). The absolute abundance of microbial data (OTUs) was log transformed and the significance of all canonical axes (n=6) were tested. Additionally, a mantel test was performed using the mantel function of the ade4 package in R software (version 1.0.136).

5.5.3 Indicator species analysis

An indicator species analysis was performed in R software (version 1.0.136), using the randomforest packages (version 4.6-12), with important OTUs (indicators) extracted with the importance function (Liaw and Weiner, 2002).

6.0 Results

A summary of the key results is presented below with supplemental data provided in Appendix 1.

6.1 Bulk mineralogical composition of drill core samples

The analyzed tailings material indicates various alteration zones (Figure 1). These alteration zones are grouped into three categories, which can be distinguished by colour, pH, and mineralogical composition. The mineralogical composition of the tailings material was analyzed and identified using optical examination, XRD, and SEM. Table 1 presents the colour, pH and mineralogy of the three alteration zones. All three alteration zones observed contain similar proportions of silt to sand size unconsolidated sediments. In this study, the oxidized zone is defined as a zone that contains primary silicates and secondary sulfates and oxides. The transition zone is defined as a zone that contains primary silicates, secondary sulfates and oxides, and primary and/or secondary sulfides. The unoxidized zone is define as a zone that contains primary silicates and sulfides, as analyzed by XRD. Trace iron sulfates (i.e: jarosite) has been detected select samples within the unoxidized zone by SEM, but as it is present in such low abundance (<5 %), it has not been detected by XRD.

6.1.1 Tailings material in the oxidized zone

The colour of the oxidized tailings material ranges from light yellow to dark brown (Munsell colours found in Table 1), with the contact pH values ranging from 2.6 - 4.5. The oxidized tailings material is dominantly composed of silicates and secondary mineral phases, including sulfates and oxides (Figure 2). Sulfate minerals present across oxidized tailings material include gypsum ($CaSO_4 \cdot 2H_2O$), jarosite ($KFe_3(SO_4)_2(OH)_6$), goethite (α-FeO(OH)), and schwertmannite ($Fe_8O_8(OH)_6SO_4$). Hematite (Fe_2O_3), is the dominant oxide in the oxidized tailings material (Table 1). In SEM images, secondary minerals, including iron (hydr)oxides and iron sulfate hydroxide minerals occur in alteration rims, coating primary silicate grains (Figure 5 and 6). Additionally, no sulfides were identified with XRD and SEM across all samples characterized as material from the oxidized zone.

6.1.2 Tailings material in the transition zone

The colour of the tailings material in the transition zone between oxidized and unoxidized zone ranges from light brown to black (Munsell colours found in Table 1), with a contact pH ranging from 3.6 - 5.31. The corresponding tailings material is dominantly composed of silicates, with secondary sulfates and/or (hydr)oxides as well as primary and perhaps secondary sulfide minerals (Figure 3). Sulfate mineral phases present in the transition zone include gypsum ($CaSO_4$), jarosite ($KFe3(SO_4)_2(OH)_6$), and bloedite ($Na_2Mg(SO_4)2 \cdot 4H_2O$). Oxide minerals present in the transition zone include wüstite (FeO), ferrihydrite (Ferric iron10O14(OH)2), hematite (Fe_2O_3) and bernalite ($Fe(OH)3 \cdot nH_2O$). Identified sulfide minerals include pyrite (FeS2), marcasite (FeS_2), smythite ($(Fe,Ni)^{3+}xS4$), chalcopyrite ($CuFeS_2$), covellite (CuS), chalcocite (Cu_2S), talnakhite ($Cu_9(Fe,Ni)_8S_{16}$) and violarite ($FeNi_2S_4$) (Table 1). In SEM images, secondary iron sulfate and iron-(hydr)oxide minerals occur as nano-crystalline rims, coating primary sulfide grains (Figure

7). Secondary iron-(hydr)oxide minerals also occur as isolated precipitates (Figure 8A). Sulfides embedded within silicate grains (Figure 8B) are not coated by secondary phases, and therefore have not been exposed to pore solutions.

6.1.3 Tailings material in the unoxidized zone

The colour of the tailings material in the unoxidized zone ranges from dark brown to black (Munsell colours found in Table 1), with the greater contact pH values ranging from 4.14 - 5.71. The unoxidized zone is dominantly composed of silicates and sulfides but does not contain secondary sulfate and/or oxide minerals (Figure 4) as detected by XRD. Sulfide mineral phases in the unoxidized zone include pyrrhotite (Fe_7S_8), pyrite (FeS_2), marcasite (FeS_2), chalcocite (Cu_2S), talnakhite ($Cu_9(Fe,Ni)_8S_{16}$) and chalcopyrite ($CuFeS_2$). The mineralogical compositions of the unoxidized zones are listed in Table 1. SEM images indicate sulfide grains embedded in silicates (Figure 9) and trace secondary iron-hydroxysulfate minerals, such as jarosite (Figure 10).

6.2 Bulk chemical composition of drill core samples

Samples within alteration zones (oxidized, transition and unoxidized) do not exhibit distinct concentrations of total iron (%), total sulfur (%), Ni (ppm) and Cu (ppm), as seen in Table 2. However, average total Ni (ppm) content is lower in samples within the oxidized zone, measured at 415 ppm, in comparison to samples from the transition and unoxidized zone measured at 1069 ppm and 1309 ppm, respectively. Average ferrous iron (%) concentrations exhibit an increase and ferric iron (%) concentrations exhibit a decrease within samples from the oxidized to unoxidized zone. Average concentrations of sulfur as sulfide and oxidized sulfur species exhibit a small increase from oxidized to unoxidized zones. Increase in oxidized sulfur species within samples from oxidized to unoxidized zones is unexpected. Average iron ratios (ferrous iron/ferric iron)

exhibit an increase and sulfur ratios (oxidized sulfur species/sulfur as sulfide) exhibit a decrease within sample samples from the oxidized to unoxidized zone. Additionally, the depth of which the samples were collected from does not exhibit lower and/or greater concentrations of the aforementioned geochemical parameters.

6.3 General microbial composition across all drill core samples

Genomic DNA was extracted and isolated from the collected tailings material, with bacterial diversity based on 16S rRNA gene sequence abundance and classified as relative percent abundance by taxonomic rank: phylum, class, order, family, genus and species. Microbial data was filtered in order to remove singletons and doubletons, and low abundance microorganisms from community analysis, resulting with a total of 833 classified OTUs with a relative abundance of >1%, across 41 samples and 5 locations.

Occurrence of putative iron and/or sulfur metabolizing microorganisms were described within all three alteration zones with relative proportions illustrated in Figure 11. Tailings material collected from the five different tailings dam structures contain similar distributions of OTU at the phylum level. However, relative abundance of specific orders/genera exhibit extensive variability across the identified alteration zones (figure 11, figure 12). OTUs identified as putative iron and/or sulfur oxidizing microorganisms include members of the order Acidithiobacillales, Nitrospirales, Bacillales (Alicyclobacillaceae), Hydrogenophilales, Thermogemmatisporales and the archaeal order Thermoplasmatales. Although these microbial members are present at various depths across all three alteration zones, they are observed in the highest abundance within ranges of 1 - 20 ft. Some iron and/or sulfur oxidizing and/or reducing species are present at greater depths within transitional tailings material, such as sample D7 from 38 - 39 ft, which exhibits an abundance of Bacillales (Figure 11). OTUs identified as putative iron and/or sulfur reducing microorganisms

include members of the order Desulfuromonadales, Ignavibacteriales (Melioribacteraceae), Anaerolineales, Desulfobacterales, Natranaerobiales, Syntrophobacterales and Dehalococcoidales. These microbial members were present at various depths. With the exception of Melioribacteraceae, the listed taxa were present across all three alteration zones as well, however, the highest abundance was observed at greater depths in the profile (36 ft and 45 ft), within unoxidized material. Three microbial members have been identified that have the capability of both oxidizing and/or reducing iron and/or sulfur, including Acidimicrobiales, Clostridiales and Bacillales.

As figure 12 exhibits, OTUs identified as microorganisms which underpin iron and/or sulfur oxidation exhibit higher abundance in tailings material from the oxidized zone in comparison to tailings material from the transition and unoxidized zone. Contrarily, OTUs which identify as microorganisms which underpin ferric iron and/or sulfate reduction exhibit greater abundance in tailings material from the unoxidized zone in comparison to tailings material from the oxidized and transition zone. OTUs identified as microorganisms that may oxidize iron and/or sulfur species, in addition to reducing ferric iron and/or sulfate, exhibit variability across tailings material across the three alteration zones (oxidized, transition, and unoxidized).

6.3.1 Microbial composition in the oxidized zone

Percent relative abundance of the taxonomic composition at the order level for microbial communities in the oxidized zone are presented in Figure 13. The oxidized zone has a high abundance of the Acidithiobacillales (*Acidithiobacillus* at genus level), specifically within samples C4 and D4 which have contact pH values of 2.8 and 3.4, respectively. The strict chemolithoautotroph, Nitrospirales (order level) identified as *Leptospirillium* spp., is present in abundance (8 – 25 % (relative abundance)) within samples K5, M6, and M7, with contact pH

values ranging from 2.6 - 3.6. Thermogemmatisporales (order level), identified as *Thermogymnomonas* spp., is present at 5 % relative abundance within sample A3, at contact pH of 3.9. Bacillales (order level), identified as Alicyclobacillaceae (family level), is only present in low abundance within sample C4, across all oxidized tailings materials. Ignavibacteriales (order level), identified as Ignavibacteriaceae (family level), a chemoheterotrophic bacterium, is present in low abundance within sample K3, with the highest pH value observed within oxidized tailings material at contact pH of 4.4. Hydrogennophilales (order level), identified as Hydrogenophilaceae (family level), is present in low abundance within sample C3, with a contact pH value of 4.3.

Syntrophobacterales (order level), identified as Syntrophobacteraceae (family level) is present across 9 OTUs in two oxidized zones. However, only 1 OTU has been identified at the genus level, this includes *Desulfobacca* spp., a sulfate reducer. This sulfate reducer is present at 8% relative abundance in the samples A1 and A2, and at contact pH values of 4.0 and 3.8 respectively. It is also present in sample D2 in lower abundance with 1.5 % relative abundance, at a contact pH value of 4.1.

6.3.2 Microbial composition across transitional tailings material

Percent relative abundance of the taxonomic composition at the order level for microbial communities in tailings material from the transition zone are listed in Figure 14. Acidithiobacillales (order level), identified Acidithiobacillus, at genus level is present in low abundance in the transition zone, excluding samples C1, D5 and D6, contrary to the oxidized zone. Environmental parameters are relatively uniform across these three samples, with pH values between 4.1 - 4.7 and similar mineralogical composition. Nitrospirales OTUs are represented by numerous taxa, including *Leptospirillum*, Thermodesulfovibrionaceae, Nitrospira and candidate genus 4 - 29. Nitrospirales are present across various transitional samples, with *Leptosprillum* sp.

in the highest abundance within sample M2 (22.2 % relative abundance). Within sample D6, 31.5 % relative abundance of Thermodesulfovibrionaceae is present. Sample M8 contains 12 % relative abundance of the genus 4-29. Sample K7 contains an overall relative abundance of approximately 5 %, with *Leptosprillum* sp. representing 3.2 %, and Nitrospira at 0.9 % and Thermodesulfovibrionaceae at 0.9 %. Nitrospirales occurs in lower abundance within samples samples A7, C6, and C9 (2 – 4 % relative abundance). Thermoplasmatales OTUs identified as BSLdp215 (sequence found in deep sea), is present only within sample A4. Thermogemmatisporales OTUs are, identified as *Thermogymnomonas* spp., is present only in samples C1 and C9. OTUs belonging to a sulfur oxidizer, identified as Thiobacteraceae, are present in low abundance in sample C2.

Similar to the oxidized zone, the transition zone does not exhibit a high abundance of iron and/or sulfur reducing microorganisms, with the exception of sample D6. Samples A4 and C7 contain a low abundance (2.6 – 2.9 % relative abundance) of OTUs from the Clostridiales, identified as *Desulfosporosinus meridiei*, an anaerobic sulfate reducing bacterium. Sample D6, however, contains a higher abundance of *D. meridiei*, containing 7.85 % relative abundance.

6.3.4 Microbial composition in the unoxidized zone

Percent relative abundance of the taxonomic composition at the order level for microbial communities in the unoxidized zone is presented in Figure 15. Six of the unoxidized tailings samples contain iron and/or sulfur oxidizing microorganisms. Notably, three samples, including samples D7, K6 and M9, contain OTUS belonging to iron and/or sulfur oxidizing microorganisms. The pH values of samples D7, K6 and M9 are not lower than other observed pH values of tailings material from the unoxidized zone and are at pH = 5.0, 4.9, and 5.7, respectively. Sample D7, contains abundant OTUs, measured at 67 % relative abundance and have been identified as

Alicyclobacillus sp., a ferrous iron- and sulfur-oxidizing and ferric iron-reducing bacterium. Sample K6 contains OTUs belonging to Hydrogenophiales, identified as *Thiobacillus* sp., at 2 % relative abundance. Also in low abundance (1.6 %), OTUs belong to Acidimicrobiales, is present within sample K6. OTUs belonging to Acidimicrobiales are more abundant within sample M9, as they are present at 28.7 % relative abundance.

The tailings material within the unoxidized zone contains a more diverse community of iron and/or sulfur reducing microorganisms in relation to tailings material from the transition and oxidized zones. Two of the 9 unoxidized tailings samples contain a wide variety of iron and/or sulfur reducing microorganisms, including samples A5 and C8, as seen in Figure 11. Sample A5, with a contact pH value of 5.3, exhibits a variety of OTUs belonging to putative iron and/or sulfur reducing microorganisms, including Anearolineales (relative abundance of 8.9 %), Desulfobacterales (3.4 %), Dehalococcoidales (1.2 %), Desulfuromondales (1.6 %) and Syntrophobacterales (3.48 %). Sample C8 contains similar OTUs, in differing relative abundance, including Anaerolineales (11.4 %), Desulfuromonodales (2.1 %), Desulfobacterales (1.6 %), Thermodesulfovibrionaceae (3.45 %), Natronaerobiales (1.4 %) and Syntrophobacterales (3.7 %).

Samples A10, K4, and M3, with respective contact pH values of 4.1, 4.5 and 4.3, exhibit fewer OTUs belonging to iron and/or sulfur reducing taxa. Sample A10 contains 1.8 % relative abundance of OTUs belonging to Acidithiobacillales. Similarly, sample M3 contains OTUs belonging to one taxa, although they belong to Clostridiales, measured at 7.6 % relative abundance. Lastly, sample K4 contains OTUs belonging to Acidimicrobiales, Bacillales and Clostridiales, with a sum of 7.4 % relative abundance.

6.4 Multivariate Statistical analysis

6.4.1 Non-metric multidimensional scaling analysis

A non-metric multidimensional scaling analysis (NMDS), using the metaMDS and adonis function of the vegan package in R software (version 1.0.136), has been used to evaluate the significance of how numerous environmental parameters may control microbial community groupings in samples of the oxidized, transition and unoxidized zones. The absolute abundance of microbial data (OTUs) was log transformed and subjected to the Bray-Curtis dissimilarity calculation, with 300 iterations. Quality of ordination is indicated by a stress value of 0.16, which represents reduced dimensions.

There are no microbial groupings against the following parameters and/or variables; tailings dam location, pH, total iron (%), total sulfur (%), Ni (ppm), Cu (ppm), ferrous iron (%), iron ratios, sulfur as sulfide (%), and oxidized sulfur species (%), within NMDS ordinations (Figures 17 - 25), indicating that location and increasing and/or decreasing values in the listed parameters do not drive changes in microbial community compositions of the 41 tailings samples. Higher ferric iron (%) content and sulfur ratios (sulfate/sulfur as sulfide) do, however, exhibit weak groupings within some of the samples of the oxidized and transition zones (Figure 26 and 27). This suggests that increasing ferric iron content and sulfur ratios may be more strongly correlated with particular tailings microbial communities.

A much stronger correlation within microbial communities across the 41 tailings samples is observed upon grouping variables according to alteration zone, contact pH and the colour the tailings material (Figure 28). Samples of the oxidized zone grouped to the left along NMDS1, samples of the unoxidized zone grouped to the right along NMDS1, and samples of the transition zone exhibit microbial community compositions overlapping the area for the samples of the

oxidized zone, although still separate from the area for the samples of the unoxidized zone. The three zones (oxidized, transition and unoxidized) within this NMDS plot are treated against each other for pairwise comparisons by Adonis, resulting in significant differences between microbial community compositions within the oxidized and unoxidized zones ($F = 6.6885$, $p = 0.001$) and between the transition and unoxidized zones ($F = 4.0498$, $p = 0.001$).

6.4.2 Redundancy analysis (RDA)

A redundancy analysis (RDA) has been used to evaluate relationships between microbial community compositions and environmental variables and/or field parameters across samples. The absolute abundance of microbial data (OTUs) is log transformed and the significance of all canonical axes (n=6) are tested. Additionally, a Mantel test has been performed to determine correlations between samples partition based on OTU (Bray distance) with environmental variables and field parameters (Euclidean distance).

The microbial community compositions of each sample analyzed against the following six geochemical parameters, ferrous iron, ferric iron, sulfur ratio, iron ratio, pH, and Eh, results with a cumulative proportion of variance of 23.9 % (Figure 29, Table 3, Table 4). This cumulative proportion of variance explained suggests that the given geochemical parameters play a minor role in structuring the microbial community assemblages and distributions across the given samples. Notably, pH and ORP exhibit the strongest loadings, as they explain 9.9 % of the cumulative proportion (Table 3, Table 4). However, the mantel test confirmed no correlations between OTUs and the six geochemical and environmental parameters inputted within the RDA, including ferrous iron, ferric iron, sulfur ratio, iron ratio, pH, and Eh ($r=0.0878$, $p=0.122$). Therefore, the low cumulative proportion explained in addition to low r and p values from the mantel test suggests

that environmental and geochemical parameters are not strongly linked to OTUs, and thus do not explain patterns of microbial community assemblages.

6.4.3 Indicator species analysis

Microbial community compositions significantly differ between samples of the oxidized, transition and unoxidized zone. Within each of the three alteration zones, microbial community compositions are variable. An indicator species analysis was performed to identify the dominant OTUs that characterize each alteration zone. This analysis generates a model aimed at classifying the samples into groups using randomly generated trees. Samples were grouped based on alteration zones (oxidized, transition and unoxidized) and 1000 randomly generated trees were used. The model assigns an indicator value (mean decrease GINI) to every OTU, which indicates the OTUs importance within the classified groups (oxidized, transition and unoxidized). OTUs with greater GINI index represent prominent predictors of the model and indicator species for each zone can be found in Figure 30, along with their relative abundance. Figure 30 shows that an OTU identified as Acidimicrobiales, is characteristic of tailings material within the oxidized zone. Samples in the transition zone contain the indicator species Alicyclobacillaceae, another ferrous- and sulfur-oxidizing bacterium, whereas samples in the unoxidized zone contain the indicator species *Desulfosporosinus* sp. (Figure 30).

7.0 Discussion

Microbial community compositions and structures are often associated to their surrounding geochemical environments (Singh, 1997; Konhauser, 2007). Within this study, no significant correlations are observed and calculated between total metals content and microbial community compositions. However, microbial community compositions are differentiated between tailings

material from the oxidized and unoxidized zone, of which contain differing mineralogical compositions. This discussion addresses the relationships between the geochemical and mineralogical composition of the three alteration zones, and their key microbial members.

7.1 Project approach; analyzing mineralogical, geochemical and microbial data

Jamieson (2011) suggests that risks associated with mine wastes are established in the materials geochemical and mineralogical compositions. Risks include acidic drainage characterized by abundant sulfate and metal contamination and contaminated neutral and/or alkaline drainage comprising toxic elements (Jamieson, 2011). Accurate geochemical and mineralogical analyses of these materials is crucial when examining mine waste environments. However, a key component within these environments, the microbiota, should not be omitted, as the mineralogy, geochemistry and microbiology of these systems are all interconnected. Improved resolution on the proceeding biogeochemical processes may thus be attained by evaluating and interpreting the mineralogy, geochemistry and microbiology of these materials.

7.2 Bulk mineralogical composition of tailings materials

The analyzed tailings materials are physically grouped into the three alteration zones (1) oxidized, (2) transition and (3) unoxidized. These three zones have distinct mineralogical compositions, which display different degrees of weathering, ranging from sulfides in the unoxidized zone to zones predominantly composed of ferric iron oxides (oxidized zone). Lottermoser (2010) categorized minerals in tailings into the following four groups (1) primary ore and gangue minerals; (2) secondary minerals that form through weathering; (3) chemical precipitates formed during and post mineral processing; and (4) chemical precipitates that form post disposal. Minerals present within the analyzed tailings material in this study belong to the groups (1), (2) and (4).

Primary ore minerals include sulfides, such as pyrite, marcasite, smythite, chalcopyrite, covellite, violarite, chalcocite, talnakhite and pyrrhotite. Primary gangue minerals include silicates, such as quartz, clinochlore, albite, magnesiohornblende, biotite, among others. Secondary minerals include gypsum, jarosite, schwerttmanite, ferrihydrite, hematite, wuestite and bernalite.

7.2.1 Mineralogical features of tailings material in the oxidized zone

The tailings material in the oxidized zone is dominantly composed of silicates and secondary mineral phases, including sulfates and oxides. The presence of secondary sulfates and oxides formed from the weathering of sulfide minerals and the absence of sulfide minerals within this alteration zone suggests that the majority of the sulfide grains were dissolved, presumably through a combination of abiotic and biotic oxidation processes (Jamieson, 2011; Lindsay et al., 2015).

7.2.2 Mineralogical features of tailings material in the transition zone

The material in the transition zone is dominantly composed of silicates, with both secondary sulfates and/or oxides and sulfides. The presence of these minerals suggests that either the sulfide minerals have not been completely dissolved under oxidizing conditions or re-precipitated through an increase in abiotic and biotic reduction of sulfate minerals under reducing conditions. For example, SEM images of a selected sample from the transition zone shows the occurrence of altered sulfides with secondary coatings, as depicted in Figure 7, whereby iron-(hydr)oxide is coating an altered pentlandite grain. Dissolution features on the pentlandite grains, such as rod shaped etching features, suggest that the mineral grain has been partly altered by abiotic and biotic dissolution processes. Secondary minerals, such as iron-oxyhydroxides and sulfate minerals, form from the weathering of sulfide minerals within sulfidic mine wastes (Jamieson, 2011). Within mine tailings, sulfide minerals previously exposed to oxygen-rich pore solutions are commonly coated

by secondary minerals, forming an amorphous and/or nano-crystalline rim, which limit O_2 diffusion to the sulfide surface (Paktunc et al., 2004; Lindsay et al., 2015). Limited O_2 diffusion and thus minimum alteration of the sulfide grain occurs also when sulfide grains are encapsulated in silicates as depicted in Figure 8B, for the occurrence of unaltered chalcopyrite grains within an amphibole grain is present.

7.2.3 Mineralogical features of tailings material in the unoxidized zone

The tailings material in the unoxidized zone is dominantly composed of silicates, with the presence of sulfides and no secondary sulfate and/or oxide minerals present in XRD data. However, trace secondary phases, such as iron-hydroxysulfates (i.e: jarosite), have been observed with SEM. This suggests that jarosite occurs in low abundance (<5%), and therefore is not present within XRD data. Additionally, any secondary sulfate and/or oxide mineral phases that contain short range ordered crystallography will not be detected by XRD and thus samples must be analyzed with SEM in conjunction with XRD analysis. The occurrence of jarosite in low abundance suggests that the analyzed unoxidized tailings material had been exposed to oxidizing conditions, as the precipitation of jarosite is common occur post sulfide oxidation (Jambor and Dutrizac, 2000). As seen in Figure 9, chalcopyrite grains occur disseminated, although incorporated within an amphibole grain. Encapsulation of the sulfide grains within the amphibole suggests that the observed sulfides have not been altered, as the coating amphibole would limit O_2 diffusion, and thereby restrict oxidative dissolution reactions.

7.3 Microbial community structure, diversity and groupings across alteration zones

Sulfidic mine tailings harbour a population of chemolithotrophic microorganisms, within both oxic and anoxic zones. Undeterred by high metal concentrations and low pH, these microorganisms

interact with minerals and catalyze the oxidation of metal-bearing sulfides and reduction of ferric ions and sulfate in dissolved and/or solid states (Lottermoser, 2010). Studies within the last few decades, particularly DNA-based studies, have provided further insights on the microbial community complexes within sulfidic mine waste environments (Baker and Banfield, 2003; Lindsay et al., 2009; Garcia et al., 2015; Li et al., 2016; Gupta et al., 2017). The microbial diversity within these environments is not as complex as soil environments, however, a significant portion of these communities are comprised of poorly characterized species (Baker and Banfield, 2003).

7.3.1 Iron and/or sulfur oxidizers

OTUs belonging to microorganisms that contain metabolisms which underpin iron and/or sulfur oxidation are often present and more abundant within tailings material from the oxidized and transition zone, than in tailings material from the unoxidized zone. These microorganisms include members of the following orders: Acidithiobacillales, Nitrospirales, Bacillales (Alicyclobacillaceae), Hydrogenophilales, Thermogemmatisporales and the archaeal order Thermoplasmatales. However, this is not always the case, as other microorganisms that also contain metabolic activity based on iron and/or sulfur oxidation, are sometimes present within tailings material from the unoxidized zone.

Alicyclobacillaceae has been identified in high abundance within the unoxidized sample D7 and in low abundance within the unoxidized samples A5, D8, K4 and K6. This family of microorganisms contains genera of novel iron and sulfur oxidizing microorganisms, many of whom have been shown to grow on ferrous iron-bearing mineral substrates (CY, 2008; X et al 2009; Stackebrandt, 2014). The family Alicyclobacillaceae contains the genera *Alicyclobacillus*, *Tumebacillus* and *Kyrpidia* spp. (Stackebrandt, 2014). Two OTUs which identified as *Alicyclobacillu*s are present at 2.2 % relative abundance within sample A7. The genera within the

remaining listed tailings samples in the unoxidized zone could not be identified with certainty. Nonetheless, *Alicyclobacillus* spp. are mostly chemoautotrophs, gaining energy by the oxidation of inorganic compounds such as ferrous iron and elemental sulfur (Guo et al., 2009). However, the Alicyclobacillus sp. can also gain energy by the reduction of ferric iron (Korehi et al., 2013). The genera *Tumebacillus* also has the ability to oxidize sulfur for growth (Sukla et al., 2015). Contrarily, *Kyrpidia* sp. have not been proven to utilize iron and/or sulfur as an energy source. The acidophilic facultative anaerobe, *Kyrpidia* sp., is understood to use H_2 as an electron donor and CO_2 as a carbon source for energy fixation (Klenk et al., 2011; Stackebrandt, 2014). As the unoxidized sample D7 contains lower values than average and the median of total iron (%), total sulfur (%), ferrous iron, ferric iron, sulfide sulfur (%), oxidized sulfur species (%), iron ratios and sulfur ratios, within samples from the unoxidized zone, it is unknown as to why there is a high abundance of Alicyclobacillaceae present. This occurrence may be due to pore water chemistry within the sample being supersaturated with respect to ferrous iron, ferric iron and/or sulfate, as microorganisms can utilize free ions for metabolism (Konhauser, 2007). The low abundance of Alicyclobacillaceae present within the unoxidized samples A5, D8, K4 and K6 may be present due similar reasons as sample D7, or the cells may have been dormant or no longer viable, and were still analyzed via extraction methods (Cangelosi, 2014). The unoxidized sample A5 also contains aerobic *Bacillus muralis*. There is currently a lack of information available on *B. muralis*, and as such, iron and/or sulfur metabolic capabilities are unknown (Wang et al., 2016). Unoxidized samples D8, K4 and K6 contain other members of Bacillales as well, including Paenibacillaceae, *Staphylococcus* spp. and other Bacillaceae (> 1% relative abundance). These listed taxa have commonly been detected in soil environments (Xie and Yokota, 2007; Lee, 2016; Wong and Bergdoll, 2003; Mulec et al., 2016) and do not contain metabolic activity linked to iron and/or sulfur cycling.

As stated, OTUs that belong to organisms related to iron and/or sulfur cycling that are present and more abundant within tailings material in the oxidized and transition zone include Thermoplasmatales, Nitrospirales, Acidithiobacillales and Acidimicrobiales. The archaeal order Thermoplasmatales, is not present within any unoxidized tailings samples. This group hosts the most extreme acidophiles known (Castelle, 2015). Thermoplasmatales includes members that oxidize ferrous iron, such as *Ferroplasma acidiphilum*, a microorganism which thrives in iron saturated environments, such as acid mine drainage (Castelle, 2015). The absence of microorganisms within tailings material from the unoxidized zone belonging to Thermoplasmatales may be due to higher contact pH ranges, as members within this family grow at pH values below 4. For example, the genus *Picrophilus* grows at pH values of 0.5 and the microorganism *Thermoplasma acidophilum* is optimal at pH values between 1 and 2 (Siddiqui and Thomas, 2008). Both members belong to Thermoplasmatales. Additionally, the mineralogical composition of the material lacks or contains trace amounts of sources of ferrous iron within minerals that are kinetically favourable for oxidative dissolution. Nitrospirales also contains members that oxidize ferrous iron, such as the iron-oxidizing bacterium, *Leptospirillum* sp., which fix energy exclusively via the oxidation of ferrous iron, and often directly oxidize ferrous iron directly by attaching to ferrous iron-bearing mineral substrate (i.e: a sulfide mineral, such as pyrite) (Konhauser, 2007; Johnson, 2015). In fact, their survival relies on being able to attach to specific sites on the mineral surface (Konhauser, 2007). Although present and abundant across oxidized and transitional tailings material, Nitrospirales, is still present within three unoxidized tailings samples, including samples C8, K6 and M9. However, in these three unoxidized samples (C8, K6 and M9), Thermodesulfovibrio sp. is detected and is most closely related to anaerobic sulfate reducing microorganisms (Sekiguchi, 2008). The presence of *Thermodesulfovibrio* sp. may be linked to the mineralogical composition of the tailings material in the unoxidized zone, as both the reduction of sulfate and the acidic dissolution of sulfides results in the formation of H_2S which may then form into secondary sulfides, of which are present in the unoxidized zone (Crundwell,

2014). The presence of sulfate within this zone may be attributed to surrounding pore waters. Samples A5 and K6 contain Ignavibacteriales, however, the microorganism has been identified at the family taxonomic level as Melioribacteraceae. This family of microorganisms contains anaerobic members which reduce ferric iron for energy fixation (Podosokorskaya, 2013; Rempfert, 2017). The small presence of Melioribacteraceae may also correspond to the given mineralogical composition of material in the unoxidized zone, as secondary minerals containing ferric iron (i.e: jarosite) are present in trace amounts (< 5 %). The genera Acidithiobacillus is present in very low relative abundance (<2%) within the unoxidized sample A10. This genus includes species that gain energy from the oxidation of both iron and/or sulfur (Konhauser, 2007; Quatrini, 2009; Hallberg et al., 2010). The low abundance of *Acidithiobacillus* present within the unoxidized sample, A10, may be due to extraction methods attaining dormant cells, or those that are no longer viable (Cangelosi, 2014). The low abundance may also be present from ferrous iron being available within the surrounding environment, such as the surrounding pore water. The unoxidized samples A5, C8, K4 contain a low abundance of Acidimicrobiales, and a greater abundance is present within the unoxidized sample M9. Acidimicrobiales has not been identified at a greater taxonomic level within these samples. Genera within this order can oxidize and/or reduce iron and/or sulfur. For example, Aciditerrimonas ferrireducens reduces ferric iron for energy fixation, whereas *Ferrimicrobium acidiphilum* oxidized ferrous iron for energy fixation (Senko et al (2008); Itoh et al (2011)). Further identification of Acidimicrobiales is unknown, and thus the metabolic capabilities of Acidimicrobiales within samples from the unoxidized zone remains unclear.

7.3.2 Iron and/or sulfur reducers

Four of the eight microorganisms that contain metabolic activity that underpin iron and/or sulfur reduction are identified across OTUs strictly within tailings material from the unoxidized zone. These microorganisms include the members of the following families; Desulfuromonadales,

Desulfobacterales, Dehalococcoidales, and Natranaerobiales. Additionally, Anaerolineales is present within unoxidized tailings material, although it is present within one transitional tailings sample, C6. Syntrophobacterales occurs more often within oxidized and transitional material than within unoxidized material. Lastly, members of the Clostridiales also occur in all unoxidized samples with the exception of sample A10, and is frequent across oxidized and transitional tailings material.

OTUs belonging to Pelobacteraceae occurs in low abundance within the unoxidized samples A5, C8 and M9. Pelobacteraceae contains areanaerobic chemoorganotrophic iron-reducing bacteria (Bertrand et al., 2015). Additionally, Castro et al (2000) states that Pelobacteraceae is capable of reducing elemental sulfur. The low abundance of Pelobacteraceae may be due to the small abundance of ferric iron-bearing minerals, of which are kinetically favoured for reductive dissolution (i.e: jarosite). The pH range for growth of ferric iron reducing species within the order Desulfuromonadales range from 6.5-8 (Vandieken et al., 2006; Thuy and Picardal, 2015). The lack of ferric iron reducing members of Desulfuromonadales within tailings material from the oxidized and transition is likely due to the pH, as extremely acidic environments are not suitable for growth. OTUs belonging to Desulfobulbaceae and Desulfobacteraceae occur within the unoxidized samples A5 and C8. Microorganisms within these families are capable of both oxidizing and/or reducing sulfur (Pfeffer et al., 2012; Engelbrektson, 2014).

OTUs belonging to Anaerolineales are present within samples A5, C8, K6 and M9, all from the unoxidized zone. However, they are also present within one tailings sample from the transition zone, sample C6. Sample C6 contains only a small abundance of Anaerolinaceae, at 3 % relative abundance. Within tailings samples from the unoxidized zone, Anaerolineales has been identified as SHD-231, an uncultured clade and the anaerobic Anaerolinaceae (Califf et al., 2017). Currently, strains within Anaerolinaceae do not exhibit ferric iron reduction, however, Kawaichi et al (2013)

states that one strain exhibits the characteristics for ferric iron reduction. As ferric iron-reduction remains unknown across members belonging to Anaerolinearles, their presence, in correspondence to the mineralogical composition of tailings material from the unoxidized zone remains unclear.

Within the order Syntrophobacterales, only two genera are identified, including the sulfate-reducing *Desulfomonile* and *Desulfobacca* spp. (Goker et al., 2011; Elferink et al., 1999). The two genera are identified in low relative abundance (<1%), within tailings material from the oxidized zone. Their low abundance may be due to the aerobic environments within the oxidized zones. The remaining microorganisms, identified as Syntrophobacterales at the order level, have not been identified at the genus level. In addition, the genus level has not been identified within transitional tailings material. Tailings material in the unoxidized zone contain *Desulfobacca* sp., a sulfate reducing microorganism, and exhibit a greater abundance of this microorganism in comparison to tailings materials within the oxidized zone. The greater abundance in sulfate-reducing microorganisms with tailings material from the unoxidized zone suggests that some sulfides present within tailings material from the unoxidized zone have formed at low temperature from the microbial reduction of sulfate to H_2S. Additionally, as the unoxidized zone hosts anaerobic microorganisms, and exhibits only trace secondary minerals formed by oxidation, sulfate may be present from leachate of the upper oxidized layers, pore water and/or groundwater.

7.3.3 Clostridiales across alteration zones

Within the order Clostridiales, many genera (>1% relative abundance) have been identified within unoxidized tailings material. This includes *Sulfobacillus*, and *Desulfurisporosinus* spp. as the most abundant and least abundant include *Pelotomaculum*, *Gracilibacter*, *Oxobacter*, WCHB1-84, *Dehalobacterium* and *Ruminococcus* spp.. The presence of OTUs belonging to Clostridiales within many samples across all three alteration zones (oxidized, transitional and unoxidized) may be a

result of the wide range of metabolic reactions within the Clostridiales order. Within this order, species are capable of oxidizing ferrous iron and/or sulfur compounds and reducing sulfate. For example, *Sulfobacillus* gains energy by oxidizing ferrous iron or sulfur compounds, whereas *Desulfurisporasinus* gains energy by reducing sulfate (Guo et al., 2016; Kaksonen et al., 2007).

Within oxidized tailings material, *Desulfurisporasinus* occurs exclusively within one sample (K3) at >1% relative abundance, and *Sulfobacillus* occurs within all samples at >1% relative abundance. Therefore, within the analyzed tailings material, more genera that oxidize ferrous iron or sulfur compounds as opposed to reducing ferric iron and/or sulfur species are present. This can be expected, as the oxidized tailings material contains mineralogical byproducts of ferrous iron and/or sulfide oxidation. However, sulfides were not detected by XRD analysis, and have likely been exhausted by microbial oxidation. Sulfides may be present in low abundance, or ferrous iron and/or sulfur species may be available within surrounding pore waters.

Within transitional tailings material that contain Clostridiales, the genera *Desulfurisporasinus* and *Sulfobacillus* are consistently present. However, *Desulfurisporasinus* is always in greater abundance than *Sulfobacillus*, with the exception of sample A8, where the relative abundances are 3.8% for both genera. The higher abundance of *Desulfurisporasinus* may be correlated to the mineralogy of the tailings material in the transition zone, as *Desulfurisporasinus* reduces sulfate for energy fixation and sulfate minerals are present. Sulfate may be present in surrounding pore waters as a by-product of microbial oxidation of the present sulfide minerals within tailings material from the transition zone.

Unoxidized tailings material exhibits OTUs belonging to both genera as well. However, *Sulfobacillus* is only present in low abundance (<1%), within the unoxidized samples C8, K6 and M3. *Desulfurisporasinu*s, the novel sulfate-reducing genera, is abundant within all unoxidized

tailings samples. The low abundance of *Sulfobacillus* is to be expected, as unoxidized material does not exhibit secondary iron-(hydr)oxide and/or sulfate minerals and sulfides are still detected, thereby suggesting anoxic conditions whereby microbial ferrous iron and sulfur oxidation is not yet pervasive. More samples exhibit *Sulfobacillu*s within transitional tailings material than unoxidized tailings material. This correlates with the observed mineralogical composition, as transitional tailings material exhibits secondary iron- (hydr)oxide and/or sulfate minerals, as they may form as a byproduct of ferrous iron and/or sulfur oxidation of sulfides by *Sulfobacillus*. The greater abundance of *Desulfurisporasinus* within unoxidized tailings material may be correlated to the presence of sulfides. Therefore, suggesting that not all sulfides may be of primary origin, as some may form through microbially-mediated reactions resulting in the formation of monosulfides, and by the presence of H_2S (from the acidic dissolution of sulfides) chemically reacting with other metals.

7.4 Trends and groupings observed across microbial taxa; linkages between environmental parameters and mineralogical compositions

7.4.1 How location and environmental parameters influenced microbial community compositions across tailings samples

Key microbial taxa influence the precipitation and/or dissolution of various mineralogical phases within acidic and low temperature environments such as sulfidic mine wastes. As discussed in Section 5.4, key iron and sulfur related microorganisms are observed within material where iron and sulfur sources are readily available. That is, they are often present within samples where iron and/or sulfur are present in kinetically favoured mineralogical phases. The location of the sampled tailings material correlates with the materials age, as material within specific locations were deposited earlier. For this reason, it was questioned if the microbial community structure would exhibit shifts in response to location, as the location directly links to materials age. Indeed, it was hypothesized that the age of the material would affect the alteration stage, as with prolonged and/or

more periods of exposure to oxygenated conditions, some minerals would oxidize. Non-metric multidimensional scaling was used to observe ordination patterns in microbial communities across locations, with the assumption that older tailings material may exhibit similar microbial communities. As seen in Figure 16, microbial community structures do not exhibit any groupings and/or trends with sample location. This finding suggests that not all tailings material from one tailings dam exhibits similar alteration stages and environmental conditions, and thus, samples will not host similar microbial communities within the same tailings dam profile.

As previously stated, iron and sulfur related microorganisms can ultimately reconfigure their surrounding environments, by altering pH regimes and/or by precipitating minerals intracellularly and/or extracellularly (Singh, 1997; Konhauser, 2007). It was thus hypothesized that microbial community structures would shift in response to increases and/or decreases in environmental and geochemical parameters. Again, multidimensional scaling was used to evaluate ordination patters in microbial communities across select parameters, including the following: pH, total iron (%), total sulfur (%), total Ni (ppm), total Cu (ppm), ferrous iron (%), iron ratios, sulfur as sulfide (%), and oxidized sulfur species (%).

There were no strong groupings and/or trends observed between microbial community structures and the listed variables. Microbial community structures do not exhibit strong groupings with specific contact pH values. They do however, exhibit weak groupings within ranges of contact pH values. As seen in Figure 28, microbial community structures within unoxidized tailings material group to the right of the NMDS1 axis, where the highest contact pH values are observed, ranging from 4.1 - 5.5. Microbial community structures within oxidized tailings material group to the left of the NMDS1 axis, with pH values ranging from 2.6 - 4.4. Contact pH of transitional tailings span those observed within oxidized and unoxidized materials, with microbial community structures grouping in between. The pH values of samples are thus not distinct amongst alteration zones,

therefore suggesting that contact pH exhibits a weak linkage with microbial community structures. This is in contrary to previous studies, such as Lui et al (2014) and Chen et al (2014), where pH was observed as the primary factor driving microbial community structures within acidic copper-bearing tailings material and simulating pyrite weathering experiments, respectively.

Microbial community structures did not exhibit groupings with total iron (%), total sulfur (%), total Ni (ppm) and total Cu (ppm), perhaps due to the mineralogical origin of these elements, as some of the total element concentrations are incorporated within silicates (Southam and Beveridge, 1992). For example, total iron (%) represents iron from all mineralogical phases, as a 4-acid digestion was utilized. As many iron-bearing silicates are present across samples (i.e: hornblende, actinolite, biotite), an unknown percentage of iron within the total amount is derived from silicates and other gangue mineralogical phases. This suggests that microbial community structures will not link with total metals and/or nonmetals, as total metal concentrations do not link solely to minerals that are kinetically favourable for microbial oxidation and/or reduction. Similar relationships were exhibited by Lui et al (2014), where bulk metal concentrations and microbial community structures did not exhibit any significant correlations. Liu et al (2014) attributed this occurrence to silicates hosting a considerable abundance of metal concentrations, and as previously stated, are not favourable for microbial access.

Lui et al (2014), observed significant correlations between Cu^{2+} and microbial community structures, suggesting that analyzing elemental speciation as a factor explaining microbial community structures may be beneficial. However, elemental speciation (for iron) did not exhibit strong correlations with microbial community structures in this study. The lack of microbial community groupings and/or trends amongst ferrous iron (%) and iron ratios suggests these two geochemical parameters do not influence community structures. This, again, may be due to the source of ferrous iron, as it often occurs within iron-bearing silicates and/or sulfides within the

observed mineralogy. As such, ferrous iron and thereby iron ratios, would not exhibit a large overall influence on microbial community structures, as key iron and/or sulfur related microorganisms do not often exhibit strong linkages with silicate minerals (Lui et al., 2014). The lack of microbial community groupings and/or trends amongst sulfur as sulfide (%), and oxidized sulfur species (%), was unexpected. As these two geochemical parameters are dominantly hosted within mineralogical phases that directly link to iron and/or sulfur related microorganisms, such as secondary iron(hydr)oxides, iron-sulfates and sulfides. The general lack of microbial community groupings with increases and/or decreases in sulfur as sulfide (%) and oxidized sulfur species (%) concentrations is unclear. Microbial community structures exhibit groupings amongst the alteration zones (Figure 28), which are defined by not only pH ranges and colour, but on mineralogical composition. Sulfide minerals are prominent within unoxidized material, and thereby, sulfur as sulfide (%) concentrations were expected to be greater within this alteration zone. Similarly, oxidized sulfur species were expected to be higher within the oxidized zone, as secondary iron-sulfates are prevalent within this alteration zone. However, microbial community structures exhibit weak groupings with increasing and/or decreasing sulfur ratios (oxidized sulfur species/sulfur as sulfide). As seen in Figure 26, tailings material in the oxidized and transition zone exhibit higher concentrations of oxidized sulfur species than sulfur as sulfide. Contrarily, less oxidized sulfur species are present than sulfur as sulfide within tailings material from the unoxidized zone. Therefore, total oxidized sulfur species and sulfur as sulfide does not directly link to microbial community groupings, however their concentration in relation to each other does.

Environmental and geochemical parameters, including ferrous iron, ferric iron, sulfur ratio, iron ratio, pH, and Eh, explained a total of 23.9% of the cumulative variance in the microbial community compositions. The pH and ORP exhibit the strongest loadings, accounting for 9.9% of the total variance. Therefore, RDA suggests that variation of bacterial OTU's were moderately affected by pH and ORP. Again, this is unlike what is observed in other studies, whereby pH and

ORP are recognized as the primary factors influencing microbial community structures (Lui et al., 2014). Sulfur ratios exhibit a much lesser degree of significance, however they still add to variation, as seen in the non-metric multidimensional scaling ordination (Figure 26). The Mantel test (significance test) determined comparable results, where the low r and p values of 0.0878 and 0.122 respectively indicate no correlation between OTUs and the given geochemical and environmental parameters (ferrous iron, ferric iron, sulfur ratio, iron ratio, pH, and Eh). A significance test is thereby necessary when observing the effects of geochemical and/or environmental parameters on the structuring of OTUs, as RDA exhibited moderate correlation, and the Mantel test concluded no correlations. The two analyses provide the conclusion that the given geochemical and environmental parameters are not strongly linked to OTUs. Accordingly, microbial community structures amongst tailings material from the three alteration zones (oxidized, transition and unoxidized) may not be explained by the given geochemical and environmental parameters (ferrous iron, ferric iron, sulfur ratio, iron ratio, pH, and Eh).

The geochemical surroundings of microorganisms do not exclusively associate with solid materials, as the aqueous geochemistry of surrounding pore waters are linked to tailings microbiology (Lindsay et al., 2009). Lindsay et al (2009) exhibits variation in sulfate reducing bacteria populations within sulfidic tailings material collected across small depth ranges. This finding has been attributed to the microbial dependence on local hydrogeochemical surroundings. Accordingly, the aqueous geochemistry of pore water within this study may have exhibited significant correlations with the microbial community structures.

7.4.2 How alteration stages and mineralogical compositions influenced microbial community compositions

The three observed material types, including oxidized, transitional and unoxidized, represent stages of alteration, where unoxidized material is least altered and oxidized is most. As previously

discussed, transitional and oxidized tailings material exhibit secondary minerals, such as iron-(hydr)oxides and iron-sulfates, which form as a by-product of sulfide weathering. As indicated by the NMDS plot (Figure 28), microbial community compositions are distinctly differentiated between the oxidized and unoxidized material. Microbial community compositions within the transitional material exhibits closer similarity to that of the oxidized material than of the unoxidized tailings material. Steven et al (2016) observed similar patterns in microbial community structures, where differentiation between community compositions was clearly identified between oxidized and unoxidized biogeochemical facies, with no distinct community present within transitional facies. However, within the NMDS plot illustrating clustering of microbial communities by Stegen et al (2016), community structures within the transitional facies exhibited closer similarities to the oxidized zone, as similarly observed within this study.

Alteration zones are differentiated by pH ranges and mineralogical compositions, thereby indicating that microbial community compositions are influenced by these two factors. This finding may be supported by past studies where similar relationships are exhibited, whereby mineralogical compositions impact microbial community structures. Carson et al (2007) determined that microbial community structures shift in accordance with change in mineralogical compositions within soils. Furthermore, Carson et al (2009) determined that microbial community structures are influenced by minerals within microhabitats in soils. Trace nutrients within minerals structures, such as iron in silicates, have been shown to affect the microbial community compositions of microorganisms that are adhered to mineral surfaces within carbon rich groundwater (Hiebert, 2001; Mauck and Roberts, 2007). Within pristine aquifers, similar relationships are observed, by which mineralogical composition influences the composition and structure of substrata microbial communities (Boyd et al., 2006). Mauck and Roberts (2007) suggest that the trace metal nutrient content of minerals establishes the abundance and the microbial community structure of microbial communities adhered to mineral surfaces, within

environments with limited available nutrients and terminal electron acceptors. The shifts in microbial community structures with changing mineralogy have therefore been observed, however, they have not been documented within sulfidic tailings materials. The resulting differentiated microbial communities within oxidized and unoxidized zones can therefore suggest that nutrient availability and access plays a crucial role in structure microbial communities.

7.4.3 Linkages between key indicator species and tailings material type

A total of 20 OTU's were identified as microbial "indicator species" within microbial communities of >1% relative abundance across all three material types. The identified OTU's represent microorganisms that exhibit significance in defining the microbial communities within the three alteration zones (oxidized, transition and unoxidized) studied here. Of the 20 OTU's identified as indicator species, oxidized material exhibited 5 OTUs, transition exhibited 1 OTU and unoxidized material exhibited 14 OTUs.

Within oxidized tailings material, OTUs belonging to Acidimicrobiales and Acidobacteriaceae may be potential microbial indicators. The occurrence of OTUs from the Acidimicrobiales as an indicator species within the oxidized zone was expected, as a number of bacteria belonging to the order Acidimicrobiales are acidophilic and oxidize ferrous iron for energy fixation (Clark and Norris, 1996; Whitman et al., 2012). Meena et al (2016) suggests Acidobacteriaceae be further studied in order to understand the role of Acidobacteriaceae in mineral weathering. It is however, understood that *Acidobacteria* sp. inhabit moderate AMD environments, within pH ranges of 3-6 (Baker and Banfield, 2003).

Within transitional tailings material, Alicyclobacillaeceae has been recognized as a potential microbial indicator. The family Alicyclobacillaeceae, contains extremophile bacterial species that thrive within pH ranges of 1.5-5.5. (Garrity, 2008). Additionally, several families within the

Firmicutes have been observed in a number of mine waste environments including, Iron Mountain Mine (Baker and Banfield, 2003), sulfidic mine tailings (Korehi et al., 2014) and Cu-bearing tailings (Li et al., 2016; Gupta et al., 2017). Particular species of this family have the ability to grow by oxidizing ferrous iron and sulfur, in addition to the ability to reduce ferric ion (Joe et al., 2007; Guo et al., 2009). Bridge and Johnson (1998) observed two species of Alicyclobacillaeceae grow via anaerobic ferric iron respiration, these included *Sulfobacillus acidophilus* and *Sulfobacillus thermosulfidooxidans*. Consequently, reductive dissolution of ferric iron bearing minerals (i.e: amorphous ferric hydroxide, jarosite and goethite) ensued. Dissimilatory reduction of sulfate to sulfide has not yet been observed amongst species within the Alicyclobacillaeceae family (Johnson et al., 2009). Given the mineralogical composition of samples within the transitional zone, it is evident that a family of microorganisms that has the ability to perform ferrous iron and sulfur oxidation, in addition to ferric iron reduction, is identified as a potential indicator, as it exhibits mechanisms to adapt to changing environments, such as changes in oxygen availability. It is expected that previous changes in oxygen availability occurred within tailings material from the transition zone, as this zone contains both sulfides and secondary iron-(hydr)oxides and sulfates. Therefore, microorganisms with further metabolic capabilities (i.e: ferric iron reduction and ferrous iron and sulfur oxidation) may thrive in such an environment.

Numerous OTUs were identified as microbial indicator species within unoxidized tailings material. Notable indicator species of this zone include the following: *Pelotamaculum* and *Desulfosporosinus* (often identified as *D. meridiei*). *Pelotamaculum*, a strictly anaerobic genus from the family Peptococcaceae, has been identified within sulfide bearing mine waste environments (Karnachuk et al., 2008). However, isolated species within this genus lack the ability to reduce sulfate (Klotz et al., 2011). *Desulfosporosinus* is a sulfate reducing anaerobe, and has been isolated from various mine waste environments (Alazard et al., 2010; Sanchez-Andrea et al., 2013). The presence of this sulfate reducing bacteria as an indicator species may be expected, as

unoxidized tailings material exhibit oxygen depleted environments as sulfide minerals remain sTable. As mentioned, *Desulfosporosinus* was often identified at the species level as *D. meridiei* sp., which has been isolated by Robertson et al (2001), from a hydrocarbon-contaminated aquifer in soil. Additionally, this species may be indirectly linked with the formation of secondary sulfides, as sulfate reduction may result in low temperature formation of H_2S, which may form into secondary sulfides. Sulfate may be present as a result of the oxidation of sulfides within tailings material in the upper transition and/or oxidized zones.

8.0 Conclusions and Limitations

This study exhibits microbial community structuring within sulfur-bearing mine waste correlating with alteration zones (oxidized, transition and unoxidized). Therefore, the degree of material weathering and thus, the mineralogical composition, exhibits distinct differing microbial community compositions. Alternatively, RDA and the significance test (Mantel test) provides evidence for weak to absent correlating linkages between OTUs and geochemical parameters (ferrous iron, ferric iron, sulfur ratio, iron ratio, pH, and Eh). This was unexpected, as microorganisms are often directly correlated with their surrounding geochemical parameters. This occurrence is likely due to analyzing total metals, as oppose to analyzing elemental concentrations bound within mineralogical phases of interest. For example, total iron associated with sulfides vs. total iron associated with secondary oxides and sulfates may have exhibited groupings with the microbial community composition.

The lack of correlation between the analyzed geochemical data and the strong correlation between microbial community structures and the mineralogical composition of the studied tailings material suggests that microbial communities are indeed structuring based on mineral sources of nutrients (i.e. iron and sulfur). Minerals that define each alteration zone, such us sulfates, oxides and sulfides, contain differing dissolution and/or precipitation kinetics. These minerals are kinetically

favourable in terms of dissolution and/or precipitation in comparison to other minerals, such as silicates, of which also contain sources of nutrients. It is likely that the microbial community compositions are structuring based on the presence of minerals with both favourable kinetics and sources of nutrients. In this study, total elemental concentrations represent all mineral phases, and due to the lack of mineralogical abundances, estimations on the origin of elemental concentrations cannot be determined. Accordingly, future studies may include the following: (1) rietveld analysis of XRD patterns in order to determine mineral abundances; (2) sequential extractions in order to identify elemental partitioning within solid phases of interest (i.e: % ferrous iron within secondary iron-(hydr)oxide phases vs. sulfides); and (3) Mössbauer spectroscopy in order to determine the concentration of elements within mineralogical phases of interest.

Additionally, iron and/or sulfur oxidizing and reducing microorganisms are present across all three alteration zones. It is evident that their abundance markedly changes across alteration zones. Nonetheless, the presence of both oxidizers and reducers within anaerobic and aerobic environments, respectively suggests that material may transition, if optimal environmental conditions develop. Notably, the presence of sulfate reducing microorganisms, such as *Desulfobacca* sp., within oxidized material suggests that upon optimal conditions, sulfides may form and thus, the depletion of metals and/or metalloids of concern within surrounding pore water may ensue. This finding is pertinent in regards to applications used for ameliorating environmental degradation. Understanding where iron and/or sulfur related microorganisms are present, in regards to material type, further guides ones understanding of the potential for oxidation and reduction within material at various depths. Understanding the potential for oxidation is of key importance as sulfide oxidation within sulfidic tailings material generates acidity, and the production of acidity further exhilarates mineral dissolution, releasing metals and/or metalloids to surrounding pore waters. Correspondingly, understanding the potential for reduction (i.e: sulfate reduction) is of key importance as the reduction of sulfate (in addition to the acidic dissolution of

sulfides) produces H_2S. The production of H_2S in the absence of oxygen can promote the production of secondary sulfides, which structurally incorporates metals within the mineral crystal lattice. By increasing our knowledge on the presence, occurrence, and abundances of iron and/or sulfur related microorganisms within these materials, we may improve and/or provide the opportunity for adjustments to amendments added to these materials. For instance, upon the addition of organic matter within material hosting sulfate reducing microorganisms, sulfide formation may ensue, and thus the depletion harmful metals and/or metalloids within surrounding pore or ground water (Peppas et al., 2000).

Chapter 2

9.0 Introduction

Modern developments in analytical techniques have provided new insight into the vital roles played by geomicrobial processes within geological, geochemical and environmental capacities. Combining methods from distinct disciplines, including molecular methods (genomics) and microscopy (morphological features and mineral characterization), provides the opportunity to link microbial activity to mineral precipitation, transformation, and dissolution. Molecular methods, including the isolation and characterization of DNA, are used to better understand the unseen environmental micro-biome, as it is a key mechanism used to characterize microbial communities and to elucidate geochemical potentials of the organisms and/or community composition. Probing the microbial-mineral interface also requires electron microscopy, but techniques differ notably as preservation of microbial cells is required. Conventional sample preparation techniques, including sample dehydration and chemical fixation with heavy metal stains, have allowed imaging and examination of the compositional and morphological features of microorganisms interacting with mineral phases. This study analyzes microbial-mineral assemblages within three representative tailings samples, in the interest of furthering our knowledge and understanding on biomineralization within the examined tailings material.

10.0 Objectives

Chapter 1 shows that pH ranges and bulk mineralogical compositions influence the microbial community compositions associated with the analyzed tailings material. These links provide further understanding of biogeochemical processes occurring within the tailings dam materials, both at surface and at a range of depths. However, microbial community structures and bulk mineralogical compositions obtained within Chapter 1 do not clearly identify the key microbial roles in mineral precipitation and/or dissolution within the analyzed tailings material. The

suggested relationships between minerals and microorganisms described in Chapter 1 are therefore studied in three selected samples at the nanoscale, representing three alteration zones from the same drill core. The objectives of this study are thus the characterization of mineral-bacteria interactions in general and more specifically, the identification of biotic formed minerals in the oxidized, transition and unoxidized zone.

11.0 Methods

Samples from each alteration zone were analyzed for their bulk mineralogical and chemical composition as well as for mineralogical features on the nanometer to micrometer scale. The mineralogical and chemical composition of the tailings material was analyzed and identified using optical techniques such as XRD and SEM. Staining of transmission electron microscopy (TEM) samples resulted with the binding of uranyl acetate and lead citrate to the biological specimen, allowing the imaging of both inorganic and organic substrates (see below).

The three representative tailings samples were collected from the same borehole (figure 31), with the oxidized and unoxidized tailings samples within close proximity to each other. The oxidized and unoxidized tailings samples represented a hardpan within the borehole and were collected from 21.5 ft and 22 ft below surface, respectively. The transitional tailings sample was collected from 16 ft, as there was no apparent transitional material between the selected oxidized and unoxidized tailings samples.

11.1 Field Measurements

A waterproof and portable HANNAH meter was utilized to measure the pH and ORP (mV) in situ with a 1:2 soil to water ratio. The probe was calibrated with pH 4 and 7 buffer solution, and was

rinsed and wiped with a Kimtech wipe in between samples. Colour of tailings material was determined upon sample collection with a Munsell colour chart.

11.2 X-ray Diffraction (XRD), Scanning Electron Microscopy (SEM)

Powdered samples were prepared by crushing solid tailings material with an agate mortar and pestle. The samples were measured with a Phillips PW 1729 X-ray diffractometer, using Cu Kα (1.79Å) radiation, and operating at 40 kV 30 mA for Powder X-ray Diffraction analysis. Diffraction patterns were collected over a scan range of x-x with a step size of 0.02°2Θ and dwell times of 4 seconds per step. The XRD data is listed as supplementary data in Appendix 1. Scanning Electron Microscopy was conducted with a JEOL 6400 at 20 kV using detectors for backscattered (BSE) and secondary electrons (SE) detectors as well as an energy dispersive X-ray spectrometer (EDS).

11.3 Immersion Fixation

Samples used for Transmission Electron Microscopy (TEM) were fixated by being immersed in a 1:4 volumetric ratios of 10mL glutaraldehyde (8% EM grade), 10mL distilled H_2O and 20mL of 0.2M Sorensen's phosphate buffer solution (pH 7.4) (Hayat, 1986). Samples were fixated for 2 hrs at room temperature, followed by storage in a refrigerator at 4°C.

11.4 Microtome, Staining, High Resolution Transmission Electron Microscopy and Scanning Transmission Electron Microscopy

Sections containing the fixed material, were first stained with uranyl acetate and lead citrate and subsequently microtomed with a diamond knife. Sections were examined at the nanoscale for mineralogical and chemical features, along with microbial-mineral assemblages, with a JEOL 2100 field thermionic emission analytical transmission electron microscope (TEM) at the Virginia

Tech National Center for Earth and Environmental Nanotechnology Infrastructure (NanoEarth). All measurements were taken with an accelerating voltage of 200 kV and a beam current of approximately 107 μA. EDS point analyses and maps were acquired with the instrument operating in Scanning Transmission Electron Microscope (STEM) mode using a JEOL BF detector, and Selected Area Electron Diffraction (SAED) patterns were acquired using a Gatan Orius SC200D detector.

12.0 Results

A summary of the key results is presented below with supplemental data provided in Appendix 1.

12.1 Tailings Sample from the oxidized zone

The colour of the oxidized tailings sample is 2.5Y5/6, with a contact pH value of 4.1 and ORP value of 189 mV. The sample was collected from 21.5ft below surface and was wet upon sampling, as the water Table was at 25ft. This sample is dominantly composed of; quartz, clinochlore, albite, ferroactinolite, biotite, jarosite and goethite. Angular silicate grains are coated by iron-(hydr)oxide and jarosite precipitates (Figures 5 and 6 in Chapter 1). Scanning electron microscope images display hollow concretions of goethite exhibiting chain-like structures, ranging from 1-2 um in diameter (Figure 32). Acicular goethite is also present within the same aggregate, ranging from 3-15 um in length (Figure 32). Transmission electron microscope images show microbial cells with epicellular iron-rich illite grains encrusting the outer cell wall (Figure 33). Iron-rich illite occurs separately as acicular fragments, 100 nm in length. Aluminum-rich goethite occurs as nano-size grains (25 – 50 nm) above iron-rich illite, surrounding the microbial cell wall, revealing similar precipitation characteristics as observed on SEM (Figure 32).

12.2 Tailings Sample from the Transition Zone

The colour of the tailings sample from the transition zone is 10YR3/6, with a contact pH value of 4.2 and ORP value of 215 mV. The sample has been collected from 16 ft within the borehole (above the oxidized and unoxidized samples). The sample was moist upon sample collection and is dominantly composed of quartz, clinochlore, albite, ferroactinolite, biotite, jarosite, gypsum, marcasite and Mg-rich vermiculite. The sulfides pentlandite and chalcopyrite observed by SEM were not been detected by XRD, suggesting that they only occur in trace amounts (<5 %) in the tailings sample. Transmission electron microscopy shows the occurrence of a rod-shaped bacterium, encrusted in nano-crystalline goethite (Figure 34A). The bacteria formed a common interface with the amphiboles actinolite and pargasite. The interface itself is composed of nano-crystalline goethite and ferrihydrite (Figure 34B).

12.3 Tailings Sample from the Unoxidized Zone

The colour of the tailings material from the unoxidized zone upon sample collection is Gley1 2.5/N, with a contact pH value of 4.2 and ORP value of 223 mV. The sample was collected at 22 ft below surface and was wet upon sampling. The sample is dominantly composed of quartz, clinochlore, albite, magnesiohornblende, biotite, orthopyroxene, diopside and pyrite. Sulfides grains appear unaltered and disseminated within silicate grains (Figure 9 in Chapter 1). Jarosite occurs in trace abundance, being identified with SEM (Figure 10, Chapter 1), but not by XRD. Similarly, greigite and goethite have been identified in TEM images but not with XRD and SEM. Crystals of greigite approximately 500 nm in length and 150 nm in width (Figure 35) occur on the boundary of nano-crystalline Al-rich goethite. Although the TEM Sections are very thick, one prismatic dipyramidal crystal of greigite has been resolved (Figure 35).

13.0 Discussion

This TEM-based study has allowed the identification of microbial mineral assemblages, which have not been identified with bulk-XRD and SEM. As stated in Section 4.1, illite was observed with TEM and not by SEM within the tailings material from the oxidized zone. Additionally, goethite encrusting a rod-shaped bacterium is observed by TEM and not SEM within the tailings material from the transition zone, as described in Section 4.2. Similarly, a crystal of greigite has been identified with TEM in the unoxidized sample but not with bulk XRD and SEM. It is therefore evident that TEM reveals mineralogical and morphological features that would otherwise go unnoticed when utilizing SEM. This is in accord with the studies by Schindler et al (2015, 2016, 2017), who show that nano-scale examinations of soils and tailings material can reveal both abiotic and biotic processes, that commonly remain undetected with SEM and powder XRD.

13.1 Biotic formation of iron-bearing illite

As discussed in Section 1.4.2, microbial outer cell walls provide a favoured site for mineral nucleation (Konhauser, 2007). This is due to the abundance of ionized ligands present on microbial outer cell wall, which adsorb to surrounding cations (Konhauser, 2007). Therefore, microorganisms often serve as templates for the passive mineralization of small mineral phases (<1 um). The presence of clay minerals on microbial cell walls has been identified in numerous environments, including metal-contaminated sediments sampled from mine tailings within Sudbury, ON (Ferris et al., 1997). The majority of clay minerals observed along cell walls in previous studies have d-spacings of d = 10 A and compositions similar to the illite ($K_{0.65}Al_2(Al_{0.65}Si_{3.35}O_{10})(OH)_2$), observed in this study. (Konhauser et al., 1998).

Chen et al (2014) states that there are three pathways by which clay minerals form along the cell walls: (1) Dekov et al (2007), suggest that dissolved silicate anions may bind with R-NH_3^+ groups

on cellular walls, activating silica nucleation; (2) Dissolved silicate anions may also adhere to different charged sites along the cell wall, including $COOH^-$ and PO_4^{3-} groups (Urrutia and Beverage, 1994; Hinrichs et al., 1999; Devok et al., 2007); (3) Konhauser (1999, 2007), suggests that (Fe, Al)-silicate colloids may bind with exopolymers and/or iron adsorbed to the cell surface, ultimately leading to the formation of clay minerals. Although the formation of silica-bearing minerals encrusting cell walls is a common feature in the environment, the reactions involved in their initial formation remain unclear (Konhauser, 1999, 2007; Chen et al., 2014).

The low temperature formation of illite is believed to be strictly abiotic, where its formation proceeds through the smectite-to-illite (S-I) reactions (Liu et al., 2015). This formation involves an increase in illite percentage, and thus is a reaction representing a gradual change from smectite to illite. Smectite, a 2:1 phyllosilicate contains a layered structure, in which an octahedral cationic sheet is in between two tetrahedral cationic sheets (Velde and Meunier, 2008); i.e. they are considered 2:1. The transition of smectite to illite may be linked to an addition of K, where an increasing activity of K results in the formation of more illite layers or in the neoformation of illite without smectite precursor (Velde and Meunier, 2008).

As previously stated, smectite illitization is often described as a physical-chemical process, and excludes any biological roles (Fang et al., 2017). However, Kim et al. (2004), show that smectite illitization can be microbially facilitated under ambient conditions. Furthermore, studies show that sulfate reducing bacteria and dissimilatory iron reducing bacteria are able to reduce structurally incorporated ferric iron within smectite, resulting in reductive dissolution of smectite and thereby, the microbially mediated formation of illite (Kim et al., 2004; Liu et al., 2015; Liu et al., 2012). These observations suggest that the observed illite along the cell wall of the bacterium (Figure 32) has been formed via the biotic reductive dissolution of a ferric iron-bearing smectite precursor, and its subsequent crystallization in the presence of K-rich pore solutions. The smectite precursor

most likely formed through multiple abiotic mechanisms, initiated by the binding of silicate anions to cellular cations, such as adsorbed ferric iron and/or exopolymers. The observed microbial cells may have simply served as a nucleation site for clay formation (Ferris et al., 1991).

13.2 Biotic formation of ferrrihydrite and the transformation of ferrihydrite into goethite

The formation of goethite in aqueous solution occurs commonly during a three step process: (1) oxidation of aqueous ferrous iron; (2) abiotic or biotic formation of ferrihydrite and (3) transformation of ferrihydrite into goethite (Schwertman et al., 2004; Konhauser, 2007; Das et al., 2010).

As goethite encrusts the preserved rod-shaped bacterium in Figure 34 and ferrihydrite is present at the microbial-mineral interface within the transitional sample, a sequence of microbially mediated reactions, encompassing the formation of ferrihydrite, may be adduced. Passively, microorganisms can serve as nucleation sites, supporting the precipitation of ferrihydrite or goethite on cellular surfaces. The hydrolysis of ferric iron and the subsequent polymerization of ferric iron results in the precipitation of ferrihydrite, as described in reaction 1 within Section 1.3.5, or in the precipitation of goethite (Cedennec and Lecerft, 2006; Huang et al., 2012). The initial precipitation of ferrihydrite (Ksp ~ 10 -39) is kinetically controlled, as its crystal structure is less thermodynamically sTable than goethite (Ksp ~ 10 -41) (Cornell and Schwermann, 2003; Michel et al., 2007).

The transformation of ferrihydrite into goethite occurs through dissolution-precipitation reactions has been observed within both acidic and basic medias (Schwertmann et al., 2004). These reactions include the dissolution of ferrihydrite, followed by the nucleation and formation of goethite (Bowles et al., 2011). Solid-state transformation between these two mineralogical phases cannot

occur due to the presence of face-sharing $Fe(OOH)_6$ octahedra within the structure of ferrihydrite, as goethite contains an edge- and corner-sharing octahedra within its structure (Drits et al., 1993). Determining the underlaying preserved microorganism may adduce if the ferrihydrite was biomineralized, or if it formed by abiotic processes and used the microbial surface as a nucleation site. However, community level 16S RNA gene sequencing data and morphology of the rod-shaped bacteria does not determine the genera of the observed bacteria. Further studies would be needed to attain this information, including FISH stains or other targeted microscopy methods. Alyciclobacillaceae has been detected at 4.8 % relative abundance, with 2 OTUs identified as *Alicyclobacillus* at 2.2 % relative abundance. The remaining genera could not be identified with certainty across OTUs. *Alicyclobacillus* gains energy by the oxidation of ferrous iron and elemental sulfur (Guo et al., 2009), and its presence may thereby be linked to the biomineralization of ferrihydrite.

Contrarily, the presence of goethite above the illite coating of the preserved cell within the tailings sample from the oxidized zone (Figure 32) may be the result of an abiotic process simply due to the oxidation of ferrous and subsequent hydrolysis of ferric iron. The hollow concretions of goethite within the same tailings sample (from the oxidized zone) may exhibit the micro-scale feature of what is observed at the nano-scale. The size variations of the hollow concretions with <1 - 2.5 um in diameter suggests that the concretions represent an area of which microbial cells and agglomerates of cells may have populated.

13.3 Biotic formation of Greigite

Greigite, an iron-sulfide mineral, has been identified as a precursor phase for pyrite formation (Hunger and Benning, 2007). Greigite is an authigenic ferromagnetic mineral (Rowen and Roberts,

2006; Konhauser, 2007) and has been mineralized intracellularly by biologically controlled processes (Bazylinski and Frankel, 2000).

Bazylinski and Frankel (2000) state that some anaerobic sulfate-reducing bacteria can mediate greigite formation, as they form H_2S as a product of sulfate respiration. The reactions are abiotic and include the reaction between sulfide ions and iron (Bazylinksi and Frankel, 2000; Konhauser, 2007).

Biomineralized greigite exhibits various morphologies as pleomorphic, pseudorectangular prismatic, cubo-octahedral and bullet-shape (Bazylinski, 2001), whereby the greigite crystals can show random orientations within rod-shaped cells (Kasana et al., 2006). The morphological feature of the greigite-bearing bacterium with an approximate length of 400 nm exhibit a prismatic morphology. This morphology has been observed within intracellularly formed greigite, however the crystals often align in a chain-like manner (Lefevre et al., 2011). The isolated greigite crystal found within this study may be attributed to sample preparation techniques or by separation from the microorganism over time.

This sample does not contain sulfate-reducing microorganisms. The only iron and/or sulfur related microorganism present includes Acidithiobacillus, and is present in very low relative abundance (<2%). As stated in Chapter 1, the presence of Acidithiobacillus may be due to extraction methods attaining dormant cells, or those that are no longer viable (Cangelosi, 2014). The presence of Acidithiobacillus may be attributed to the presence of ferrous iron, which may have been available within the surrounding environment, such as in the surrounding pore water, as it has the ability to oxidize iron and/or sulfur (Quatrini, 2009; Hallberg et al., 2010). For these reasons, the precise mechanism for the past greigite formation within the unoxidized sample remains challenging to

determine, as the formation of greigite may have been microbially mediated under different environmental conditions, and in association with different microorganisms.

14.0 Conclusion

This research shows the importance of using a combination of both microscopy (SEM and TEM) and bulk 16s rRNA sequencing techniques when analyzing microbial-mineral interfaces and assemblages. Bulk mineralogy observed by XRD within Chapter 1 provides linkages between microbial community compositions, bulk mineralogy and contact pH ranges. However, this data did not provide evidence for biomineralization and/or products of microbially mediated reactions. This study shows that examination at the nano-scale provides evidence for (1) the biotic formation of ferrihydrite and smectite and their subsequent transformation into goethite and illite, respectively; and (2) the occurrence of past sulfate reducing processes and the subsequent formation of of greigite. Illite, a clay-like mineral, was not identified with XRD and SEM techniques alone. However, TEM data illustrated the importance of smectite in regards to the formation and occurrence of goethite. Similarly, greigite was not identified with XRD and SEM techniques but was present at the nano-scale, as observed with TEM. This ultimately concludes the importance of using a combination of methods in order to further understand biomineralization and microbe-mineral assemblages.

15.0 General Conclusions

This study provides evidence for interconnected relationships amongst microorganisms and the mineralogical and geochemical compositions within sulfur-bearing tailings material. Key findings of Chapter 1 of this study include the following: (1) A lack of strong correlation between microbial community compositions and structures with geochemical parameters; (2) Microbial community compositions structuring based on the mineralogical composition of material and contact pH range,

thereby suggesting that microbial community compositions change structure with the degree of material weathering; and (3) Iron and/or sulfur related bacteria as indicator species amongst alterations zones. OTUs that identify as microorganisms with the potential to oxidize iron and/or sulfur are indicators of tailings material from the oxidized zone. OTUs that identified as microorganisms with the potential to oxidize iron and/or sulfur and reduce ferric iron as indicators of tailings material from the transition zone. OTUs that identified as microorganisms with the potential to reduce sulfate as indicators of tailings material from the unoxidized zone. Additionally, OTUs that identified as microorganisms which underpin iron and/or sulfur oxidation were in higher abundance within tailings material from the oxidized zone, than in tailings material from the transition and unoxidized zone. OTUs that identified as microorganisms which underpin iron and/or sulfate reduction are in higher abundance within tailings material from the unoxidized zone, than in tailings material from the oxidized and transition zone. This change in microbial community structure may be linked to the mineralogical composition of the alteration zone, as shown by NMDS. These findings present the potential for hypothesizing key microbial members within sulfur-bearing tailings based on mineralogical composition and degree of alteration.

Chapter 1 did not provide evidence for biomineralization and/or products of microbially mediated reactions. For this reason, Chapter 2 focused on microscopy work of three representative tailings samples, with one from each alteration zone (oxidized, transition and unoxidized) in order to analyze and identify biominerals, in addition to microbe-mineral interactions within the samples. Key findings of Chapter 2 of this study include the following: (1) The formation of ferrihydrite at the microbial-mineral interface; (2) Goethite encrusting microorganisms; (3) The formation of illite enveloping microbial cell walls; and (4) Low temperature sulfides, such as greigite, present within tailings material from the unoxidized zone. These findings suggest evidence for the biotic formation of ferrihydrite and smectite, and their subsequent formation into goethite and illite, respectively. Additionally, the presence of low temperature sulfides (greigite) within the

unoxidized zone, exhibits evidence for microbial reduction of sulfate, resulting in the formation of H_2S and the subsequent formation of sulfides. These biominerals, whether formed for microbial physiological benefit, or as a by-product of microbial activity, we're not detected in Chapter 1. As these minerals play an important role in metal attenuation (i.e: gregite, ferrihydrite, greigite), it is of value to both identify and understand where they may be present within specific types of tailings material. For this reason, additional microscopy, including SEM and TEM, should be performed in order to fully deduce and examine the variation of biomineralized mineralogical phases and microbial-mineral interactions across the select samples. These findings are of interest as the ultimate environmental fate of various elements is fundamentally controlled by redox and microbial processes and thus further understanding of microbe-mineral interactions is of great significance when evaluating tailing environments.

This study improves our understanding of biogeochemical processes occurring within the analyzed tailings material and provides improved resolution on the relationships between microbial communities and the tailings material of which they host. However, the mineralogical, geochemical and microbial communities within the analyzed tailings material does not encapsulate the illustration of all biogeochemical processes occurring. In additional and supplementary studies, a unified approach with focus on weathering processes is recommended. This approach should require but may not be limited to knowledge on temperature and seasonal variations, hydrogeology, pore water chemistry, and process aids (i.e: environmental amendments, processing chemicals used during metal extraction, etc).

Tables

Table 1 Alteration zone, mineralogical composition analyzed by X-Ray diffraction, pH and Munssel colour of the total 41 tailings samples.

Sample ID	Zone	Silicates	Sulfates	Oxides	Sulfides	pH	Munsell Colour
A1	Oxidized	Quartz, Clinochlore, Albite, Muscovite, Alunite	Gypsum	Wuestite		4.0	10YR 4/6
A2	Oxidized	Quartz, Clinochlore, Albite, Amphibole, Biotite	Jarosite			3.8	10YR 4/4
A3	Oxidized	Quartz, Clinochlore, Albite	Gypsum, Jarsosite			3.9	10YR 3/6
A9	Oxidized	Quartz, Clinochlore, Albite, Ferroactinolite, Biotite	Jarosite, Goethite			4.1	2.5Y 5/6
C3	Oxidized	Quartz, Clinochlore, Albite, Magnesiohornblende, Biotite, Montmorillonite	Gypsum, Jarsosite			4.3	5Y 4/4
C4	Oxidized	Quartz, Albite, Biotite, Magnesiohornblende, Clinochlore, Protoenstatite	Jarosite, Gypsum			2.8	10YR 3/6
C5	Oxidized	Quartz, Clinochlore, Albite, Biotite, Magnesiohornblende, Diopside	Jarosite, Gypsum			3.0	10YR 3/6
D2	Oxidized	Quartz, Clinochlore, Albite, Ferroactinolite, Biotite, Microcline		Hematite		4.1	5Y 2.5/2
D4	Oxidized	Quartz, Clinochlore, Albite, Magnesiohornblende, Biotite, Microcline	Jarosite, Gypsum	Hematite		3.4	2.5Y 4/3
K1	Oxidized	Quartz, Clinochlore, Albite, Ferroactinolite, Phlogopite, Microcline	Jarsosite	Hematite		4.1	2.5Y 3/3
K3	Oxidized	Quartz, Clinochlore, Albite, Ferroactinolite, Biotite, Microcline	Gypsum			4.4	2.5Y 3/3
K5	Oxidized	Quartz, Clinochlore, Albite, Magnesiohornblende, Biotite	Gypsum, Schwertmannite			3.6	10YR 3/3
M1	Oxidized	Quartz, Clinochlore, Albite, Ferroactinolite, Biotite	Jarosite			4.3	10YR 3/6
M4	Oxidized	Quartz, Clinochlore, Albite,Magnesiohornblende, Biotite	Jarosite			3.4	10YR 4/6
M6	Oxidized	Quartz, Clinochlore, Albite, Microcline	Jarosite			2.6	10YR 5/8
M7	Oxidized	Quartz, Clinochlore, Albite, Ferroactinolite, Biotite, Microcline	Jarosite			3.3	10YR 3/6
A4	Transition	Quartz, Clinochlore, Albite, Ferroactinolite, Magnesiohornblende, Biotite	Gypsum, Jarosite		Pyrite	3.9	Gley 1 2.5/N
A7	Transition	Quartz, Clinochlore, Albite, Ferroactinolite, Biotite	Gypsum, Jarosite		Marcasite, Smythite	4.2	10YR 3/6
A8	Transition	Quartz, Clinochlore, Albite, Magnesiohornblende, Biotite	Gypsum, Jarosite		Pyrite	4.1	Gley 1 2.5/N mottled 2.5Y 5/6
C1	Transition	Quartz, Clinochlore, Albite, Magnesiohornblende, Biotite, Montmorillonite	Jarosite		Smythite	4.2	10YR 4/4
C2	Transition	Quartz, Clinochlore, Albite, Ferroactinolite, Biotite		Wuestite, Ferrihydrite	Chalcopyrite, Covellite	5.0	10YR 5/4 mottled Gley 1 2.5/N
C6	Transition	Quartz, Clinochlore, Albite, Magnesiohornblende, Biotite	Gypsum		Pyrite	5.2	5Y 4/2

Sample ID	Zone	Silicates	Sulfates	Oxides	Sulfides	pH	Munsell Colour
C7	Transition	Quartz, Clinochlore, Albite, Ferroactinolite, Biotite	Gypsum, Jarosite		Pyrite	5.3	Gley 1 2.5/N mottled 5Y 4/3
C9	Transition	Quartz, Clinochlore, Albite, Magnesiohornblende, Biotite, Microcline		Wuestite, Hematite	Violarite	4.1	10YR 4/2
D1	Transition	Quartz, Clinochlore, Albite, Ferroactinolite, Biotite	Jarosite		Chalcocite	4.2	10YR 4/6
D3	Transition	Quartz, Clinochlore, Albite, Biotite	Gypsum, Jarosite	Hematite	Chalcopyrite	4.2	2.5Y 4/3
D5	Transition	Quartz, Clinochlore, Albite, Actinolite	Jarosite		Pyrite	4.1	Gley 1 2.5/N mottled 2.5Y 3/1
D6	Transition	Quartz, Clinochlore, Albite, Magnesiohornblende, Biotite, Microcline	Jarosite		Chalcopyrite, Chacocite	4.7	Gley 1 2.5/N
K7	Transition	Quartz, Clinochlore, Albite, Magnesiohornblende, Biotite	Bloedite		Pyrite	4.6	5Y 4/2
M2	Transition	Quartz, Clinochlore, Albite, Magnesiohornblende, Biotite	Gypsum	Hematite	Chalcopyrite	3.6	5Y 3/2
M5	Transition	Quartz, Clinochlore, Albite, Magnesiohornblende, Biotite	Gypsum		Talnakhite	4.5	Gley 1 2.5/N
M8	Transition	Quartz, Clinochlore, Albite, Biotite		Bernalite	Pyrite, Violarite	5.0	5Y 3/2
C8	Unoxidized	Quartz, Clinochlore, Albite, Biotite, Ferroactinolite			Pyrite	5.5	Gley 1 2.5/N
A5	Unoxidized	Quartz, Clinochlore, Albite, Magnesiohornblende, Biotite			Pyrrhotite	5.3	Gley 1 2.5/N
A10	Unoxidized	Quartz, Clinochlore, Albite, Magnesiohornblende, Biotite, Orthopyroxene, Diopside			Pyrite	4.1	Gley 1 2.5/N
D7	Unoxidized	Quartz, Clinochlore, Albite, Biotite, Ferroactinolite			Chalcocite, Marcasite	5.0	2.5Y 3/2 mottled Gley 1 2.5/N
D8	Unoxidized	Quartz, Clinochlore, Albite, Magnesiohornblende, Biotite			Talnakhite	4.8	Gley 1 2.5/N
K4	Unoxidized	Quartz, Clinochlore, Albite, Biotite, Ferroactinolite, Muscovite			Chalcopyrite	4.5	Gley 1 2.5/N
K6	Unoxidized	Quartz, Clinochlore, Albite, Magnesiohornblende, Biotite			Talnakhite	4.9	Gley 1 2.5/N
M3	Unoxidized	Quartz, Clinochlore, Albite, Magnesiohornblende, Biotite, Clinopyroxene			Talnakhite	4.3	Gley 1 2.5/N
M9	Unoxidized	Quartz, Clinochlore, Anorthite, Ferroactinolite, Biotite, Enstatite			Digenite	4.2	Gley 1 2.5/N

Table 2 Geochemical and Environmental Parameters of Analyzed Tailings Samples

Sample ID	Alteration Zone	Depth (ft)	Contact pH	ORP (mV)	Fe (%)	S (%)	Ni (ppm)	Cu (ppm)	Ferrous iron (%)	Ferric iron (%)	Fe Ratios	S as Sulfide (%)	Oxidized S species (%)	Sulfur Ratio
A1	Oxidized	2	4	241	6.8	1.0	311	1610	4.3	2.5	1.7	0.05	0.95	19.0
A2	Oxidized	14	3.8	280	14.4	0.9	371	710	6.7	7.7	0.9	0.02	0.90	45.0
A3	Oxidized	21	3.9	243	12.8	1.1	532	1280	6.7	6.1	1.1	0.02	1.10	55.0
A9	Oxidized	21.5	4.1	189	13.8	1.6	976	700	7.2	6.6	1.1	0.02	1.61	80.5
C3	Oxidized	16	4.3	125	9.0	1.1	808	2780	5.8	3.2	1.8	0.04	1.02	25.5
C4	Oxidized	19	2.8	484	12.2	1.3	356	529	5.2	7.0	0.7	0.01	1.30	130.0
C5	Oxidized	21	3.8	265	10.7	1.3	378	557	5.0	5.7	0.9	0.01	1.32	132.0
D2	Oxidized	2	4.1	189	6.8	0.1	300	223	5.6	1.2	4.5	0.02	0.07	3.5
D4	Oxidized	4	3.4	366	8.3	0.8	301	622	5.4	2.9	1.8	0.02	0.73	36.5
K1	Oxidized	2	4.5	275	10.2	0.6	325	423	6.2	4.0	1.5	0.02	0.54	27.0
K3	Oxidized	10	4.4	199	8.7	0.6	625	947	6.8	2.0	3.4	0.02	0.53	26.5
K5	Oxidized	12	3.6	375	8.7	0.8	425	1030	6.5	2.2	3.0	0.02	0.75	37.5
M1	Oxidized	4	4.3	231	10.4	0.7	279	448	6.0	4.4	1.4	0.01	0.64	64.0
M4	Oxidized	1	3.4	232	10.4	0.6	291	368	6.3	4.1	1.5	0.01	0.54	54.0
M6	Oxidized	2	2.6	433	2.7	0.2	47.4	32.8	1.5	1.2	1.3	0.01	0.15	15.0
M7	Oxidized	5	3.3	282	10.7	0.6	316	269	6.0	4.7	1.3	0.01	0.62	62.0
A4	Transition	22	3.9	264	11.5	1.6	1070	4020	10.0	1.4	7.0	0.14	1.46	10.4
A7	Transition	16	4.2	215	12.1	1.6	516	786	5.8	6.3	0.9	0.01	1.54	154.0
A8	Transition	21	4.1	157	13.4	2.1	1715	779	6.9	6.4	1.1	0.04	2.10	52.5
C1	Transition	4	4.2	213	10.9	1.1	706	2210	5.6	5.3	1.1	0.06	1.01	16.8
C2	Transition	7	5	183	8.8	1.4	3720	2700	6.7	2.1	3.1	0.24	1.14	4.8
C6	Transition	25	5.2	-27	8.4	0.7	481	533	5.6	2.8	2.0	0.02	0.66	33.0
C7	Transition	33	5.3	94	9.6	0.4	436	292	7.5	2.2	3.5	0.01	0.39	39.0
C9	Transition	6	4.1	218	6.5	0.5	421	558	4.7	1.8	2.6	0.04	0.45	11.3
D1	Transition	1	4.2	4	7.6	0.4	295	483	6.8	0.8	8.0	0.03	0.41	13.7
D3	Transition	14	-	-	10.1	1.0	641	1750	6.6	3.5	1.9	0.06	0.90	15.0
D5	Transition	28	4.1	4	9.6	1.5	751	810	5.4	4.2	1.3	0.05	1.44	28.8
D6	Transition	31	4.7	5	9.9	1.1	820	691	7.2	2.8	2.6	0.03	1.08	36.0
K7	Transition	8	4.6	124	6.5	0.9	787	4520	5.6	0.9	6.3	0.25	0.68	2.7
M2	Transition	13	3.6	334	9.6	0.8	401	845	6.6	3.0	2.2	0.02	0.81	40.5
M5	Transition	21	4.5	171	11.4	1.9	1060	608	7.4	4.0	1.9	0.07	1.81	25.9
M8	Transition	8	5	14	14.7	4.0	3280	1720	7.2	7.5	1.0	0.44	3.54	8.0
A5	Unoxidized	36	5.3	6	18.2	4.3	2300	1080	12.3	5.9	2.1	0.24	4.05	16.9
A10	Unoxidized	22	4.1	223	10.7	1.4	2460	1145	9.1	1.6	5.7	0.07	1.30	18.6
C8	Unoxidized	45	5.5	-18	11.5	1.9	1175	686	8.9	2.6	3.4	0.19	1.70	8.9
D7	Unoxidized	39	5.5	153	8.6	0.9	522	641	5.9	2.8	2.1	0.03	0.83	27.7
D8	Unoxidized	48	4.8	158	9.3	1.4	889	550	6.1	3.2	1.9	0.05	1.31	26.2

Sample ID	Alteration Zone	Depth (ft)	Contact pH	ORP (mV)	Fe (%)	S (%)	Ni (ppm)	Cu (ppm)	Ferrous iron (%)	Ferric iron (%)	Fe Ratios	S as Sulfide (%)	Oxidized S species (%)	Sulfur Ratio
K4	Unoxidized	11	4.5	242	9.0	1.2	1050	1660	6.8	2.2	3.1	0.05	1.16	23.2
K6	Unoxidized	21	4.9	87	9.6	1.4	1605	1420	7.9	1.6	4.8	0.23	1.19	5.2
M3	Unoxidized	14	4.3	249	8.8	0.9	664	1650	7.6	1.2	6.4	0.04	0.82	20.5
M9	Unoxidized	14	5.7	-22	10.6	1.4	1115	867	8.6	1.9	4.5	0.06	1.37	22.8

Table 3 Eigenvalues and their contribution to the Bray distance

	dbRDA1	dbRDA2	dbRDA3	dbRDA4	dbRDA5	dbRDA6
Eigenvalue	4.40271	0.60882	0.48007	0.32124	0.26475	0.16279
Proportion Explained	0.09932	0.04311	0.03399	0.02275	0.09875	0.01153
Cumulative Proportion	0.09932 %	0.14243 %	0.17642 %	0.19916 %	0.21791 %	0.22943 %

Table 4 Biplot scores for constraining variables

	dbRDA1	dbRDA2	dbRDA3	dbRDA4	dbRDA5	dbRDA6
pH	-0.94037	-0.20773	0.2317	0.02632	0.07801	0.10991
ORP	0.89909	-0.04218	-0.3707	-0.05155	0.20733	0.08246
Ferrous iron	-0.65568	-0.10435	-0.3951	-0.29769	-0.50012	0.25366
Ferric iron	0.08975	0.77845	0.1063	-0.18704	-0.03324	0.58187
Fe ratio	-0.29564	-0.54934	-0.4556	0.45337	-0.33606	-0.29119
S ratio	0.17313	0.79081	-0.3965	-0.09867	0.42078	0.02529

** bold text represents values with strongest loadings*

Figure 1 Field images of sampled tailings material representing three alteration zones; (A) Oxidized tailings material, (B) Transitional tailings material, (C) Unoxidized tailings material

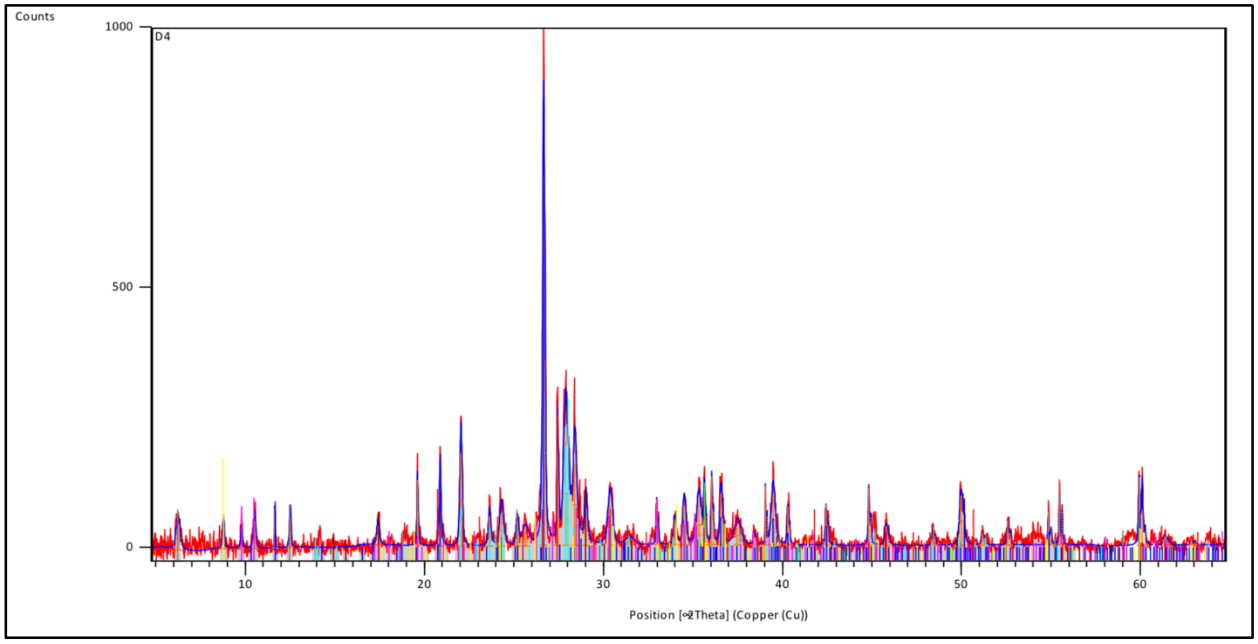

Figure 2 XRD pattern of oxidized tailings material, exhibiting the following crystalline mineral phases; Quartz (SiO2), Hematite (Fe2O3), Clinochlore ((Mg,Al,Fe)6(Si,Al)4O10(OH)8), Jarosite ((K,H3O)Fe3(SO4)2(OH)6), Albite (Na,Ca)Al(Si,Al)3O8, Magnesiohornblende ({Ca2}{Mg4Al}(AlSi7O22)(OH)2), Biotite (KFeMg2(AlSi3O10)(OH)2), Microcline (KAlSi3O8), and Gypsum (CaSO4(H2O)2)

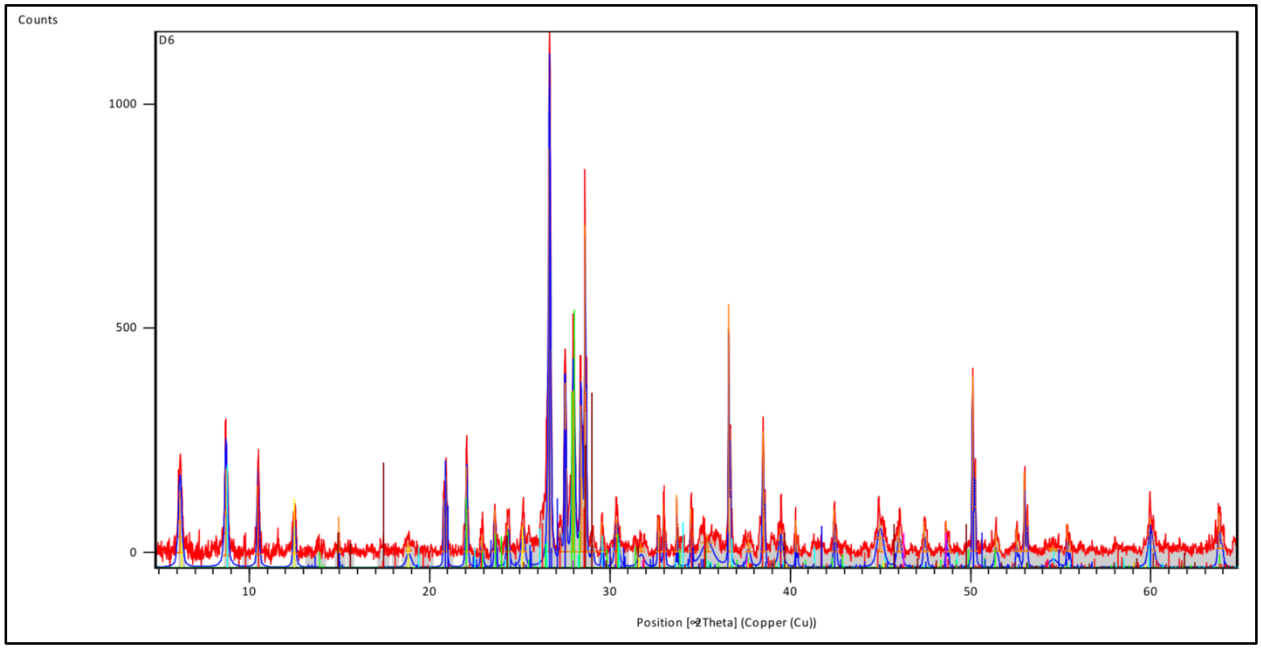

Figure 3 XRD pattern of transitional tailings material, exhibiting the following crystalline mineral phases; Quartz, Albite, Biotite, Jarosite, Chalcopyrite ($CuFeS_2$), Chalcocite (Cu_2S), Clinochlore ($(Mg,Al,Fe)_6(Si,Al)_4O_{10}(OH)_8$), Magnesiohornblende and Microcline

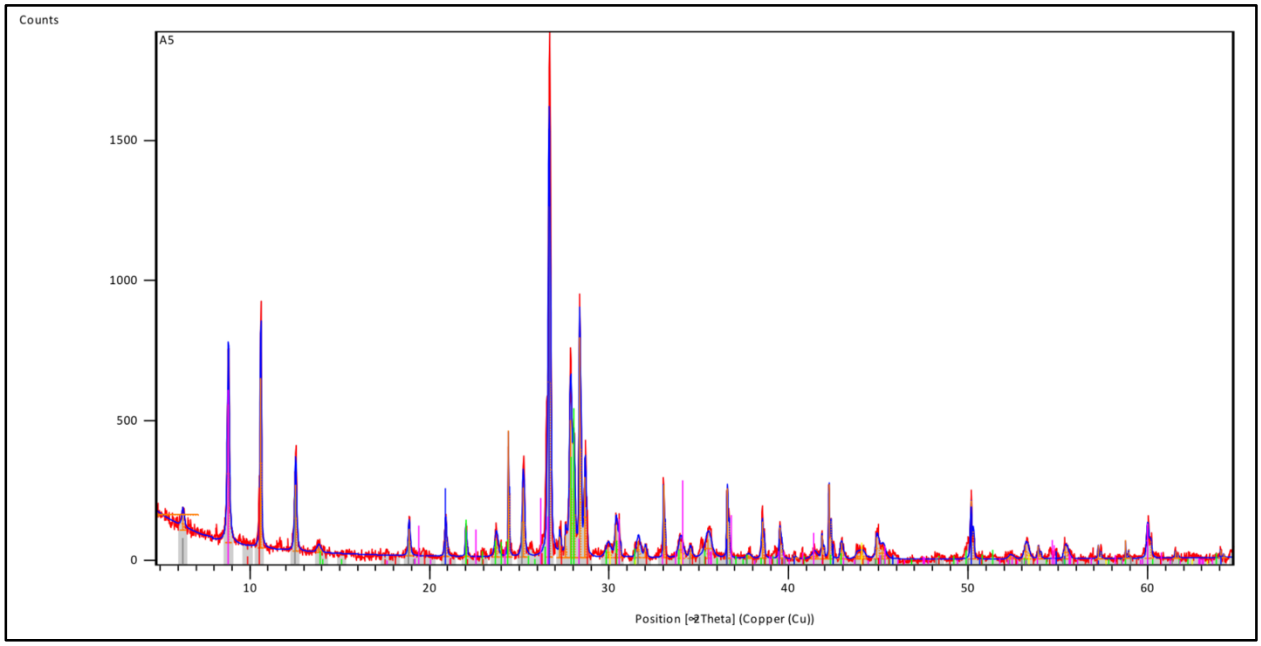

Figure 4 XRD pattern of unoxidized tailings material, exhibiting the following crystalline mineral phases; Quartz, Albite, Clinochlore, Biotite, Pyrrhotite (Fe_7S_8) and Magnesiohornblende

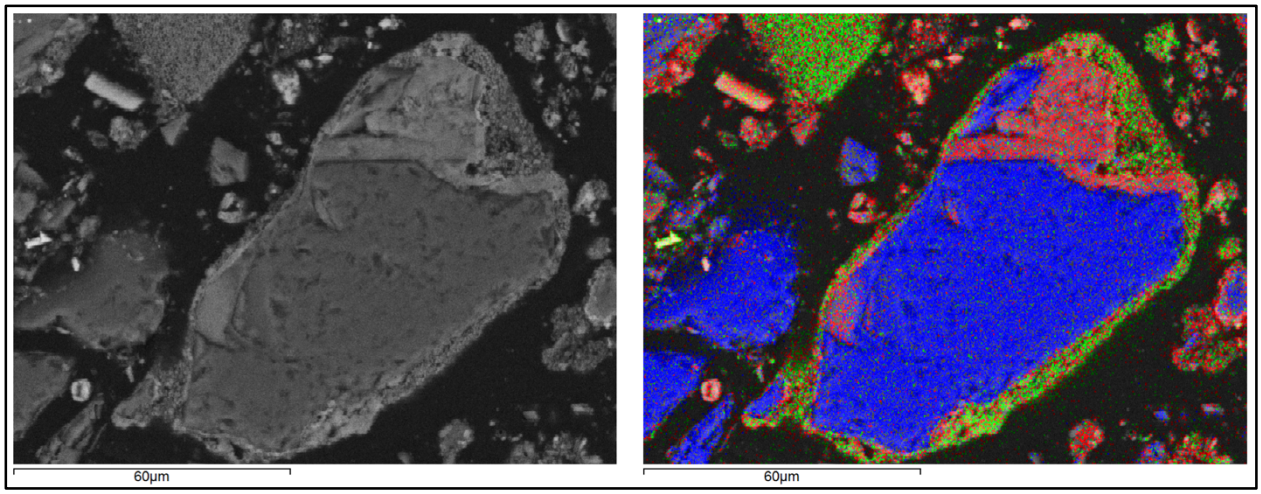

Figure 5 SEM images of oxidized tailings material; (A) Nano-crystalline Fe(hydr)oxide ($Fe(OH)_2$) coating an amphibole grain ($AX_2Z_5((Si,Al,Ti)_8O_{22})(OH,F,Cl,O)_2$) (B) Coating exhibits enrichment in Fe (green) and O (blue), with enclosed amphibole enriched in Si, obtained by Energy-dispersive X-ray spectroscopy

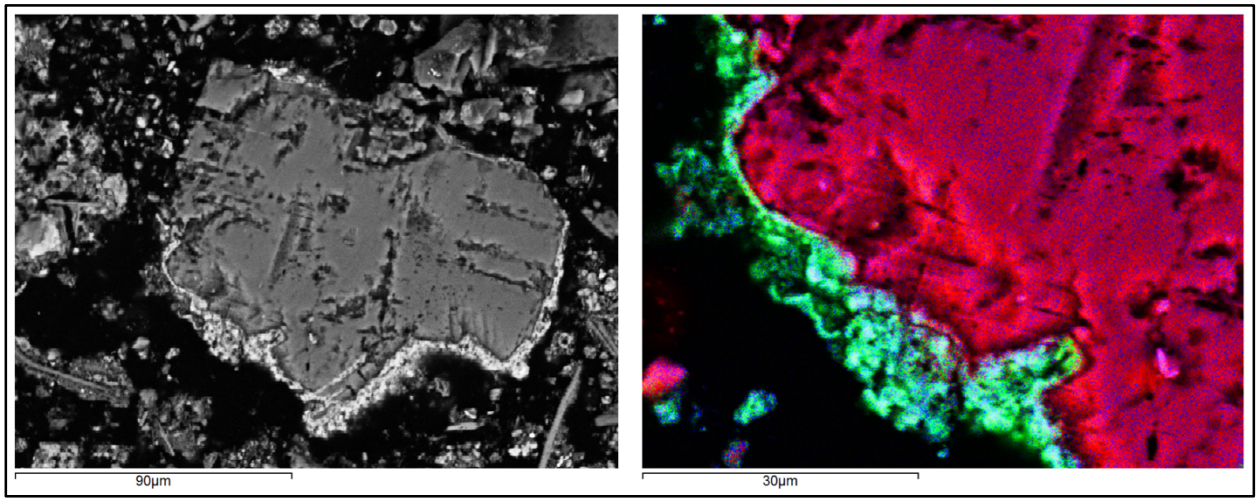

Figure 6 SEM images of oxidized tailings material; (A) Nano-crystalline Jarosite (KFerric iron 3(SO4)2(OH)6) coating quartz grain (SiO2) (B) Coating exhibits enrichment in S (green) and Fe (red), with enclosed quartz grain enriched in Si, obtained by Energy-dispersive X-ray spectroscopy

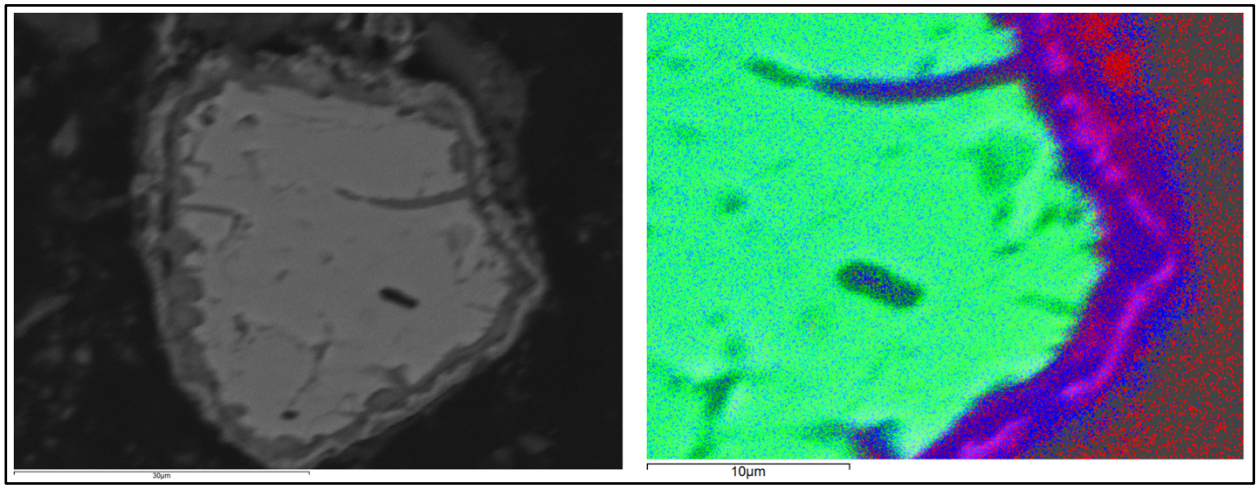

Figure 7 SEM images of transitional tailings material; (A) Altered anhedral pentlandite grain $(FeNi_9)S_8$, enclosed by nano-crystalline Fe(hydr)oxide rim (B) Coating exhibits two layers of Fe(hydr)oxides, with differing Fe ratios, blue represents Fe and red represents O. The pink layer represent a layer depleted in Fe content. Green represents S

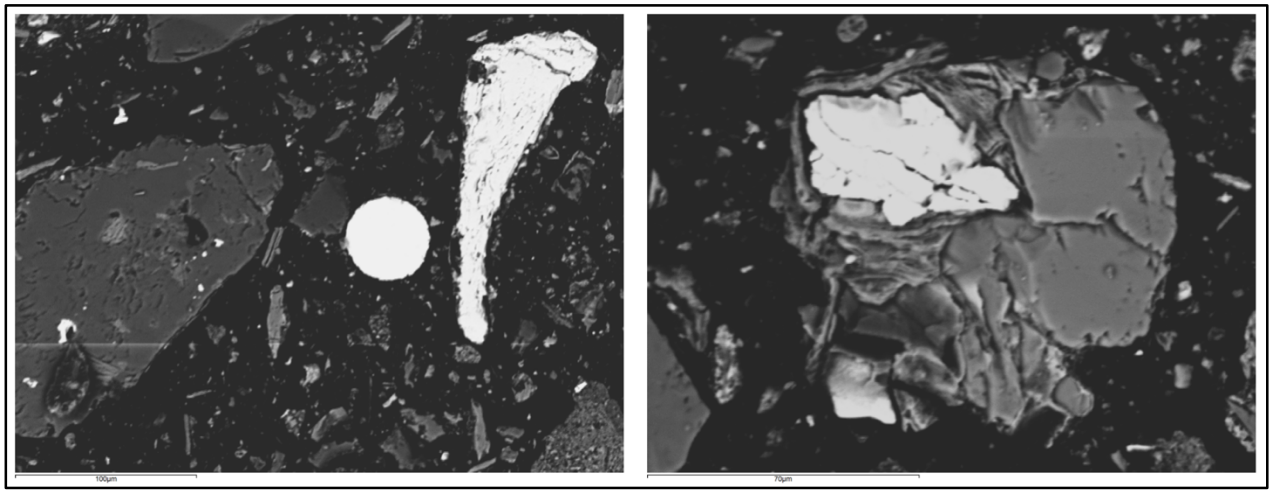

Figure 8 SEM image of transitional tailings material; (A) Isolated Plagioclase grain ((Na,Ca) $(Si,Al)_4O_8$ exhibiting no coatings on the left side of the smelter particle, and encompassing Fe-(hydr)oxide (Fe_3O_4) grains ranging from 4-10 um in diameter. Isolated anhedral Fe(hydr)oxide grain is present to the right of the smelter particle, and does not enclose other minerals (B) Unaltered chalcopyrite grain ($CuFeS_2$) encapsulated in amphibole grain $((AX_2Z_5((Si,Al,Ti)_8O_{22})(OH,F,Cl,O)_2)$

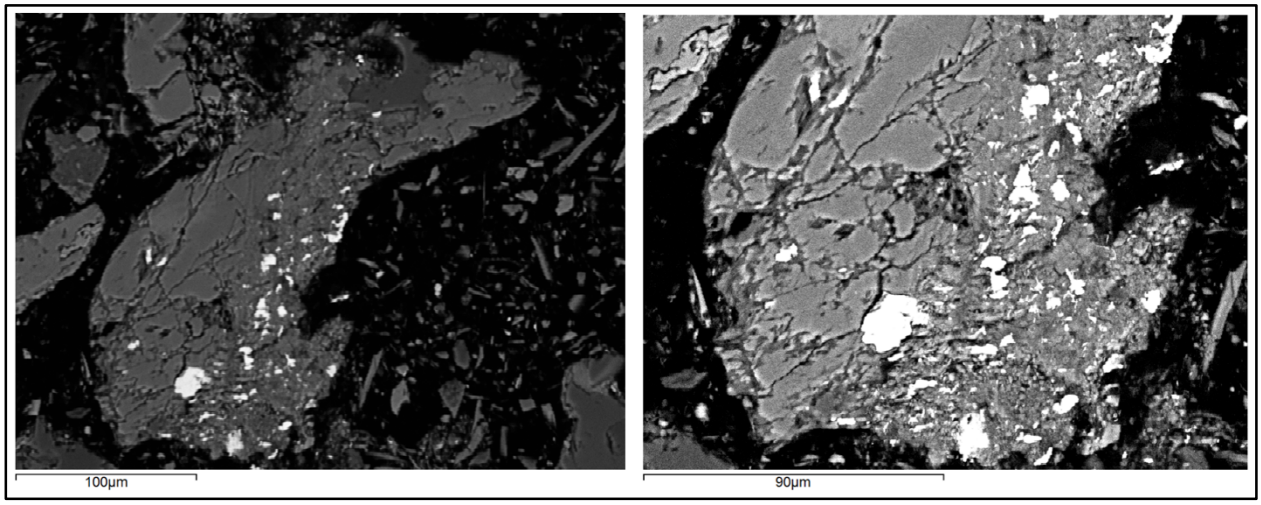

Figure 9 SEM images of unoxidized tailings material; Unaltered and disseminated chalcopyrite and Fe-oxide grains incorporated in euhedral amphibole grain

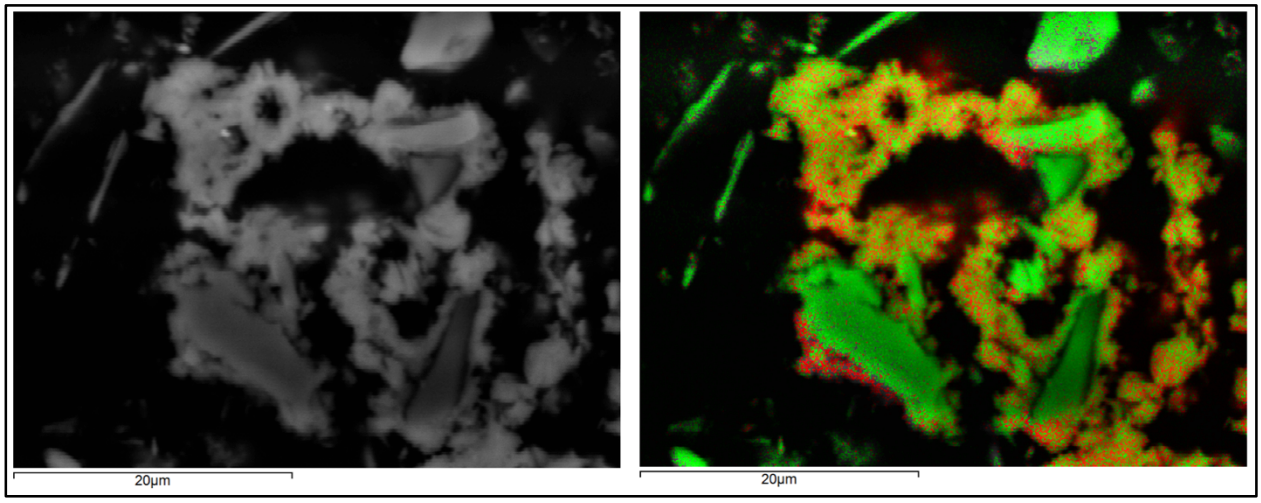

Figure 10 SEM images of unoxidized tailings material; (A) Amorphous jarosite coating silicate grains and occurring isolated (B) Green represents zones enriched in Fe and red represents zones enriched in S

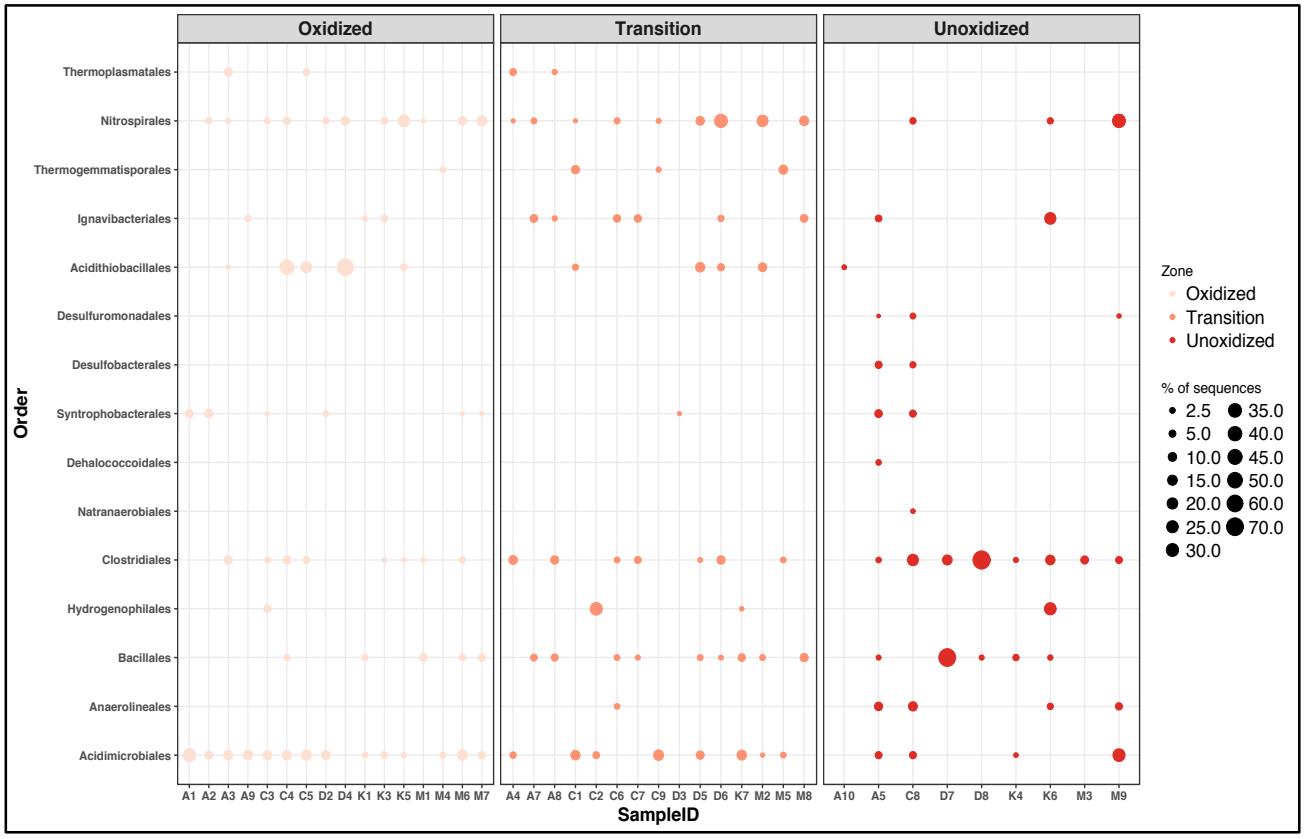

Figure 11 Taxonomy (order level) dot plot of Fe and/or S related bacteria across 41 tailings samples. The size of the dot represents the % of sequences or each microorganism listed. Light pink dots, on the left of the Figure represent oxidized samples.

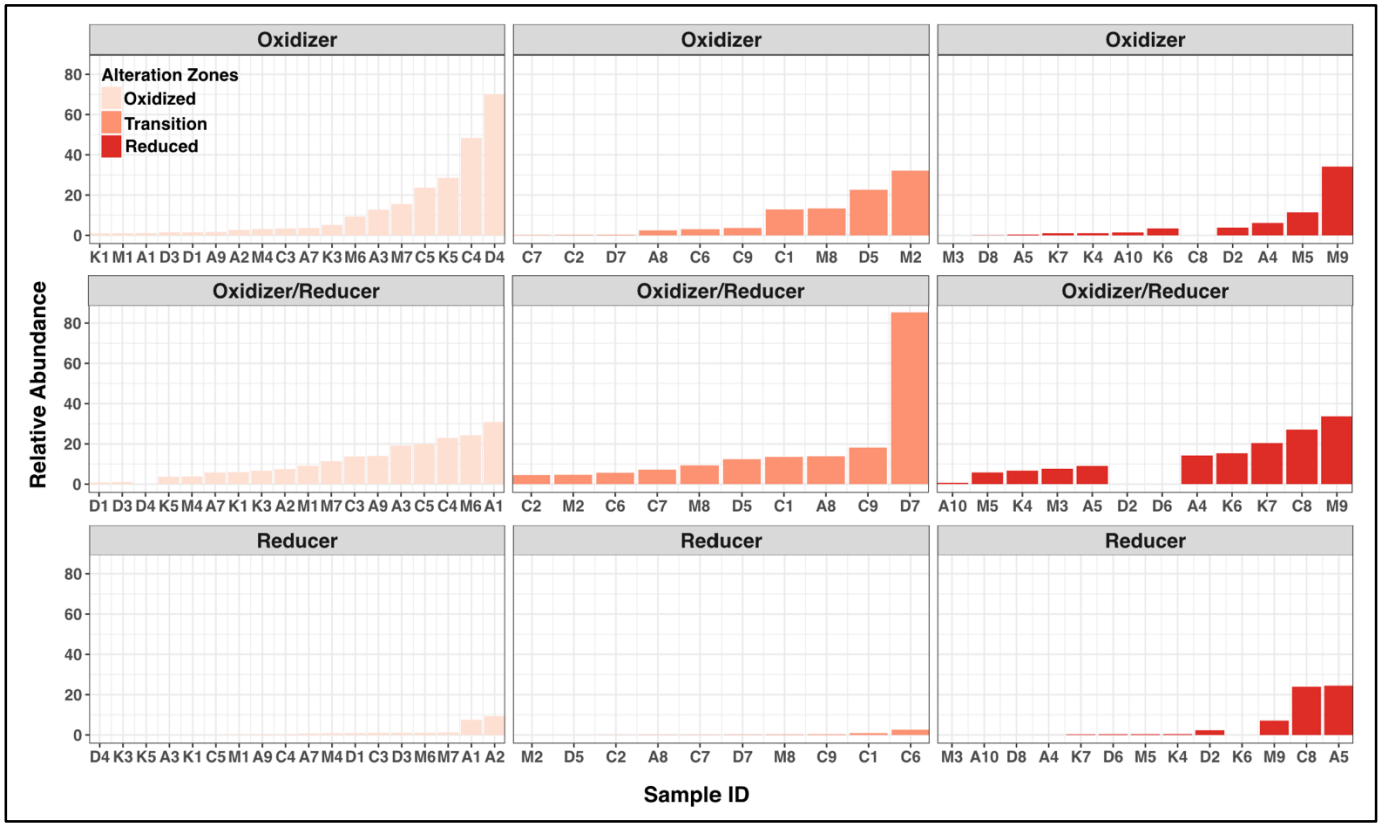

Figure 12 Bar plot exhibiting changes in abundances of total iron and/or sulfur related bacteria. Light pink represents tailings samples from the oxidized zone, peach represents tailings samples from the transition zone, and red represents tailings samples from the unoxidized zone.

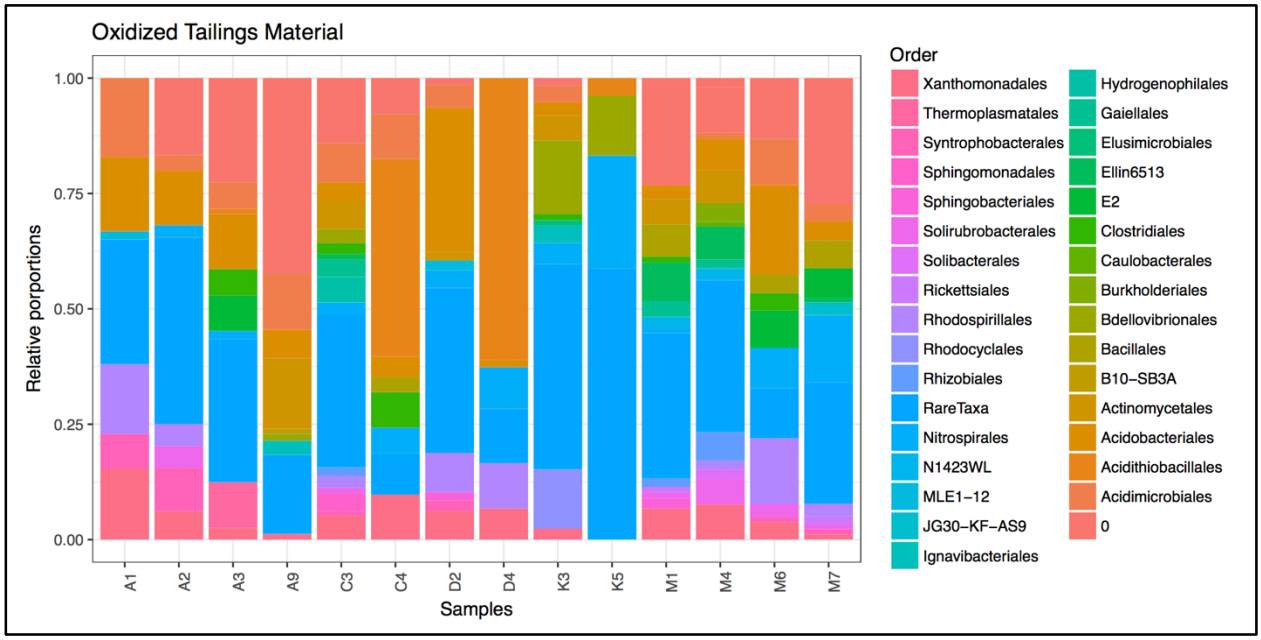

Figure 13 Percent relative abundance of the taxonomic composition at the order level for microbial communities analyzed within oxidized tailings material across 5 tailing dam structures in Sudbury, ON

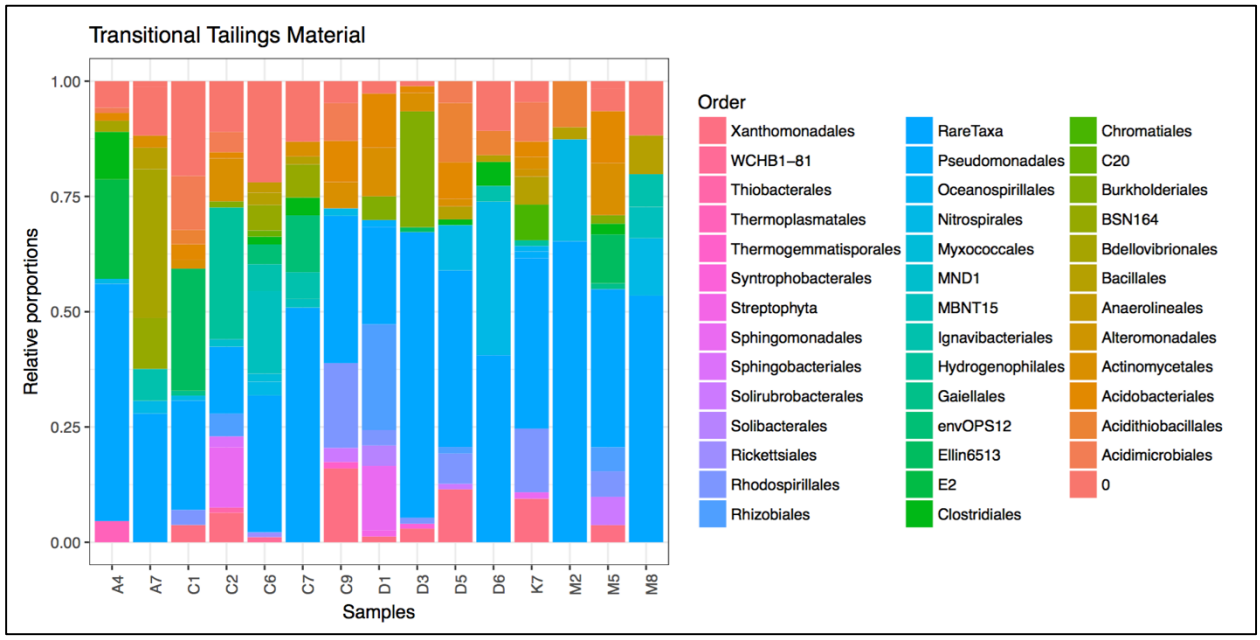

Figure 14 Percent relative abundance of the taxonomic composition at the order level for microbial communities analyzed within transitional tailings material across 5 tailing dam structures in Sudbury, ON.

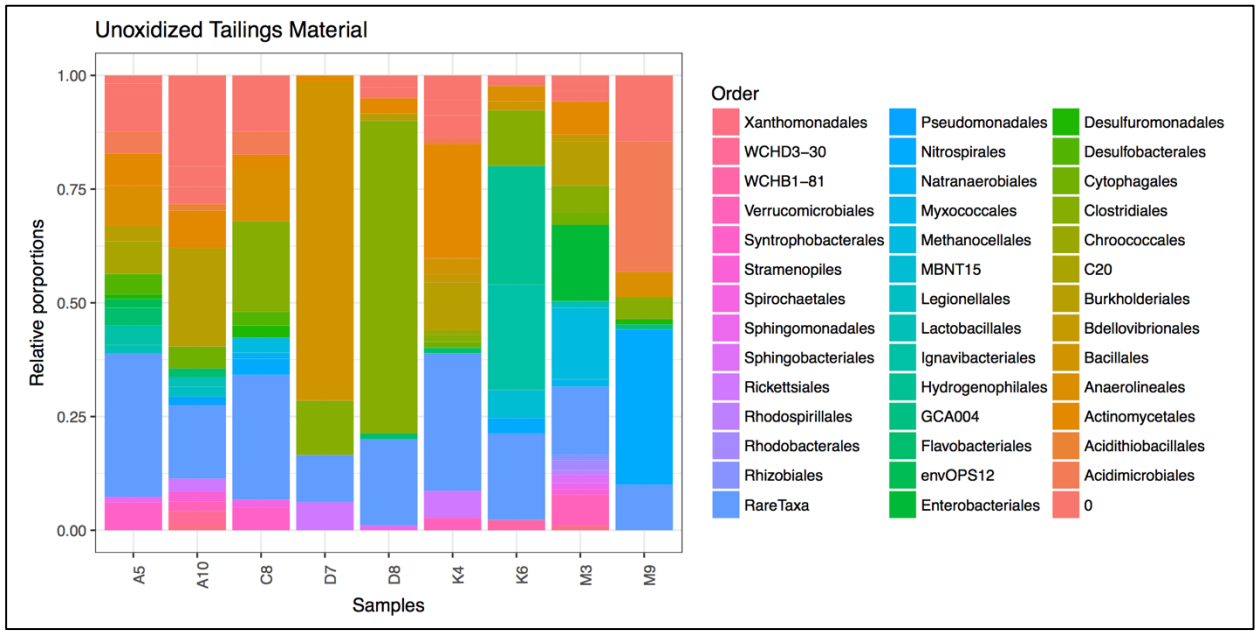

Figure 15 Percent relative abundance of the taxonomic composition at the order level for microbial communities across unoxidized tailings material across 5 tailings dam structures in Sudbury, ON.

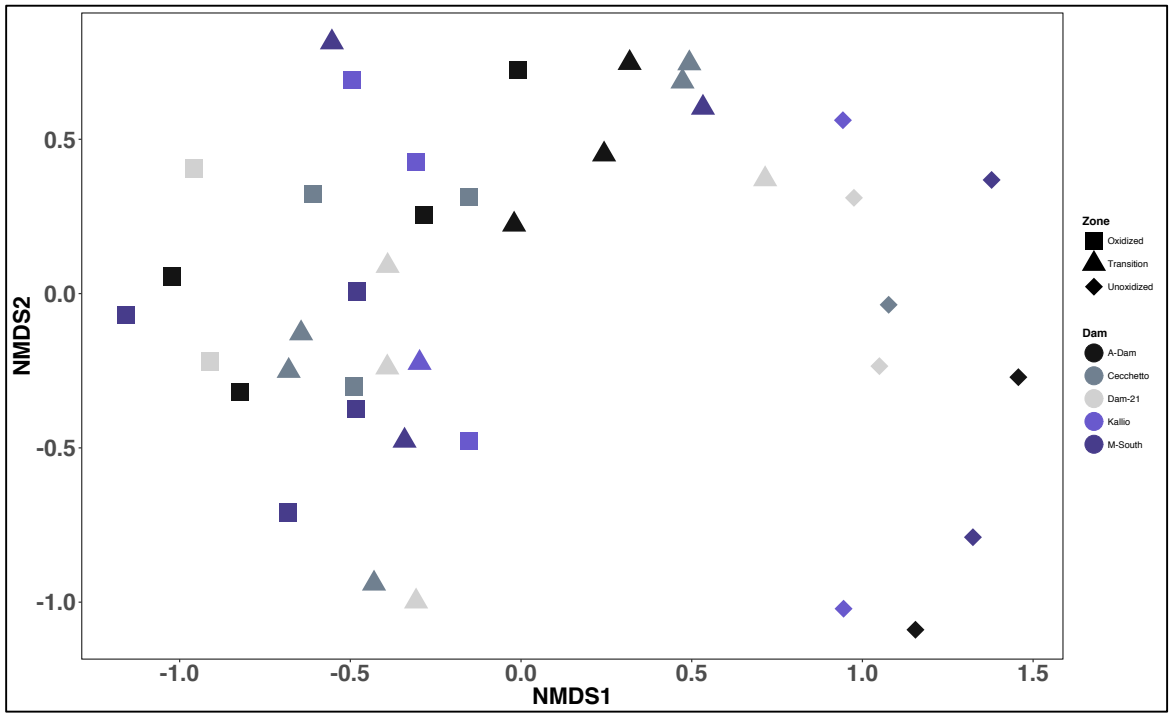

Figure 16 NMDS plot: Microbial community compositions vs. location

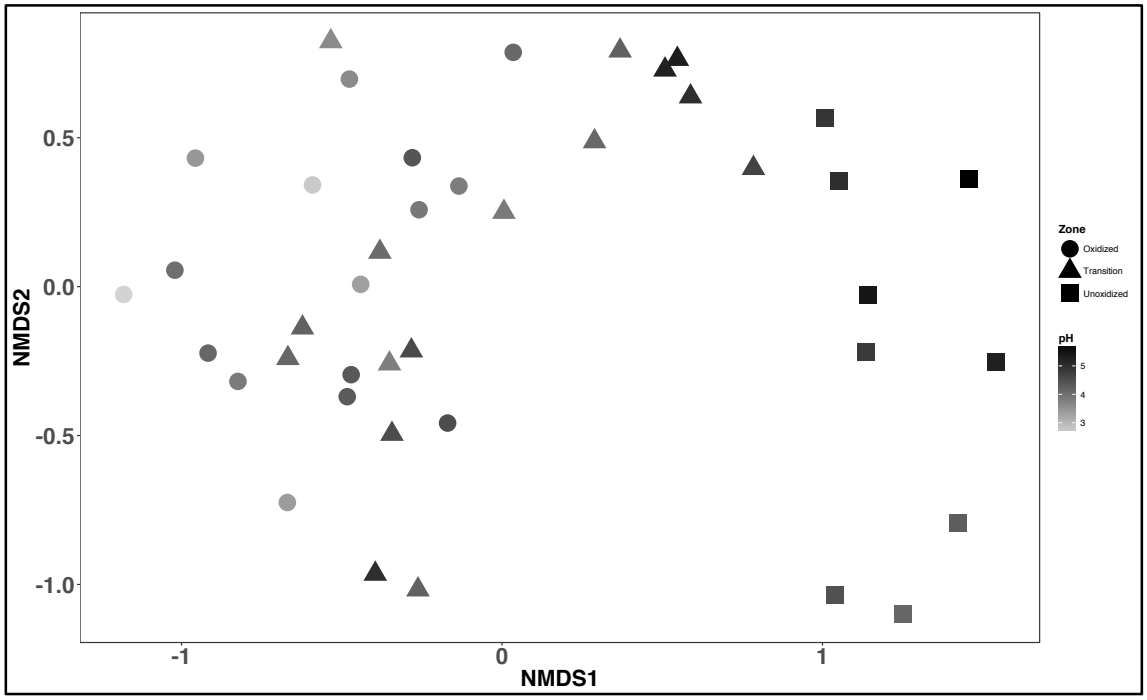

Figure 17 NMDS plot: Microbial community compositions vs. contact pH

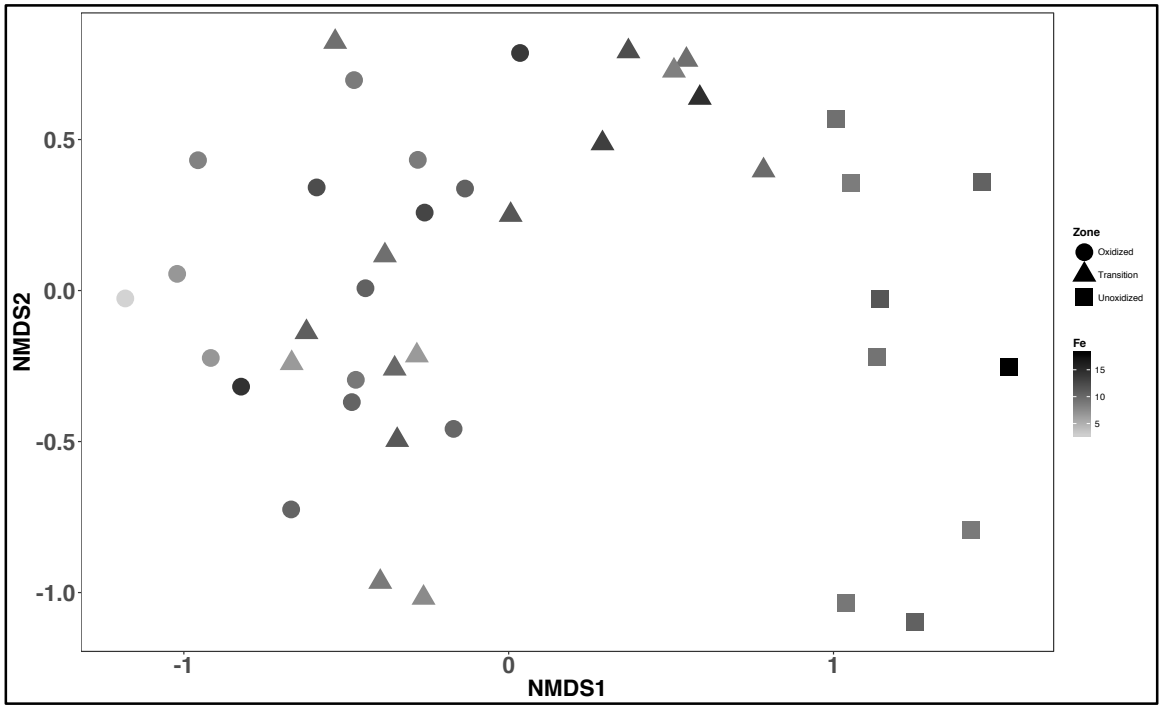

Figure 18 NMDS plot: Microbial community compositions vs. total iron (Fe) content (%)

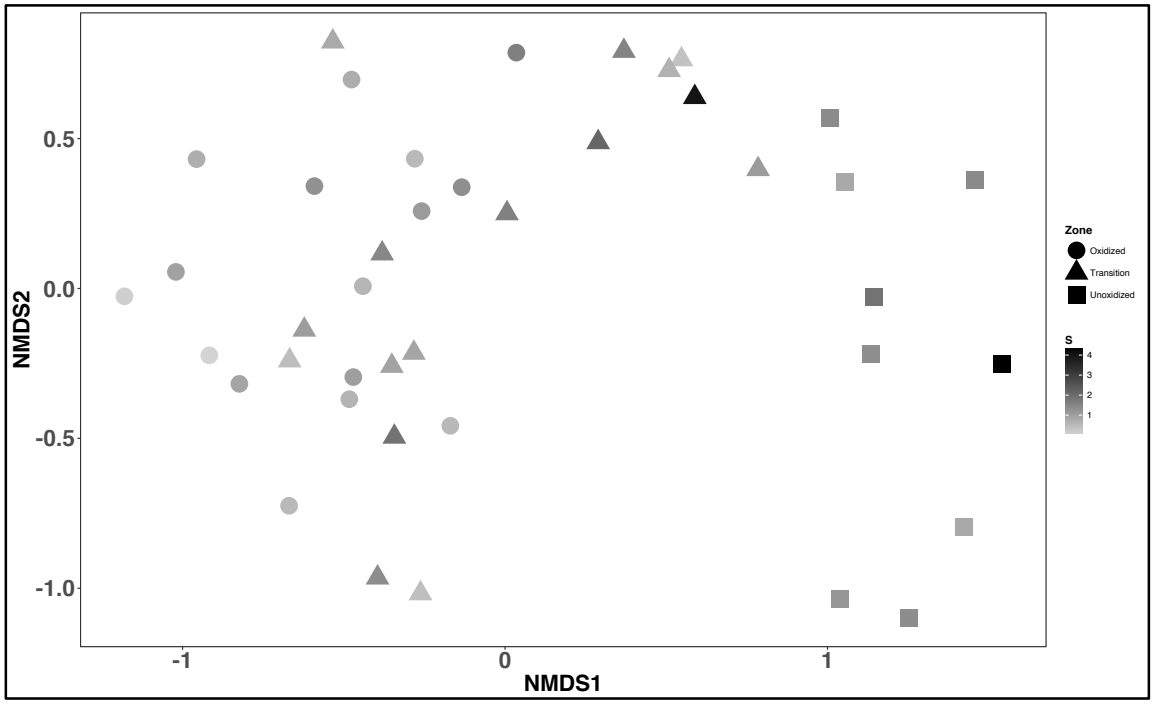

Figure 19 NMDS plot: Microbial community compositions vs. total sulfur (S) content (%)

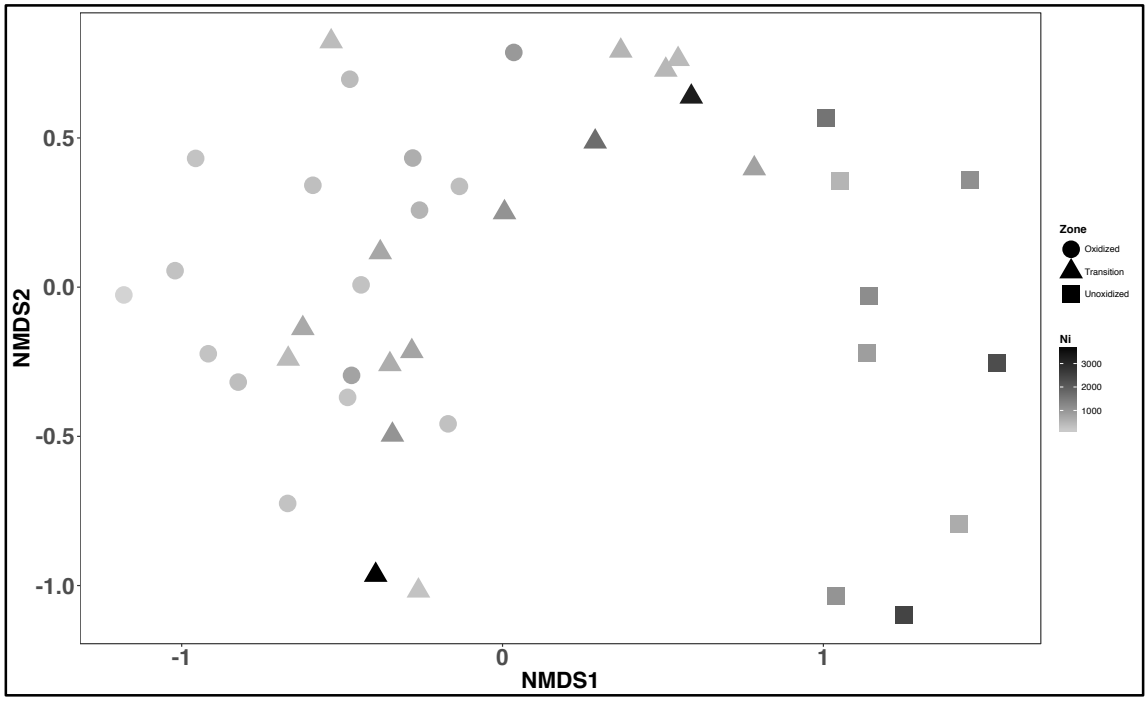

Figure 20 NMDS plot: Microbial community compositions vs. total Ni content (ppm)

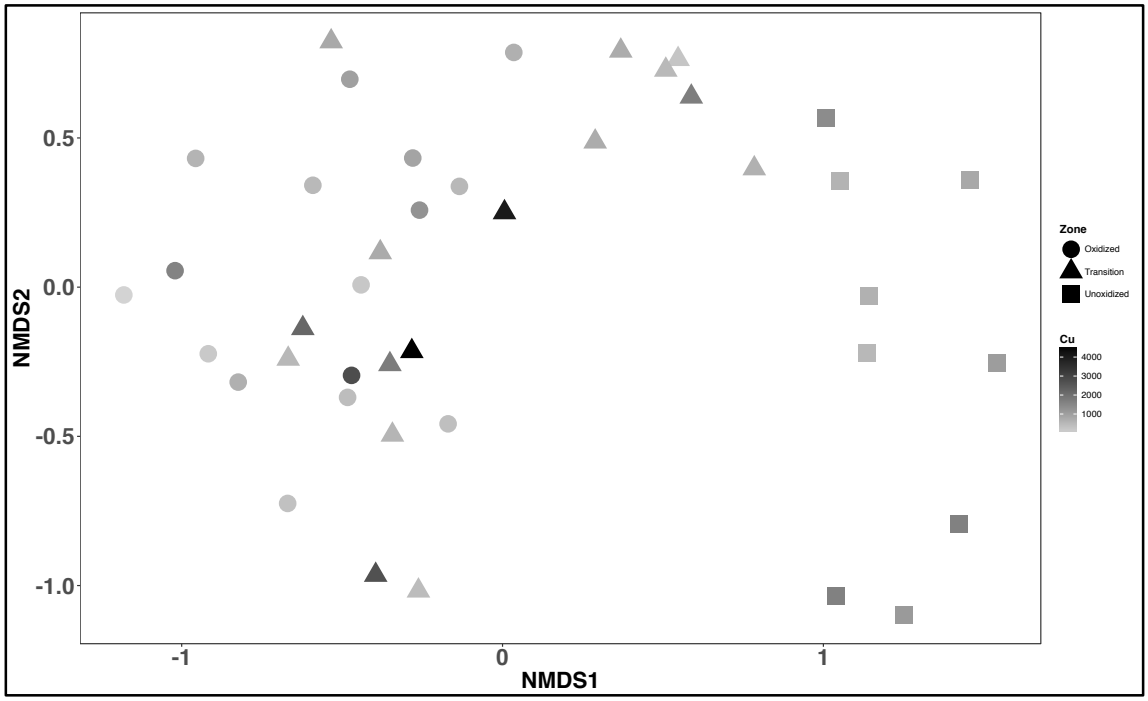

Figure 21 NMDS plot: Microbial community compositions vs. total Cu content (ppm)

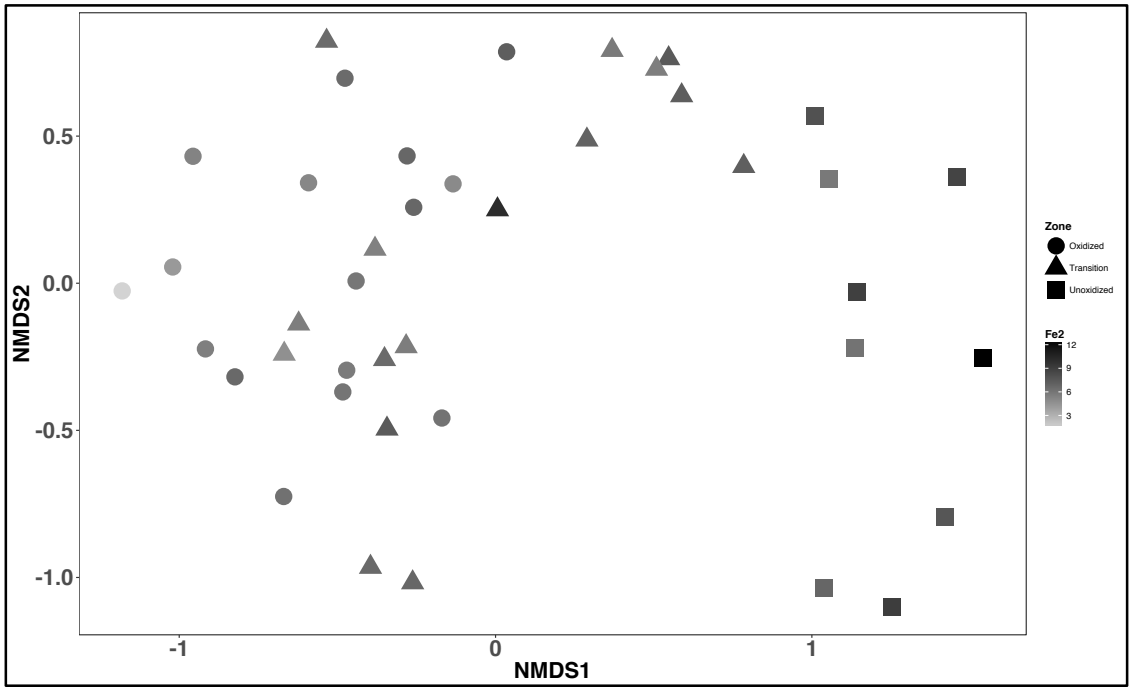

Figure 22 NMDS plot: Microbial community compositions vs. total ferrous iron content (%)

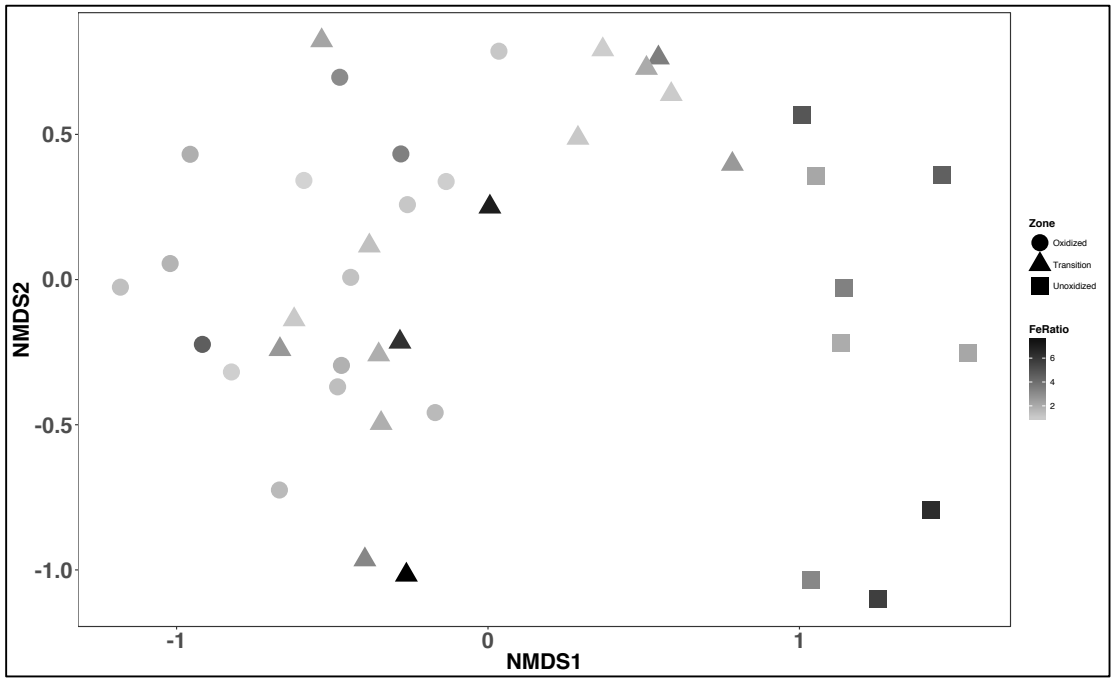

Figure 23 NMDS plot: Microbial community compositions vs. total Fe ratio

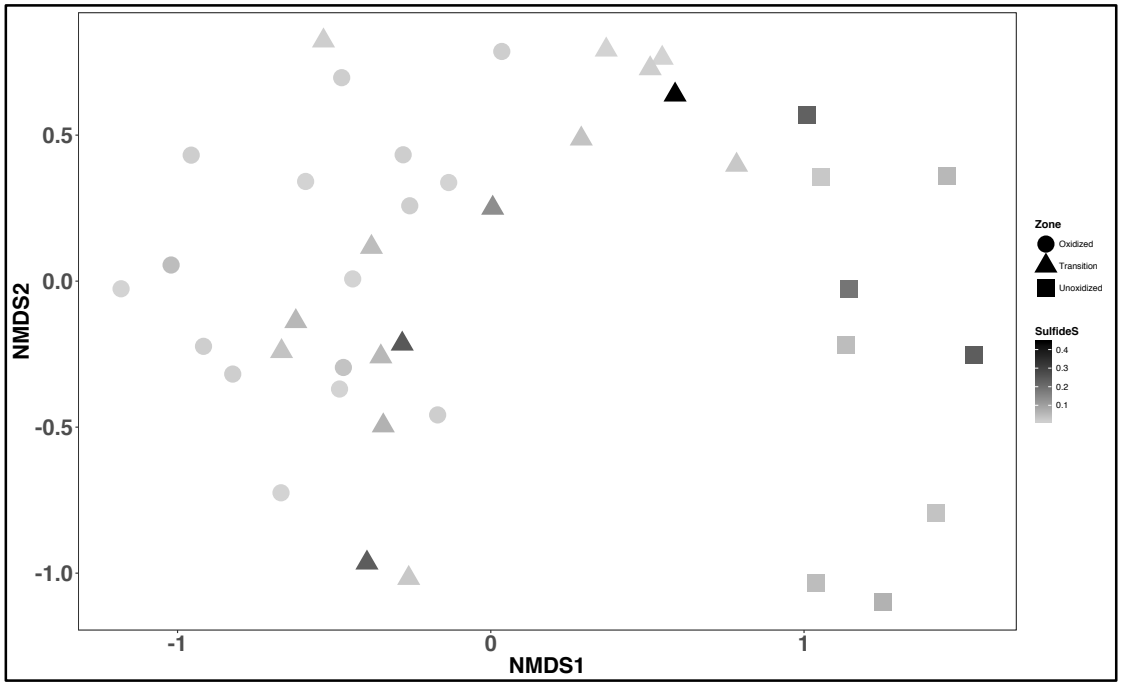

Figure 24 NMDS plot: Microbial community compositions vs. total sulfur as sulfide content (%)

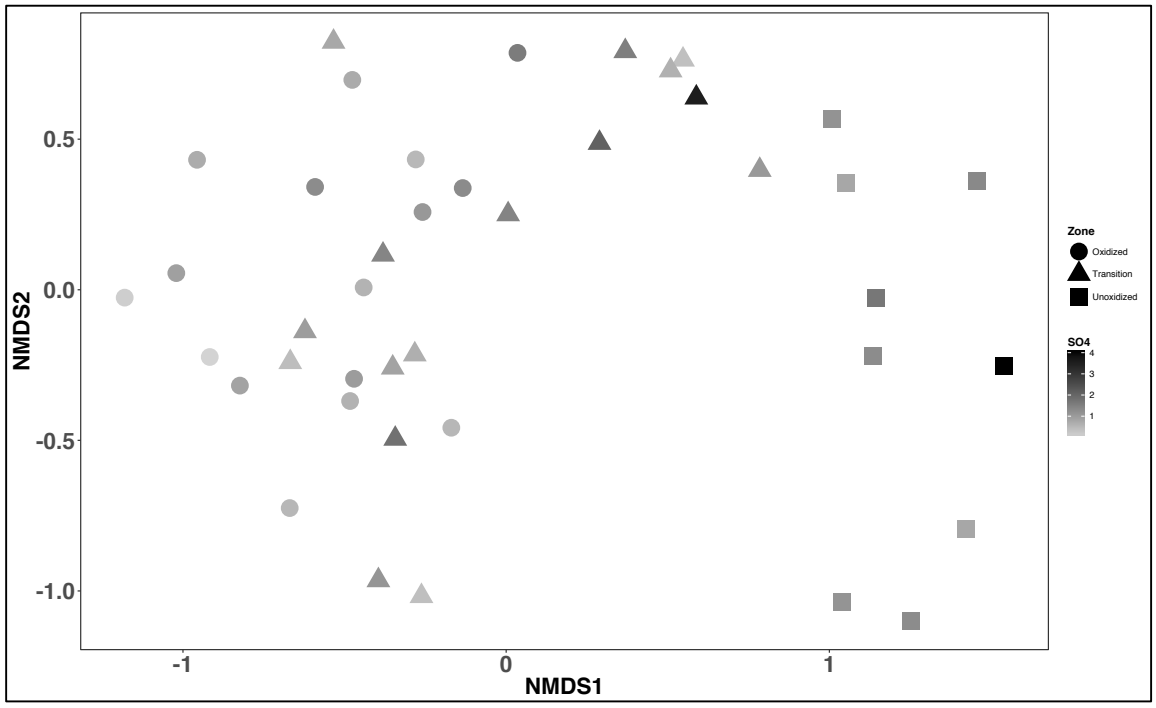

Figure 25 NMDS plot: Microbial community compositions vs. total sulfate content (%)

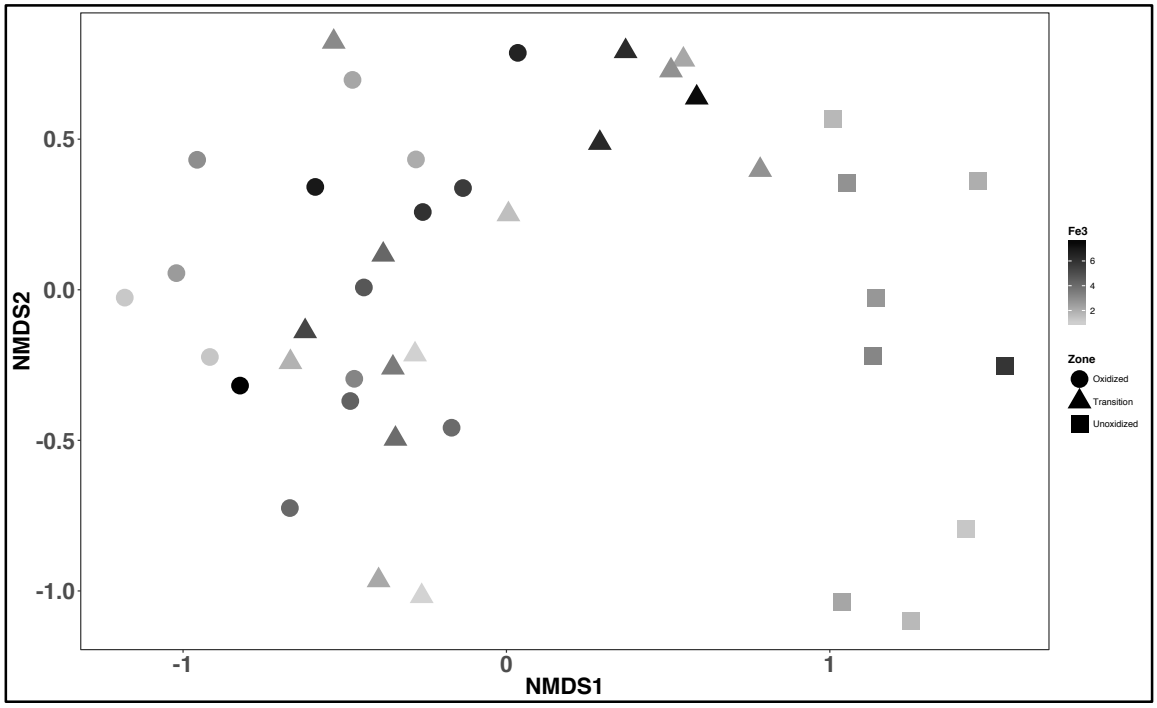

Figure 26 NMDS plot: Microbial community compositions vs. total ferric iron content (%)

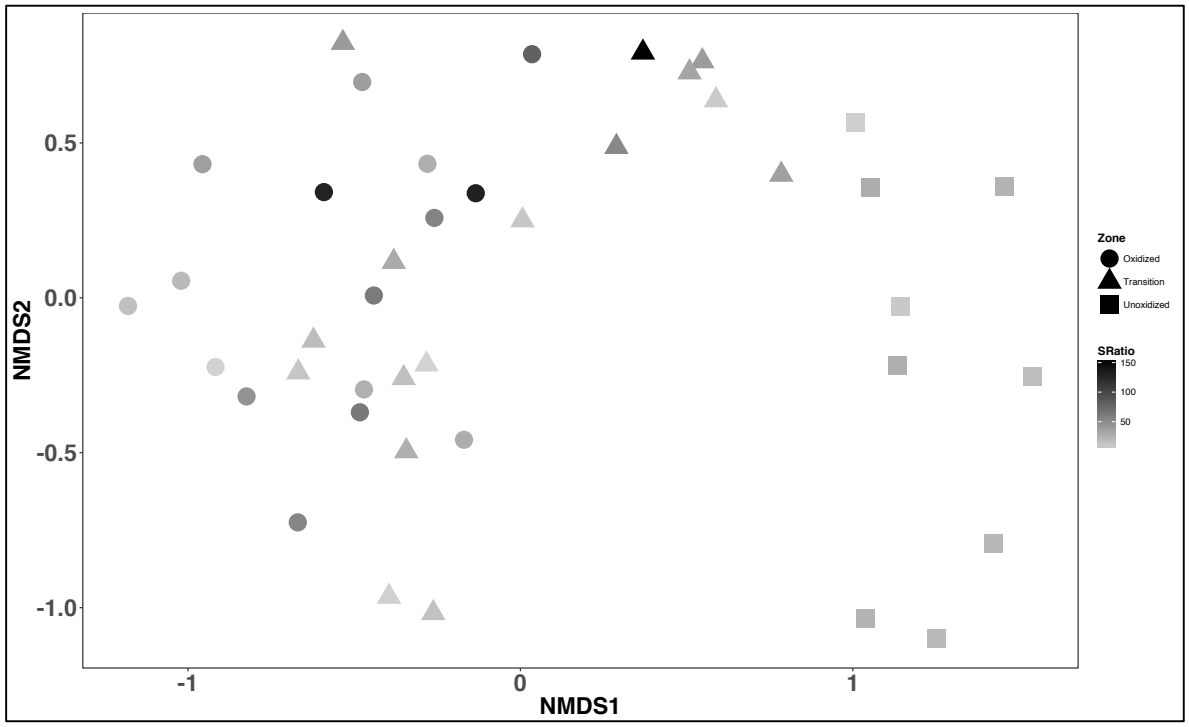

Figure 27 NMDS plot: Microbial community compositions vs. sulfur ratio

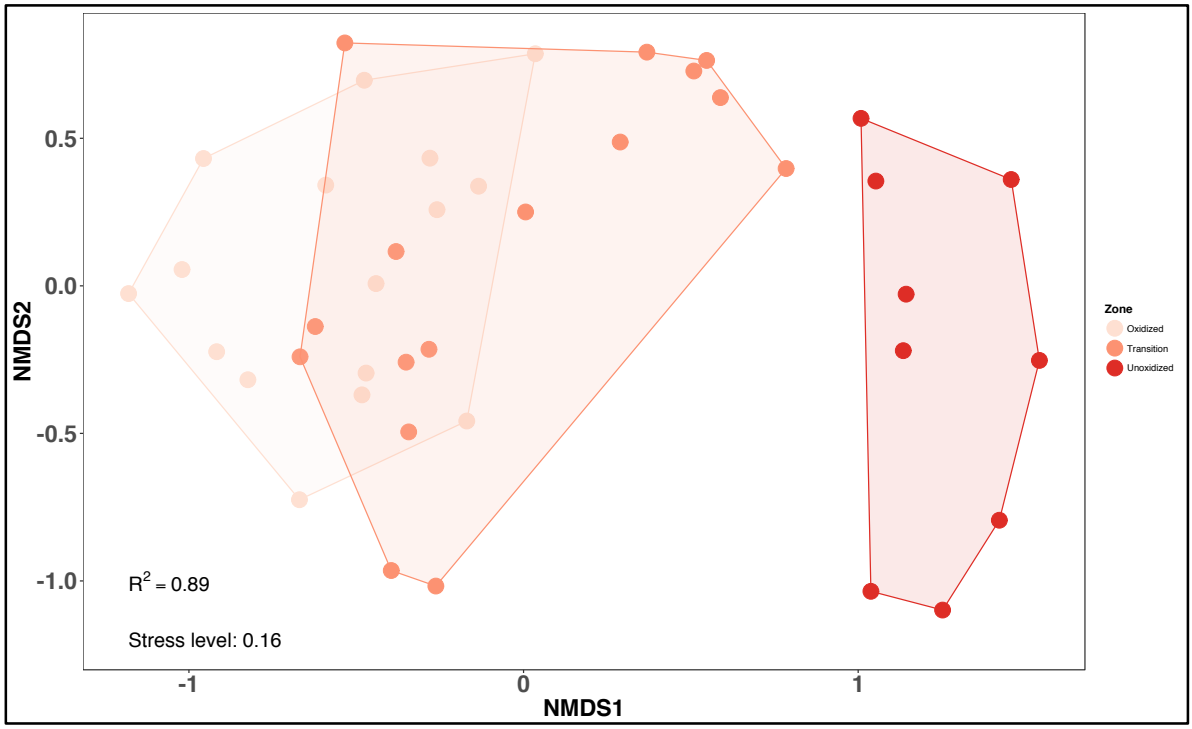

Figure 28 NMDS plot: Microbial community compositions vs. alteration zones

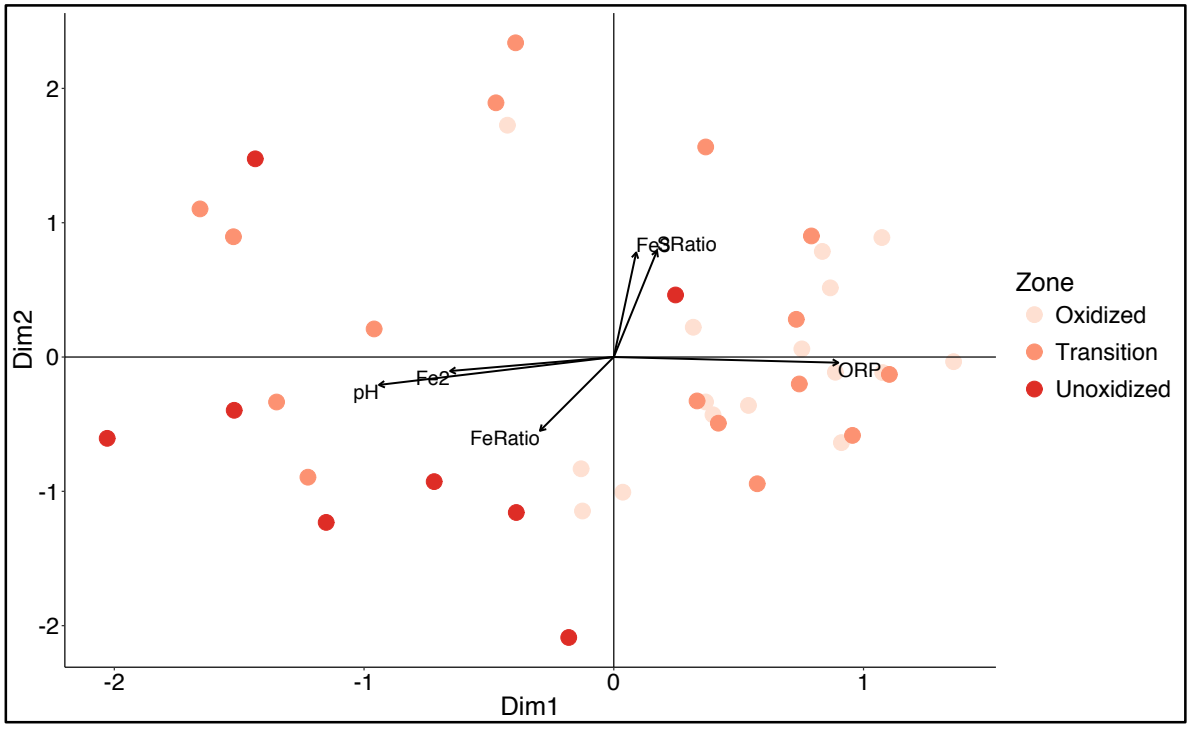

Figure 29 Redundancy analysis (RDA) exhibiting effects of environmental parameters and variables on microbial community compositions of samples. Black line vectors represent environmental parameters and variables including the following; pH, ORP, ferrous iron, ferric Fe, iron Ratio and sulfur ratio

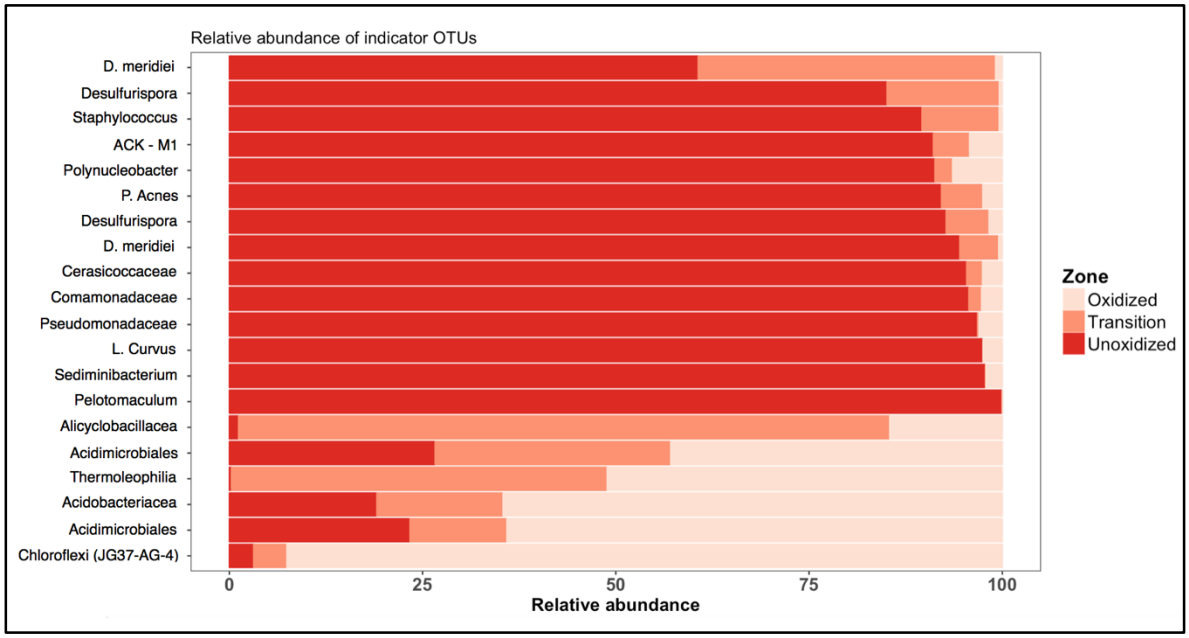

Figure 30 Indicator species analysis, exhibiting the dominant microbial members that characterize each zone (oxidized, transition, unoxidized)

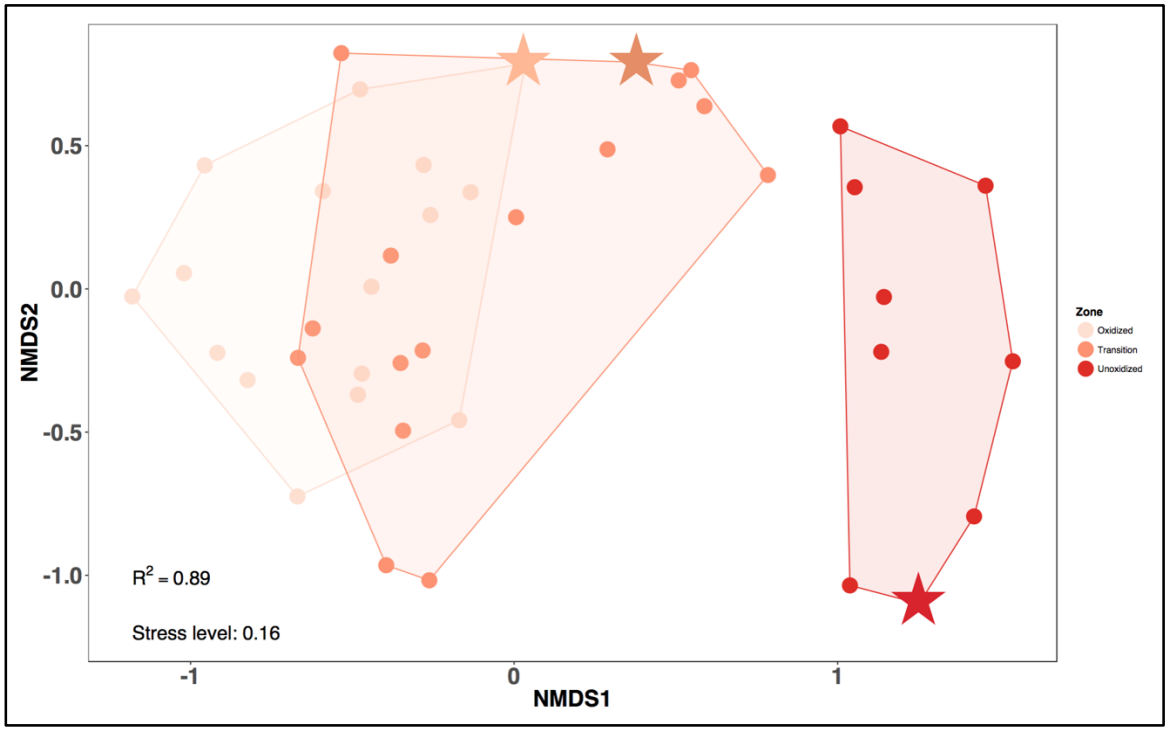

Figure 31 NMDS plot: microbial community structures with differing alteration zones Alteration zones are depicted as in Figure 27. Stars represent the three samples chosen for microscopic analysis, one in each alteration zone.

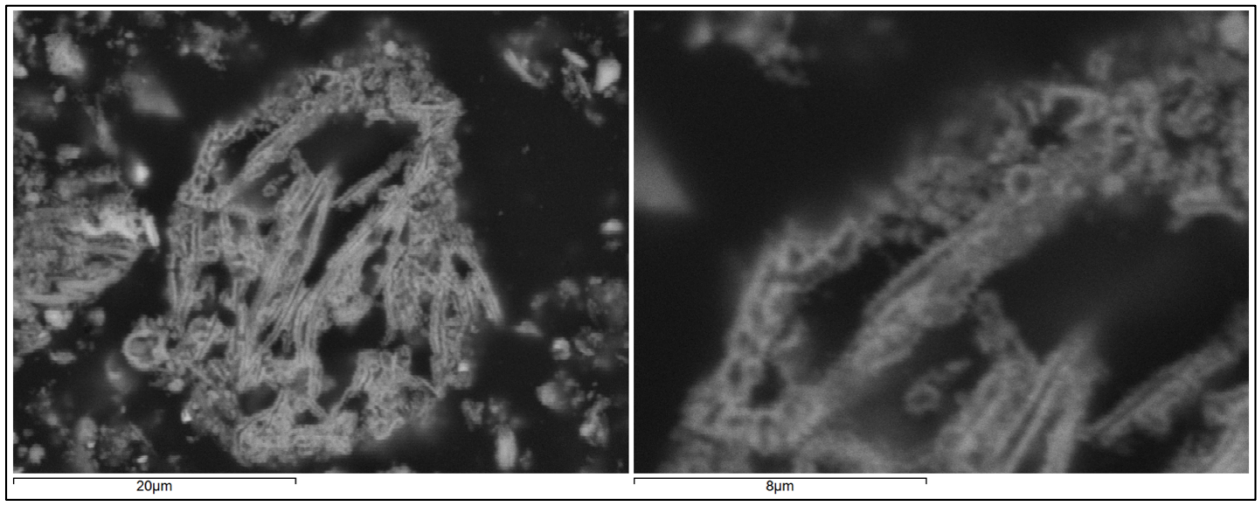

Figure 32 SEM images of oxidized tailings sample; (A) Acicular and hallow concretions of goethite (α-Ferric ironO(OH)) (B) Higher magnification of hallow concretions of goethite forming a chain-line structure

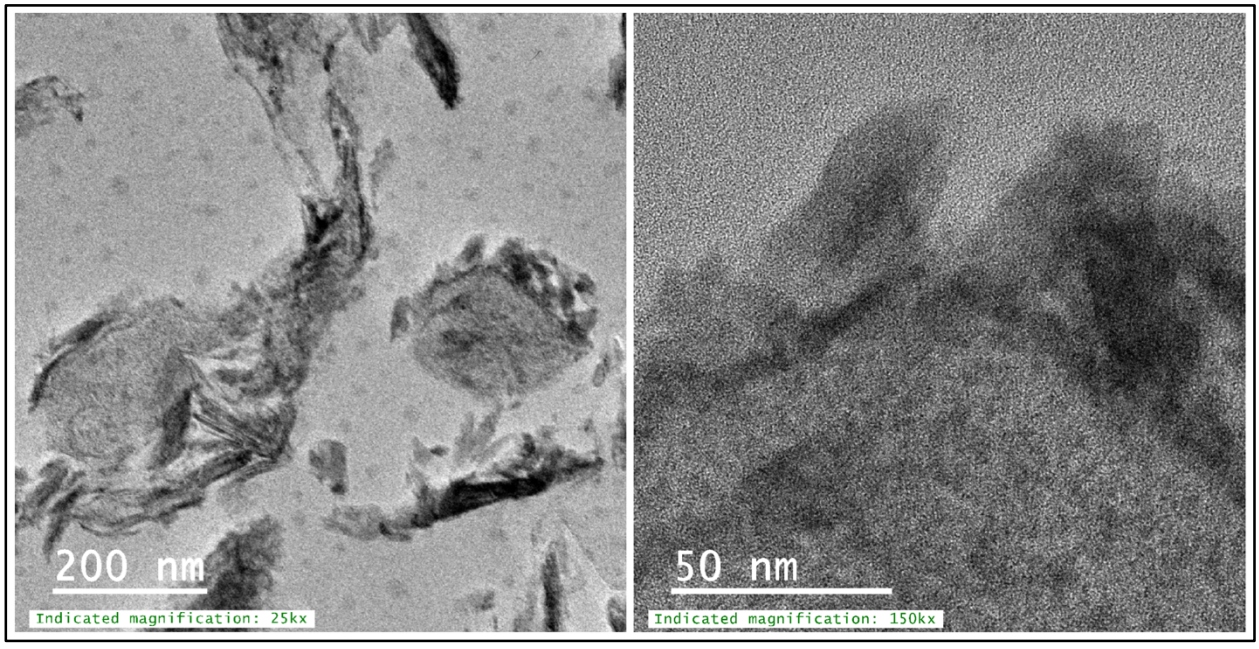

Figure 33 TEM images of tailings sample from the oxidized zone; (A) Iron-rich illite occurs as isolate acicular fragments and encrusting the two imaged microbial cells (B) Goethite occurring as nano-size grains above iron-rich illite, coating microbial outer cell wall

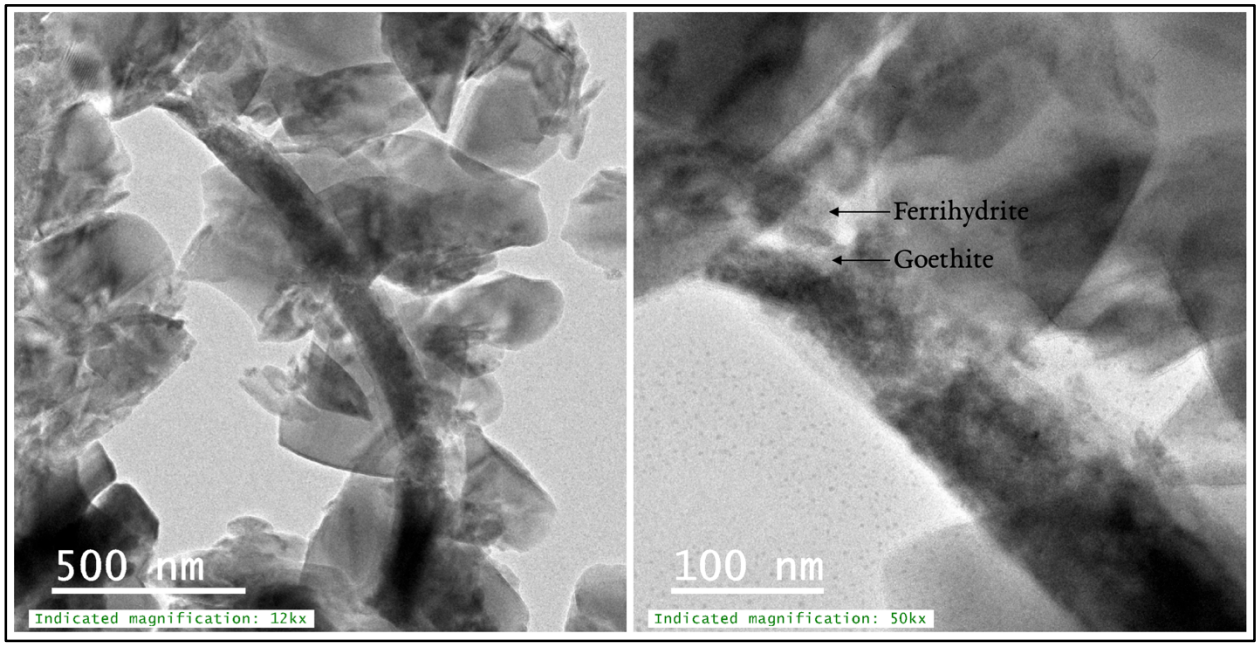

Figure 34 TEM images of tailings sample from the transition zone; (A) Rod-shaped bacterium encrusted with goethite, forming an interface with amphiboles, actinolite and pargasite (B) Ferrihydrite present in between goethite (coating microorganism) and amphibole grain

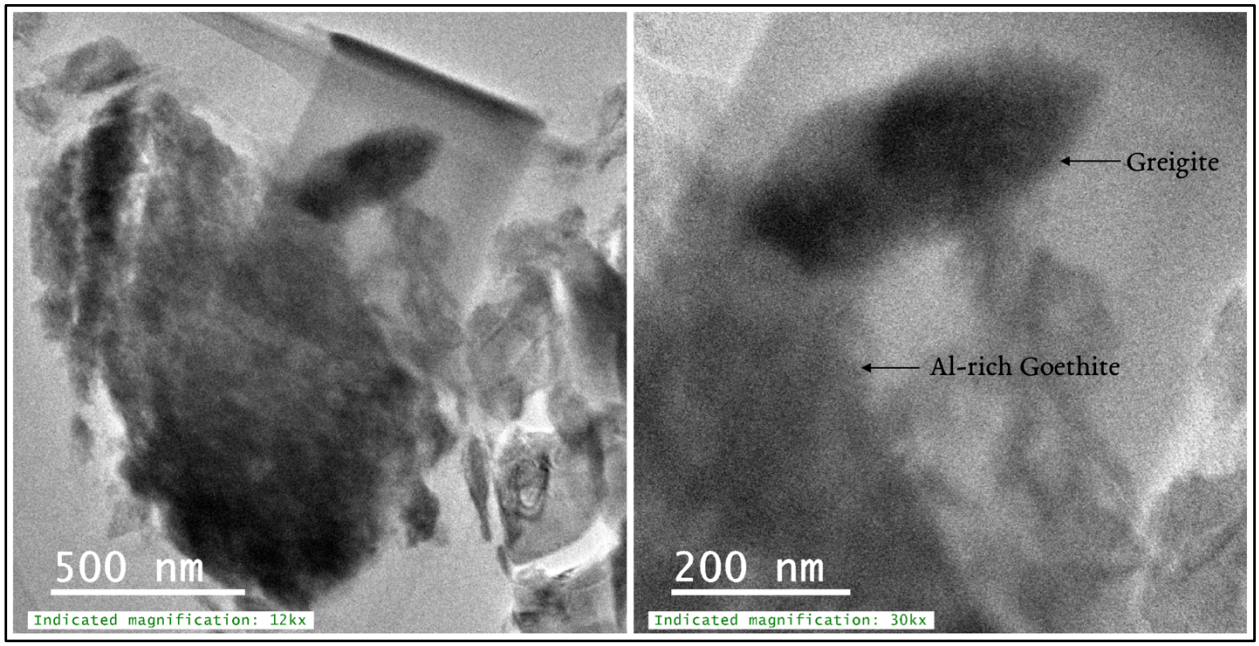

Figure 35 TEM images of tailings sample from the unoxidized zone; Greigite crystals occurring at the boundary of Al-rich goethite

References

Akai, J., Akai, K., Ito, M., Nakano, S., Maki, Y., & Sasagawa, I. (1999). Biologically induced iron ore at Gunma iron mine, Japan. American Mineralogist,84(1-2), 171-182.

Alazard, D., Joseph, M., Battaglia-Brunet, F., Cayol, J., & Ollivier, B. 2010. Desulfosporosinus acidiphilus sp. nov.: a moderately acidophilic sulfate-reducing bacterium isolated from acid mining drainage sediments. Extremophiles. 14, 305-312.

An, T. T., & Picardal, F. W. 2015. Desulfuromonas carbonis sp. nov., an Fe(III)-, S0- and Mn(IV)-reducing bacterium isolated from an active coalbed methane gas well International Journal of Systematic and Evolutionary Microbiology. 65, 1686-1693.

Baker, B. J., & Banfield, J. F. 2003. Microbial communities in acid mine drainage. FEMS Microbiology Ecology. 44, 139-152.

Bazylinski, D. A., & Frankel, R. B. (2000). Biologically Controlled Mineralization of Magnetic Iron Minerals by Magnetotactic Bacteria. Environmental Microbe-Metal Interactions, 109-144.

Bazylinski, D.A. 2002. Bacterial Mineralization. Encyclopedia of Materials: Science and Technology (Second Edition), 441-447.

Bennett, P.C., J. R. Rogers, W. J. 2001. Silicates, Silicate Weathering, and Microbial Ecology. Geomicrobiology Journal, 18 (1), 3-19.

Bilgin, A. A., Silverstein, J., & Jenkins, J. D. (2004). Iron respiration by Acidiphilium cryptum at pH 5. FEMS Microbiology Ecology,49(1), 137-143.

Bowles JFW, Howie RA, Vaughan DJ, Zussman J (2011) Non-silicates: Oxides, Hydroxides and Sulphides. Rock-Forming Minerals Vol. 5A, Geological Society, London. 920 pp

Califf, K. J., Schwarzberg-Lipson, K., Garg, N., Gibbons, S. M., Caporaso, J. G., Slots, J., Kelley, S. T. 2017. Multi-omics Analysis of Periodontal Pocket Microbial Communities Pre- and Posttreatment. MSystems, 2 (3).

Canfield, E.M., 1989. Reactive iron in marine sediments. Geochimica et Cosmochimica Acta, 53, 619-632.

Cangelosi, G. A., & Meschke, J. S. 2014. Dead or Alive: Molecular Assessment of Microbial Viability. Applied and Environmental Microbiology,80(19), 5884-5891.

Carson, J. K., Rooney, D., Gleeson, D. B., & Clipson, N. 2007. Altering the mineral composition of soil causes a shift in microbial community structure. FEMS Microbiology Ecology,61(3), 414-423.

Carson, J. K., Campbell, L., Rooney, D., Clipson, N., & Gleeson, D. B. 2009. Minerals in soil select distinct bacterial communities in their microhabitats. FEMS Microbiology Ecology,67 (3), 381-388.

Castelle, C. J., Roger, M., Bauzan, M., Brugna, M., Lignon, S., Nimtz, M., Guiral, M. 2015. The aerobic respiratory chain of the acidophilic archaeon Ferroplasma acidiphilum : A membrane-bound complex oxidizing ferrous iron. Biochimica et Biophysica Acta (BBA)-Bioenergetics, 1847 (8), 717-728.

Castro, H. 2000. Phylogeny of sulfate-reducing bacteria. FEMS Microbiology Ecology, 31 (1), 1-9.

Chen, Y., Li, J., Chen, L., Hua, Z., Huang, L., Liu, J., . . . Shu, W. (2014). Biogeochemical Processes Governing Natural Pyrite Oxidation and Release of Acid Metalliferous Drainage. Environmental Science & Technology,48(10), 5537-5545.

Chen, Y., Li, Y.L., Zhou, G.T., Li, H., Lin, Y., Xiao, X., Wang F. 2014. Biomineralization mediated by anaerobic methane-consuming cell consortia. Scientific Reports.

Clark, D. A., & Norris, P. R. 1996. Acidimicrobium ferrooxidans gen. nov., sp. nov.: mixed-culture ferrous iron oxidation with Sulfobacillus species. Microbiology, 142 (4), 785-790.

Cornell, R. M., & Schwertmann, U. 2006. The Iron Oxides: Structures, Properties, Reactions, Occurrences and Uses (2nd ed.). Wiley-VCH.

Crundwell, F. (2014). The mechanism of dissolution of minerals in acidic and alkaline solutions: Part III. Application to oxide, hydroxide and sulfide minerals. *Hydrometallurgy,149*, 71-81.

Cudennec, Y., & Lecerf, A. 2006. The transformation of ferrihydrite into goethite or hematite, revisited. Journal of Solid State Chemistry, 179 (3), 716-722.

Cummings, D.E., March, A.W., Bostick, B., Spring, S., Caccavo, F., Fendorf, S., Rosenzweig, R.F. 2000. Evidence for Microbial Fe(III) Reduction in Anoxic, Mining-Impacted Lake Sediments (Lake Coeur d'Alene, Idaho) Applied and Environmental Microbiology 66(1), 154–162.

Das, S., Hendry, M. J., & Essilfie-Dughan, J. 2011. Transformation of Two-Line Ferrihydrite to Goethite and Hematite as a Function of pH and Temperature. Environmental Science & Technology, 45 (1), 268-275.

De Yoreo, J. J., Gilbert, P. U., Sommerdijk, N. A., Penn, R. L., Whitelam, S., Joester, D., Dove, P. M. 2015. Crystallization by particle attachment in synthetic, biogenic, and geologic environments. Science, 349.

Dekov, V. M., Kamenov, G. D., Stummeyer, J., Thiry, M., Savelli, C., Shanks, W. C., Vértes, A. 2007. Hydrothermal nontronite formation at Eolo Seamount (Aeolian volcanic arc, Tyrrhenian Sea). Chemical Geology,245(1-2), 103-119.

Dick, G. J., & Lam, P. 2015. Omic Approaches to Microbial Geochemistry. Elements,11, 403-408.

Dockrey, J., Lindsay, M., Mayer, K., Beckie, R., Norlund, K., Warren, L., & Southam, G. (2014). Acidic Microenvironments in Waste Rock Characterized by Neutral Drainage: Bacteria–Mineral Interactions at Sulfide Surfaces. Minerals,4(1), 170-190.

Dutrizac, J. E., & Jambor, J. L. 2000. Jarosites and Their Application in Hydrometallurgy. Reviews in Mineralogy and Geochemistry, 40 (1), 405-452.

Elferink, O. S. J. W. H., Vliet, W. M., Bogte, J. J., & Stams, A. J. 1999. Desulfobacca acetoxidans gen. nov., sp. nov., a novel acetate-degrading sulfate reducer isolated from sulfidogenic granular sludge. International Journal of Systematic Bacteriology, 49 (2), 345-350.

Emerson D., 2000. Microbial Oxidation of Fe(ll) and Mn (ll) at circumneutral pH. Environmental microbe-metal interactions. ASM Press, Washington, DC. 31-52.

Engelbrektson, A., Hubbard, C. G., Tom, L. M., Boussina, A., Jin, Y. T., Wong, H., . . . Coates, J. D. 2014. Inhibition of microbial sulfate reduction in a flow-through column system by (per)chlorate treatment. Frontiers in Microbiology.

Fang, Q., Churchman, G. J., Hong, H., Chen, Z., Liu, J., Yu, J., Furnes, H. 2017. New insights into microbial smectite illitization in the Permo-Triassic boundary K-bentonites, South China. Applied Clay Science, 140, 96-111.

Ferris, F., Fyfe, W., & Beveridge, T. 1991. Bacteria as Nucleation Sites for Authigenic Minerals. Diversity of Environmental Biogeochemistry Developments in Geochemistry,319-325.

Ferris, F. G. 1997. Formation of authigenic minerals by bacteria. In: Biological-Mineral Interactions. Mineralogical Associaiton of Canada Short Course Series, 25, 295-323

Fortin, D., & Beveridge, T. J. (1997). Microbial sulfate reduction within sulfidic mine tailings: Formation of diagenetic Fe sulfides. Geomicrobiology Journal,14(1), 1-21.

Fortin, D., & Langley, S. 2005. Formation and occurrence of biogenic iron-rich minerals. Earth-Science Reviews, 72 (1-2), 1-19.

Fossing, H., Nielson, H.P., Schultz, H., et al. 1995. Concentration and transport of nitrate my mat-forming sulfur bacterium *Thioploca*. Nature, 374.

Glasauer, S., Langley, S., & Beveridge, T. J. (2001). Sorption of Fe (Hydr)Oxides to the Surface of Shewanella putrefaciens: Cell-Bound Fine-Grained Minerals Are Not Always Formed De Novo. *Applied and Environmental Microbiology,67*(12), 5544-5550.

Göker, M., Teshima, H., Lapidus, A., Nolan, M., Lucas, S., Hammon, N., Klenk, H. 2011. Complete genome sequence of the acetate-degrading sulfate reducer Desulfobacca acetoxidans type strain (ASRB2T). Standards in Genomic Sciences, 4(3), 393-401.

Goldhaber, M.B., 1983. Experimental study of the metasTable sulfur oxyanion formation during pyrite oxidation at pH 6-9 at 30°C. American Journal of Science, 283, 193-217

Gunsinger, M. R., Ptacek, C. J., Blowes, D. W., & Jambor, J. L. (2006). Evaluation of long-term sulfide oxidation processes within pyrrhotite-rich tailings, Lynn Lake, Manitoba. Journal of Contaminant Hydrology, 83, 149-170.

Guo, X., You, X., Liu, L., Zhang, J., Liu, S., & Jiang, C. 2009. Alicyclobacillus aeris sp. nov., a novel ferrous- and sulfur-oxidizing bacterium isolated from a copper mine. International Journal of Systematic and Evolutionary Microbiology, 59 (10), 2415-2420.

Guo, W., Zhang, H., Zhou, W., Wang, Y., Zhou, H., & Chen, X. 2016. Sulfur Metabolism Pathways in Sulfobacillus acidophilus TPY, A Gram-Positive Moderate Thermoacidophile from a Hydrothermal Vent. Frontiers in Microbiology, 7.

Gupta, A., Dutta, A., Sarkar, J., Paul, D., Panigrahi, M. K., & Sar, P. 2017. Metagenomic exploration of microbial community in mine tailings of Malanjkhand copper project, India. GenomicsData, 12, 11-13.

Hallberg, K. B., González-Toril, E., & Johnson, D. B. 2010. Acidithiobacillus ferrivorans, sp. nov.; facultatively anaerobic, psychrotolerant iron-, and sulfur-oxidizing acidophiles isolated from metal mine-impacted environments. Extremophiles, 14 (1), 9-19.

Hansel, C. M., Ferdelman, T. G., Tebo, B. M. 2015. Cryptic cross-linkages among biogeochemical cycles: Novel insights from reactive intermediates. Elements,11, 409-414.

Hayat, M. 1986. Rinsing, Dehydration, and Embedding. Basic Techniques for Transmission Electron Microscopy, 56-125.

Hinrichs, K., Hayes, J. M., Sylva, S. P., Brewer, P. G., & Delong, E. F. 1999. Methane-consuming archaebacteria in marine sediments. Nature, 398 (6730), 802-805.

Hunger, S., & Benning, L. G. 2007. Greigite: a true intermediate on the polysulfide pathway to pyrite. Geochemical Transactions, 8(1).

Ingledew, W.J., Cox, J.C., Halling, P.J., 1997. A proposed mechagnism for energy conservation during Fe(ll) oxidation by Thiobacillus ferro-oxidans: chemiosmotic coupling to net H+ influx. FEMS Mirobiology Letters, 2, 193-197.

Itoh, T., Yamanoi, K., Kudo, T., Ohkuma, M., & Takashina, T. 2010. Aciditerrimonas ferrireducens gen. nov., sp. nov., an iron-reducing thermoacidophilic actinobacterium isolated from a solfataric field. International Journal of Systematic And Evolutionary Microbiology, 61 (6), 1281-1285.

Blowes, D.W., Jambor, J.L., 1990. The pore-water geochemistry and the mineralogy of the vadose zone of sulfide tailings, Waite Amulet, Quebec, Canada. Appl. Geochem. 5, 327–346.

Jambor, J.L., Owens, D.R. 1993, Mineralogy of the tailings impoundment at the former Cu-Ni deposit of Nickel Rim Mines Ltd., eastern edge of the Sudbury structure, Ontario. Division Report MSL 93-4 (CF), CANMET, Energy, Mines and Resources, Canada

Jambor, J.L. 1994. Mineralogy of sulfide-rich tailings and their oxidation products. Environmental Geochemistry of Sulfidic Mine Wastes. Mineralogical Association of Canada, 22, 59-102

Jamieson, H. E. 2011. Geochemistry and Mineralogy of Solid Mine Wastes: Essential Knowledge for Predicting Environmental Impact. Elements, 7, 381-386.

Jiang, C., Liu, Y., Liu, Y., You, X., Guo, X., & Liu, S. 2008. Alicyclobacillus ferrooxydans sp. nov., a ferrous-oxidizing bacterium from solfataric soil. International Journal of Systematic and Evolutionary Microbiology, 58 (12), 2898-2903.

Johnson, D. B., Ghauri, M. A., & McGinness, S. 1993. Biogeochemical cycling of iron and sulphur in leaching environments. FEMS Microbiology Reviews, 11, 63-70.

Johnson, D. B., & Roberto, F. F. 1997. Heterotrophic Acidophiles and Their Roles in the Bioleaching of Sulfide Minerals. Biomining,259-279.

Johnson, D. B., Bridge, T. A. M. 1998. Reduction of Soluble Iron and Reduction Dissolution of Ferric Iron-Containing Minerals by Moderately Thermophilic Iron-Oxidizing Bacteria. Applied and Environmental Microbiology, 2181-2186

Johnson, D.B., 2015. Bergeys manual of systematics of Archaea and Bacteria. John Wiley & Sons, Inc.

Kaksonen, A. H., Spring, S., Schumann, P., Kroppenstedt, R. M., & Puhakka, J. A. 2007. Desulfurispora thermophila gen. nov., sp. nov., a thermophilic, spore-forming sulfate-reducer isolated from a sulfidogenic fluidized-bed reactor. International Journal of Systematic and Evolutionary Microbiology,57(5), 1089-1094.

Karnachuk, O. V., Gerasimchuk, A. L., Banks, D., Frengstad, B., Stykon, G. A., Tikhonova, Z. L., Pimenov, N. V. 2009. Bacteria of the sulfur cycle in the sediments of gold mine tailings, Kuznetsk Basin, Russia. Microbiology,78(4), 483-491.

Kawaichi, S., Ito, N., Kamikawa, R., Sugawara, T., Yoshida, T., & Sako, Y. 2013. Ardenticatena maritima gen. nov., sp. nov., a ferric iron- and nitrate-reducing bacterium of the phylum Chloroflexi isolated from an iron-rich coastal hydrothermal field, and description of Ardenticatenia classis nov. International Journal of Systematic and Evolutionary Microbiology, 63 (8), 2992-3002.

Kim, J. 2004. Role of Microbes in the Smectite-to-Illite Reaction. Science, 303 (5659), 830-832.

Klenk, H., Lapidus, A., Chertkov, O., Copeland, A., Rio, T. G., Nolan, M., . . . Eisen, J. A. 2011. Complete genome sequence of the thermophilic, hydrogen-oxidizing Bacillus tusciae type strain (T2T) and reclassification in the new genus, Kyrpidia gen. nov. as Kyrpidia tusciae comb. nov. and emendation of the family Alicyclobacillaceae da Costa and Rainey, 2010. Standards in Genomic Sciences, 5 (1), 121-134.

Klotz, M., & Bryant, D. 2011. The microbial sulfur cycle. Frontiers Research Topics.

Konhauser, K. O., & Urrutia, M. M. 1999. Bacterial clay authigenesis: a common biogeochemical process. Chemical Geology, 161 (4), 399-413.

Konhauser, K. (2007). Introduction to Geomicrobiology. Blackwell Science Ltd.

Korehi, H., Blöthe, M., Sitnikova, M. A., Dold, B., & Schippers, A. (2013). Metal Mobilization by Iron- and Sulfur-Oxidizing Bacteria in a Multiple Extreme Mine Tailings in the Atacama Desert, Chile. *Environmental Science & Technology,47*(5), 2189-2196.

Korehi, H., Blöthe, M., & Schippers, A. 2014. Microbial diversity at the moderate acidic stage in three different sulfidic mine tailings dumps generating acid mine drainage. Research in Microbiology, 165(9), 713-718.

Larrson, L., Gunnel, O., Holst, O., Karlsson, H.T. 1993. Oxidation of pyrite by Acidianus brierleyi: importance of close contact between pyrite and the microorganism. Biotechnology Letters, 15, 99-104.

Lee, S. D. 2016. Paenibacillus cavernae sp. nov., isolated from soil of a natural cave. International Journal of Systematic and Evolutionary Microbiology, 66(2), 598-603.

Lefevre, C. T., Menguy, N., Abreu, F., Lins, U., Posfai, M., Prozorov, T., . . . Bazylinski, D. A. 2011. A Cultured Greigite-Producing Magnetotactic Bacterium in a Novel Group of Sulfate-Reducing Bacteria. Science, 334 (6063), 1720-1723.

Li, Y., Jia, Z., Sun, Q., Zhan, J., Yang, Y., & Wang, D. 2016. Ecological restoration alters microbial communities in mine tailings profiles. Scientific Reports,6(1).

Lindsay, M. B., Condon, P. D., Jambor, J. L., Lear, K. G., Blowes, D. W., & Ptacek, C. J. 2009. Mineralogical, geochemical, and microbial investigation of a sulfide-rich tailings deposit characterized by neutral drainage. Applied Geochemistry,24(12), 2212-2221.

Lindsay, M. B., Moncur, M. C., Bain, J. G., Jambor, J. L., Ptacek, C. J., & Blowes, D. W. 2015. Geochemical and mineralogical aspects of sulfide mine tailings. Applied Geochemistry,57, 157-177.

Liu, D., Dong, H., Bishop, M. E., Zhang, J., Wang, H., Xie, S., Eberl, D. D. 2012. Microbial reduction of structural iron in interstratified illite-smectite minerals by a sulfate-reducing bacterium. Geobiology,10(2), 150-162.

Liu, J., Hua, Z., Chen, L., Kuang, J., Li, S., Shu, W., & Huang, L. 2014. Correlating Microbial Diversity Patterns with Geochemistry in an Extreme and Heterogeneous Environment of Mine Tailings. Applied and Environmental Microbiology,80(12), 3677-3686.

Liu, D., Dong, H., Wang, H., & Zhao, L. 2015. Low-temperature feldspar and illite formation through bioreduction of Fe(III)-bearing smectite by an alkaliphilic bacterium. Chemical Geology,406, 25-33.

Lottermoser, B. 2007 Mine Wastes Characterization, Treatment and Environmental Impacts (2nd ed.). Springer Berlin.

Lovley, D.R., Woodward. J.C., Chapelle F.H, Landa, R. 1991. Microbial reduction of uranium. Nature, 350, 413-416

Lovley, D. (1993). Dissimilatory Metal Reduction. Annual Review of Microbiology,47(1), 263-290.

Lovley, D.R., Holmes, D.E., Nevin, K.P., 2004. Dissimilatory Fe(lll) and Mn (IV) reduction. Advances in Microbial Physiology, 49, 219-286

Lower, S.K., Hochella, M.F Jr., Beveridge, T.J., 2001. Bacterial recognition of mineral surfaces: nanoscale interactions between Schwanella and –FeOOH. Science, 292, 1360-1363

Mandic-Mulec, I., Stefanic, P., & Elsas, J. D. 2016. Ecology of Bacillaceae. The Bacterial Spore: from Molecules to Systems,59-85.

Mauck, B. S., & Roberts, J. A. 2007. Mineralogic Control on Abundance and Diversity of Surface-Adherent Microbial Communities. Geomicrobiology Journal,24(3-4), 167-177.

McGregor, R. G., Blowes, D. W., Jambor, J. L., Robertson, W. D. 1998. The solid-phase controls on the mobility of heavy metals at the Copper Cliff tailings area, Sudbury, Ontario, Canada. Journal of Contaminant Hydrology,33, 247-271.

Melton, E. D., Swanner, E. D., Behrens, S., Schmidt, C., & Kappler, A. 2014. The interplay of microbially mediated and abiotic reactions in the biogeochemical Fe cycle. Nature Reviews Microbiology.

Menndez-Garcia, C., Pelã¡ez, A. I., Mesa, V., Sã¡nchez, J., Golyshina, O. V., & Ferrer, M. 2015. Microbial diversity and metabolic networks in acid mine drainage habitats. Frontiers in Microbiology,6.

Michel, F.M., Ehm, L., Antao, S.M., Lee, P.L., Chupa, P.J., Liu, G., Strongin, D.R., Schoonen, M.A.A., Phillips, B.L., Parise, J.B. 2007. The Structure of Ferrihydrite, a Nanocrystalline Material. Science, 316.

Moncur, M., Jambor, J., Ptacek, C., & Blowes, D. (2009). Mine drainage from the weathering of sulfide minerals and magnetite. Applied Geochemistry,24(12), 2362-2373.

Mori, J. F., Lu, S., Handel, M., Totsche, K. U., Neu, T. R., Iancu, V. V., Kusel, K. 2016. E Schwertmannite formation at cell junctions by a new filament-forming Fe(II)-oxidizing isolate affiliated with the novel genus Acidithrix. Microbiology, (162), 62-71.

Nielson, A.E., Sohnel, O., 1971. Interfacial tensions electrolyte crystal-aqueous solutions, from nucleation data. Journal of Crystal Growth, 11, 233-242.

Nordstrom, D. K., Blowes, D. W., & Ptacek, C. J. (2015). Hydrogeochemistry and microbiology of mine drainage: An update. Applied Geochemistry,57, 3-16.

Oggerin, M., Tornos, F., Rodríguez,, N., Del Moral, C., Sánchez-Román, M., & Amils, R. 2013. Specific jarosite biomineralization by Purpureocillium lilacinum, an acidophilic fungi isolated from Río Tinto. Environmental Microbiology,15, (8), 2228-2237.

Pace, D. L., Mielke, R. E., Southam, G., & Porter, T. L. (2006). Scanning force microscopy studies of the colonization and growth of A. ferrooxidans on the surface of pyrite minerals. Scanning,27(3), 136-140.

Peppas, A., Komnitsas, K., & Halikia, I. (2000). Use of organic covers for acid mine drainage control. Minerals Engineering,13(5), 563-574.

Pfeffer C, Larsen S, Song J, Dong M, Besenbacher F, Meyer RL et al. 2012. Filamentous bacteria transport electrons over centimeter distances. Nature, 491, 218–221.

Podosokorskaya, O. A., Kadnikov, V. V., Gavrilov, S. N., Mardanov, A. V., Merkel, A. Y., Karnachuk, O. V., Kublanov, I. V. 2013. Characterization ofMelioribacter roseusgen. nov., sp. nov., a novel facultatively anaerobic thermophilic cellulolytic bacterium from the class Ignavibacteria, and a proposal of a novel bacterial phylum Ignavibacteriae. Environmental Microbiology,15(6), 1759-1771.

Quatrini, R., Appia-Ayme, C., Denis, Y., Jedlicki, E., Holmes, D. S., & Bonnefoy, V. 2009. Extending the models for iron and sulfur oxidation in the extreme Acidophile Acidithiobacillus ferrooxidans. BMC Genomics,10(1), 394.

Rempfert, K. R., Miller, H. M., Bompard, N., Nothaft, D., Matter, J. M., Kelemen, P., Templeton, A. S. 2017. Geological and Geochemical Controls on Subsurface Microbial Life in the Samail Ophiolite, Oman. Frontiers in Microbiology,8.

Roden E.E., Zachara, J.M., 1996, Microbial reduction of crustalline iron (lll) oxides: influenceof oxide surfaces area and potential for cell growth. Environmental Science and Technology, 30, 1618-1628.

Sahinkaya, E., Ozkaya, B., Kaksonen, A.H., Puhakka, J.A., 2007. Sulfidogenic fluidized-bed treatment of metal-containing wastewater at 8 and 65 C degrees temperatures is limited by acetate oxidation. Water Research 41 (12), 2706- 2714.

Sánchez-Andrea, I., Stams, A. J., Hedrich, S., Ňancucheo, I., & Johnson, D. B. 2014. Desulfosporosinus acididurans sp. nov.: an acidophilic sulfate-reducing bacterium isolated from acidic sediments. Extremophiles,19(1), 39-47.

Schieber J. 2011. Iron Sulfide Formation. Encyclopedia of Geobiology, Springer Verlag,486-502

Schindler, M., Hochella, M. F. 2015. Soil memory in mineral surface coatings: Environmental processes recorded at the nanoscale. Geology,43(5), 415-418.

Schindler, M., Hochella, M. F. 2016. Nanomineralogy as a new dimension in understanding elusive geochemical processes in soils: The case of low-solubility-index elements. Geology,44(7), 515-518.

Schindler, M., Lanteigne, S., Mcdonald, A. M., & Hochella, M. F. 2016. Evidence of CU- and Ni-Bearing Surface Precipitates and Adsorption Complexes in Remediated Soils at the Nanoscale: A Tem, Micro-Raman, and Laser-Ablation ICP-MS Study of Mineral Surface Coatings. The Canadian Mineralogist, 54(1), 285-309.

Schippers, A., Breuker, A., Blazejak, A., Bosecker, K., Kock, D., & Wright, T. L. 2010. ChemInform Abstract: The Biogeochemistry and Microbiology of Sulfidic Mine Waste and Bioleaching Dumps and Heaps, and Novel Fe(II)-Oxidizing Bacteria. Hydromettallurgy,342-350

Schoonen, M.A.A., Barnes, H.L., 1991. Reactions froming pyrite and marcasite from solution: ll. Via FeS precursors below 100°C. Geochimica et Cosmochimica Acta, 55, 1505-1514

Schwertmann, U., Stanjek, H., & Becher, H. 2004. Long-termin vitrotransformation of 2-line ferrihydrite to goethite/hematite at 4, 10, 15 and 25°C. Clay Minerals,39(4), 433-438.

Senko, J. M., Wanjugi, P., Lucas, M., Bruns, M. A., & Burgos, W. D. 2008. Characterization of Fe(II) oxidizing bacterial activities and communities at two acidic Appalachian coalmine drainage-impacted sites. The ISME Journal,2(11), 1134-1145.

Sekiguchi, Y., Muramatsu, M., Imachi, H., Narihiro, T., Ohashi, A., Harada, H., Kamagata, Y. 2008. Thermodesulfovibrio aggregans sp. nov. and Thermodesulfovibrio thiophilus sp. nov., anaerobic, thermophilic, sulfate-reducing bacteria isolated from thermophilic methanogenic sludge, and emended description of the genus Thermodeulfovibrio. International Journal Of Systematic And Evolutionary Microbiology,58(11), 2541-2548.

Shock, E. L., & Boyd, E. S. 2015. Principles of Geobiochemistry. Elements,11, 395-401.

Siddiqui, K. S. 2008. Protein adaptation in extremophiles. New York: Nova Biomedical Books.

Southam, G., Beveridge, T.J. 1992. Enumeration of Thiobacilli within pH-neutral and acidic mine tailings and their role in the development of secondary mineral soil. Applied and Environmental Microbiology, 58, 1904-1912.

Southam G, Beveridge TJ: Examination of the lipopolysaccharide (O- antigen) populations of thiobacillus ferrooxidans from two mine tailings. *Appl Environ Microbiol* 59, 1283–1288 (1993)

Stackebrandt, E. 2014. The Family Alicyclobacillaceae. The Prokaryotes,7-12.

Steefel, C.I., Van Cappellen, P., 1990. A new kinetic approach to modelling water-rock interaction: the role of nucleation, precursons and Ostwald ripening. Geochimica et Cosmochimica Acta, 54, 2657-2677

Stegen, J. C., Konopka, A., Mckinley, J. P., Murray, C., Lin, X., Miller, M. D., Fredrickson, J. K. 2016. Coupling among Microbial Communities, Biogeochemistry and Mineralogy across Biogeochemical Facies. Scientific Reports,6(1).

Stumm, W., Morgan, J.J., 1996. Aquatic Chemistry, 3rd edition. John Wiley, New York

Sukla, L. B., Pradhan, N., Panda, S., Mishra, B. K. 2015. Environmental Microbial Biotechnology. Soil Biology.

Sweeney, R.E., Kaplan, I.R., 1973. Pyrite framboid formation: laboratory synthesis and marine sediments. Economic Geology, 68, 618-634.

Ulrich, G.A., Breit, G.N., Cozzarelli, I.M., Suflita, J.M., 2003. Sources of Sulfate Supporting AnaerobicMetabolism in a Contaminated Aquifer. Environ. Sci. Technol. 37, 1093-1099.

Vaughan, D. J., Corkhill, C. L. 2017. Mineralogy of Sulfides. Elements,13, 81-87.

Velde, B., Meunier, A. 2008. The Origin of Clay Minerals in Soils and Weathered Rocks.

Wang, J., Liu, B., Liu, G., Chen, Q., Pan, Z., Zheng, X., Chen, M. 2016. Draft Genome Sequence of Bacillus muralisLMG 20238T (DSM 16288), a Spore-Forming Bacterium Isolated from Deteriorated Mural Paintings. Genome Announcements,4(1).

Wolthers, M., Charlet, L., Linde, P. R., Rickard, D., & Van der Weijden, C. H. 2005. Surface chemistry of disordered mackinawite (FeS). Geochimica et Cosmochimica Acta ,69(14), 3469- 3481.

Wong, A., & Bergdoll, M. 2003. STAPHYLOCOCCUS | Properties and Occurrence. Encyclopedia of Food Sciences and Nutrition,5547-5551.
Xu, Y., & Schoonen, M. A. (1995). The stability of thiosulfate in the presence of pyrite in low-temperature aqueous solutions. Geochimica Et Cosmochimica Acta,59(22), 4605-4622.

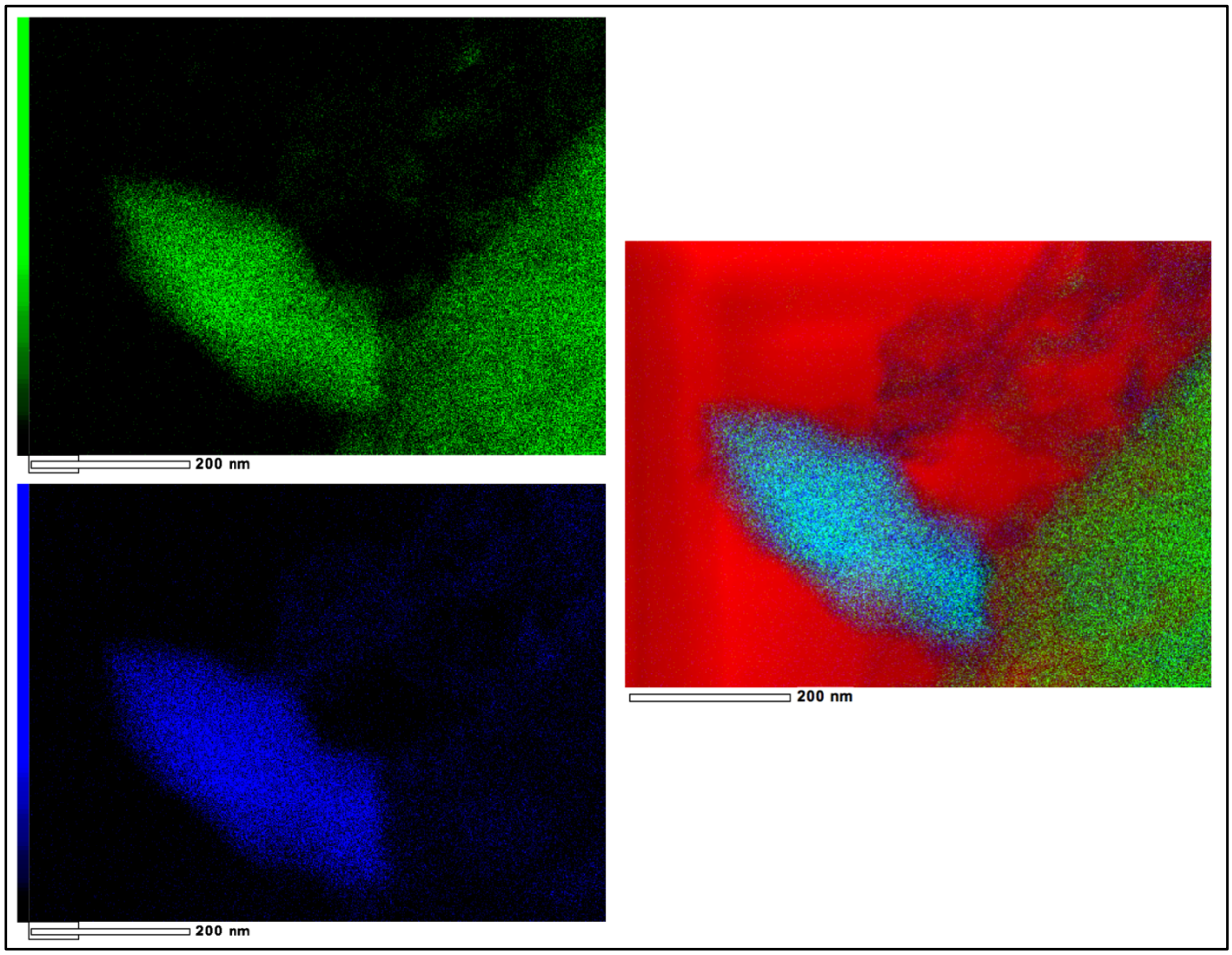

Figure 35 Iron (green) and Sulfur (blue) chemical map on TEM image of greigite crystal. Iron measures at 41.7 wt% and sulfur measures at 58.3 wt%.

Table 5 Additional geochemical parameters

Sample ID	Sulfide S %	Fe %	S %	Ferric Fe %	Ferrous iron %	Oxidized S species %	S Ratio Oxidized S Species/S as Sulfide	Fe Ratio (Fe(ll)/Fe(lll))
A1	0.1	6.8	1.0	2.5	4.3	1.0	19.0	1.7
A2	0.0	14.4	0.9	7.7	6.7	0.9	45.0	0.9
A3	0.0	12.8	1.1	6.1	6.7	1.1	55.0	1.1
A4	0.1	11.5	1.6	1.4	10.0	1.5	10.4	7.0
A5	0.2	18.2	4.3	5.9	12.3	4.1	16.9	2.1
A7	0.0	12.1	1.6	6.3	5.8	1.5	154.0	0.9
A8	0.0	13.4	2.1	6.4	6.9	2.1	52.5	1.1
A9	0.0	13.8	1.6	6.6	7.2	1.6	80.5	1.1
A10	0.1	10.7	1.4	1.6	9.1	1.3	18.6	5.7

Sample ID	Sulfide S %	Fe %	S %	Ferric Fe %	Ferrous iron %	Oxidized S species %	S Ratio Oxidized S Species/S as Sulfide	Fe Ratio (Fe(ll)/Fe(lll))
C1	0.1	10.9	1.1	5.3	5.6	1.0	16.8	1.1
C2	0.2	8.8	1.4	2.1	6.7	1.1	4.8	3.1
C3	0.0	9.0	1.1	3.2	5.8	1.0	25.5	1.8
C4	0.0	12.2	1.3	7.0	5.2	1.3	130.0	0.7
C5	0.0	10.7	1.3	5.7	5.0	1.3	132.0	0.9
C6	0.0	8.4	0.7	2.8	5.6	0.7	33.0	2.0
C7	0.0	9.6	0.4	2.2	7.5	0.4	39.0	3.5
C8	0.2	11.5	1.9	2.6	8.9	1.7	8.9	3.4
C9	0.0	6.5	0.5	1.8	4.7	0.5	11.3	2.6
D1	0.0	7.6	0.4	0.8	6.8	0.4	13.7	8.0
D2	0.0	6.8	0.1	1.2	5.6	0.1	3.5	4.5
D3	0.1	10.1	1.0	3.5	6.6	0.9	15.0	1.9
D4	0.0	8.3	0.8	2.9	5.4	0.7	36.5	1.8
D5	0.1	9.6	1.5	4.2	5.4	1.4	28.8	1.3
D6	0.0	9.9	1.1	2.8	7.2	1.1	36.0	2.6
D7	0.0	8.6	0.9	2.8	5.9	0.8	27.7	2.1
D8	0.1	9.3	1.4	3.2	6.1	1.3	26.2	1.9
K1	0.0	10.2	0.6	4.0	6.2	0.5	27.0	1.5
K3	0.0	8.7	0.6	2.0	6.8	0.5	26.5	3.4
K4	0.1	9.0	1.2	2.2	6.8	1.2	23.2	3.1
K5	0.0	8.7	0.8	2.2	6.5	0.8	37.5	3.0
K6	0.2	9.6	1.4	1.6	7.9	1.2	5.2	4.8
K7	0.3	6.5	0.9	0.9	5.6	0.7	2.7	6.3
M1	0.0	10.4	0.7	4.4	6.0	0.6	64.0	1.4
M2	0.0	9.6	0.8	3.0	6.6	0.8	40.5	2.2
M3	0.0	8.8	0.9	1.2	7.6	0.8	20.5	6.4
M4	0.0	10.4	0.6	4.1	6.3	0.5	54.0	1.5
M5	0.1	11.4	1.9	4.0	7.4	1.8	25.9	1.9
M6	0.0	2.7	0.2	1.2	1.5	0.2	15.0	1.3
M7	0.0	10.7	0.6	4.7	6.0	0.6	62.0	1.3
M8	0.4	14.7	4.0	7.5	7.2	3.5	8.0	1.0
M9	0.1	10.6	1.4	1.9	8.6	1.4	22.8	4.5

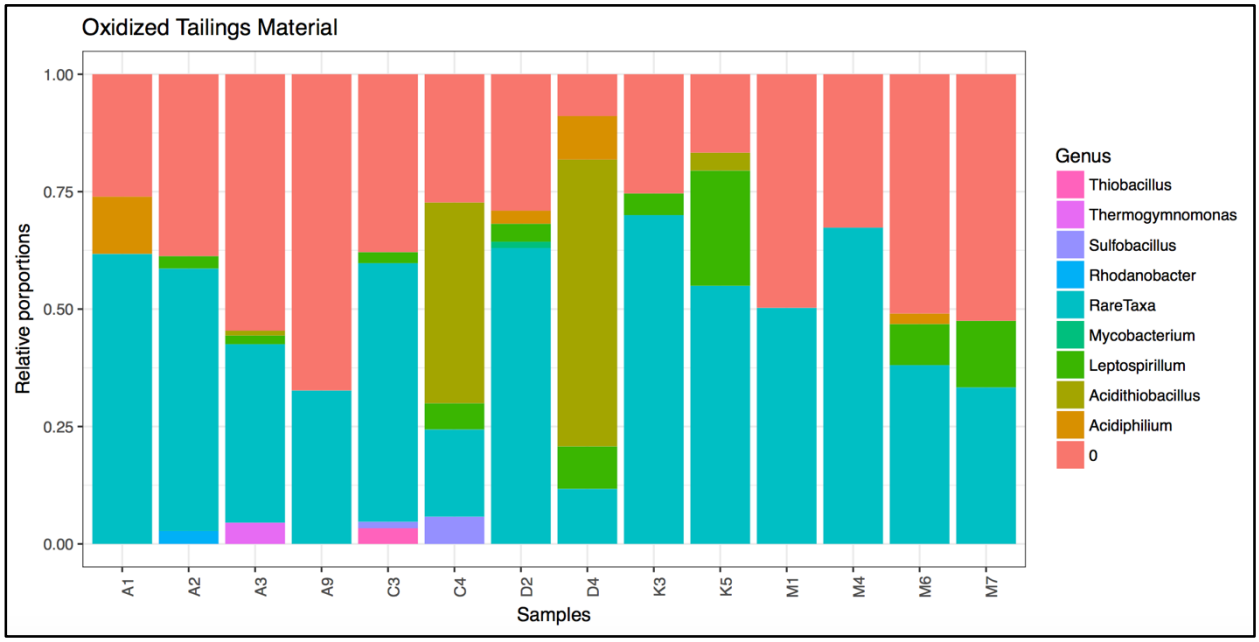

Figure 36 Microbial community data at the Genus level for tailings samples from the oxidized zone

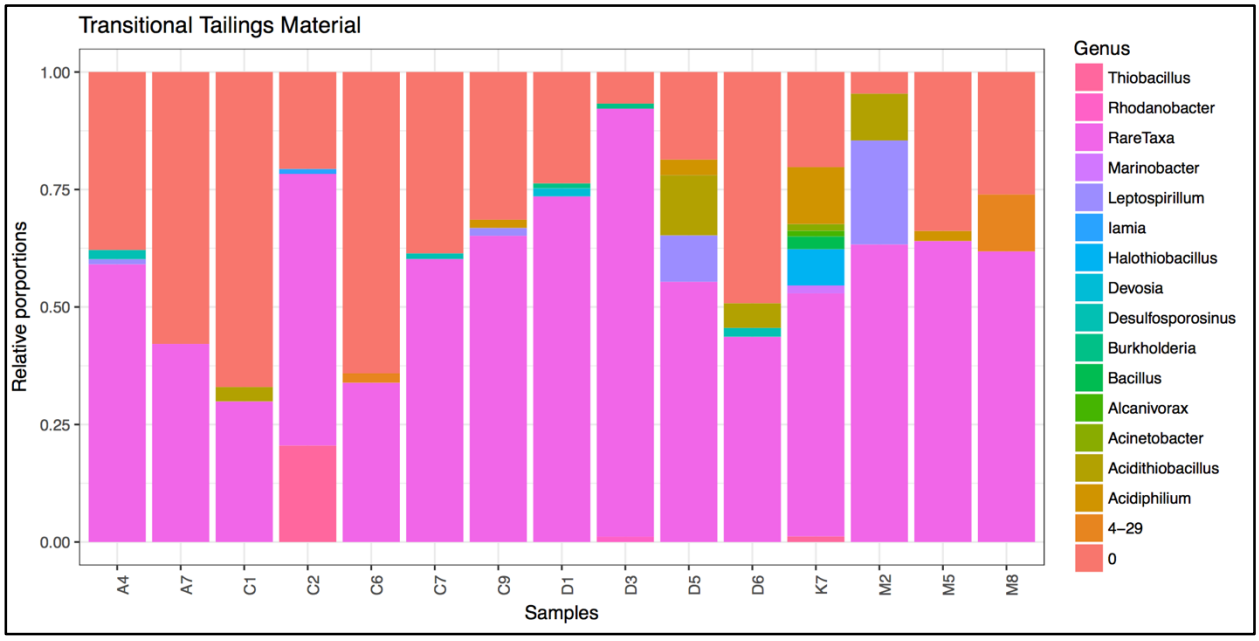

Figure 37 Microbial community data at the Genus level for tailings samples from the transition zone

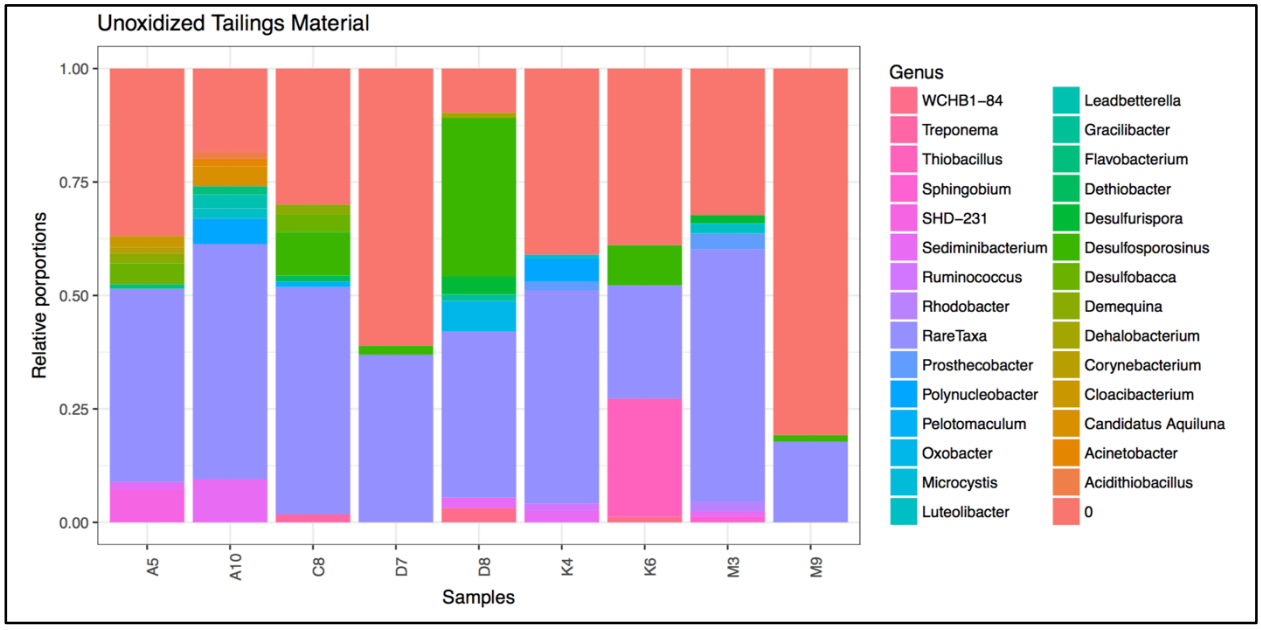

Figure 38 Microbial community data at the Genus level for tailings samples from the unoxidized zone

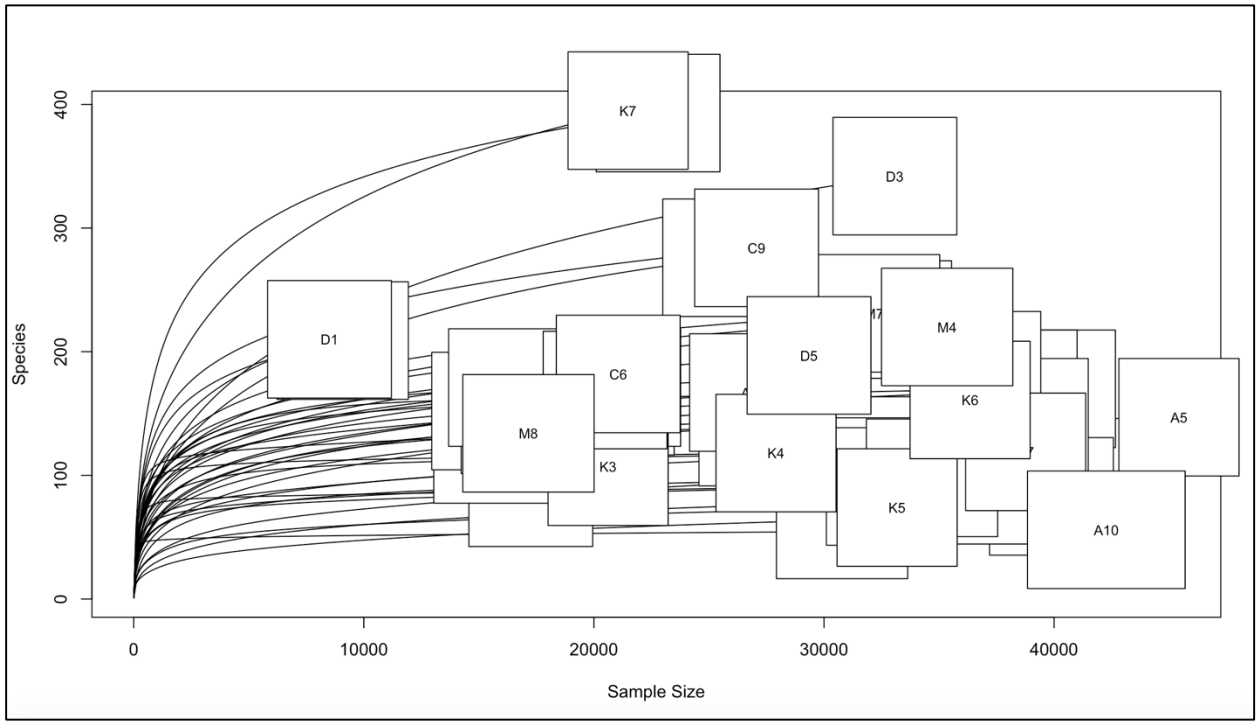

Figure 39 Rarefaction curve across 41 tailings samples, exhibiting species richness

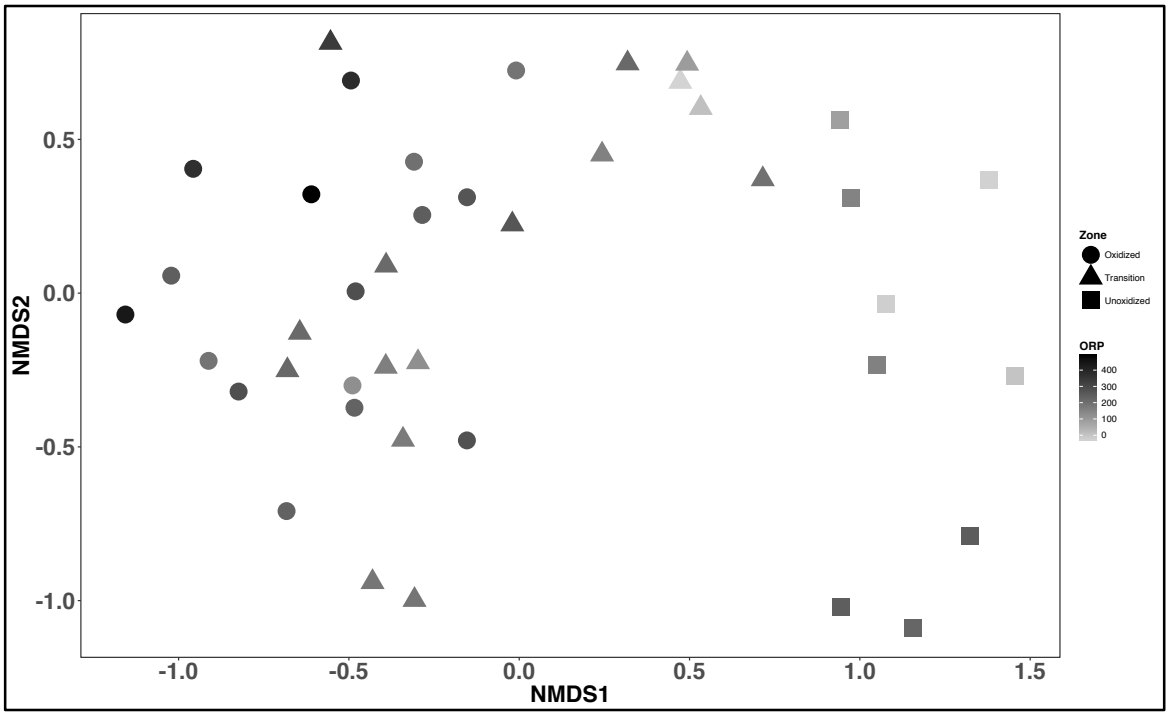

Figure 40 NMDS plot: Microbial community compositions vs. ORP (mV)

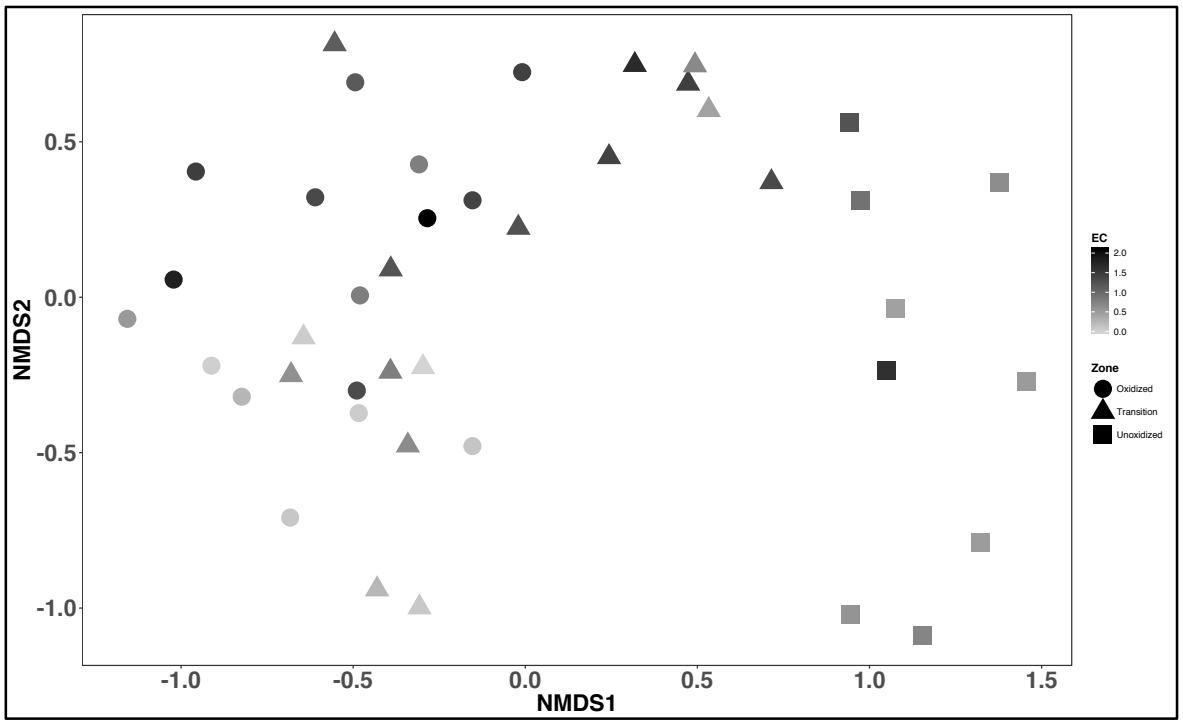

Figure 41 NMDS plot: Microbial community compositions vs. electrical conductivity (EC)

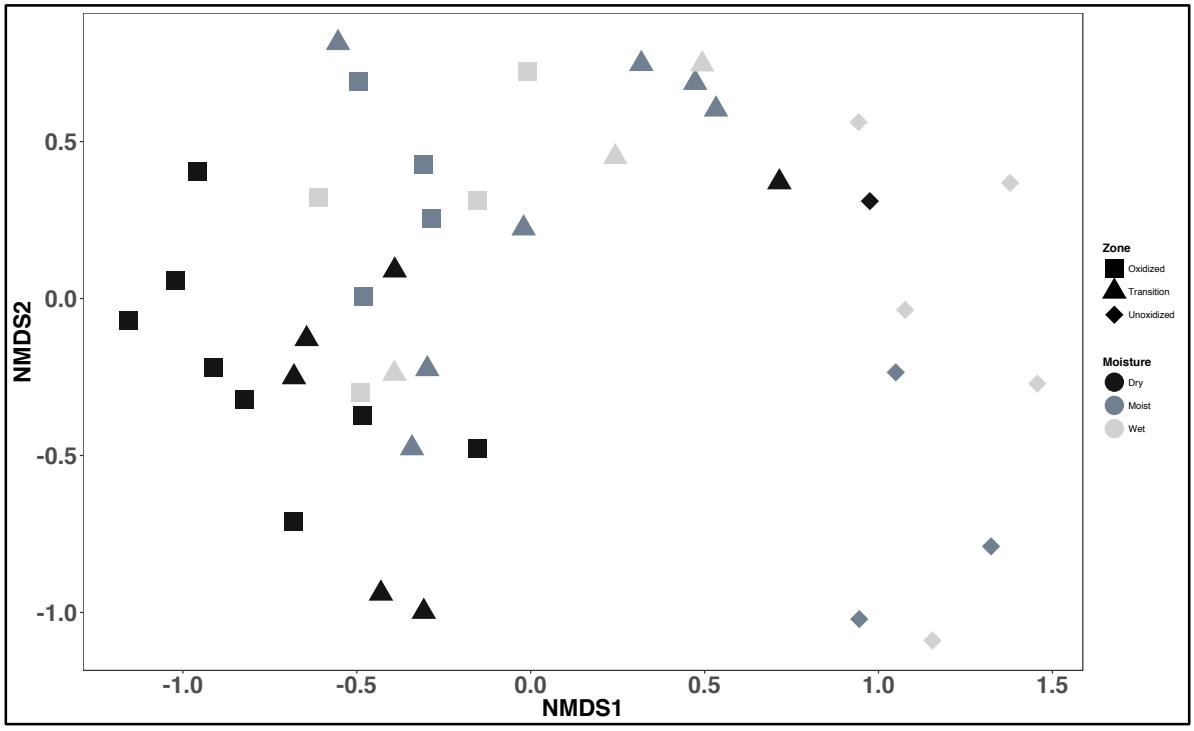

Figure 42 NMDS plot: Microbial community compositions vs. moisture content

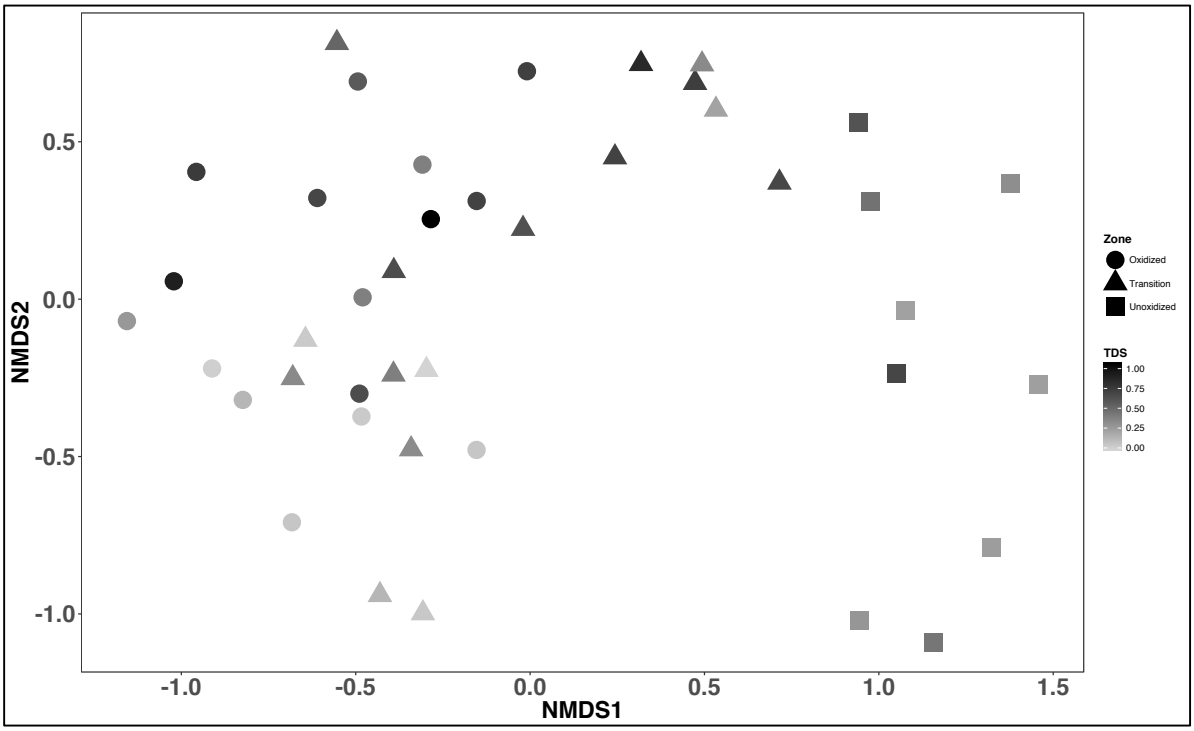

Figure 43 NMDS plot: Microbial community composition vs. TDS (ppt)